

**EXAMINING THE EFFECT OF AIR-FUEL ATOMIZATION ON THE
PERFORMANCE AND EMISSION OF HEAVY DUTY TRUCKS: A CASE STUDY
OF MERCEDES-BENZ ACTROS ENGINE MODEL 3340-LS.**

BY

KALANZI JESOUPHAT

(B.Eng. Mech & Manuf. Eng, KYU)

22/U/GMEM/428/PE

**A DISSERTATION SUBMITTED TO THE DIRECTORATE OF RESEARCH
AND GRADUATE TRAINING IN PARTIAL FULFILMENT OF THE
REQUIREMENTS FOR THE AWARD OF THE DEGREE OF MASTER OF
SCIENCE IN ADVANCED MANUFACTURING SYSTEMS ENGINEERING
OF KYAMBOGO UNIVERSITY**

DECEMBER, 2024

DECLARATION

I declare that this dissertation, entitled “**Examining the Effect of Air-Fuel Atomization on the Performance and Emission of Heavy Duty Trucks: A case study of Mercedes-Benz Actros Engine Model 3340-LS,**” is my work and has never been done before by anyone else.

Signature.....

Date

KALANZI Jesouphat

APPROVAL

This dissertation, entitled “**Examining the Effect of Air-Fuel Atomization on the Performance and Emission of Heavy Duty Trucks: A case study of Mercedes-Benz Actros Engine Model 3340-LS**”, prepared and submitted by Kalanzi Jesouphat in partial fulfillment of the requirements for the Master of Science in Advanced Manufacturing Systems Engineering of Kyambogo University, and has been under our supervision.

Dr. Maureen Nalubowa Ssempijja

Sign. Date.

Dr. Samuel Kangwagye

Sign. Date.

ACKNOWLEDGMENT

First and foremost, I thank the almighty GOD for giving me the gift of life, energy, and the finances to help me complete this research. I extend my gratitude to my supervisors who have always pushed me to progress to this final level of research; the technical support and advice they have offered is really commendable. May the almighty GOD reward them abundantly. Lastly, I thank my wife and children for the emotional support and the conducive environment they have always provided at home, for me to be able to execute my research without any misunderstandings. May the almighty GOD reward them abundantly.

DEDICATION

I dedicate this research to my dear wife and children for the love and support they have always given me towards my academics.

TABLE OF CONTENTS

DECLARATION	i
APPROVAL	ii
ACKNOWLEDGMENT	iii
DEDICATION	iv
LIST OF SYMBOLS AND ABBREVIATIONS	x
LIST OF FIGURES	xii
LIST OF TABLES	xiv
ABSTRACT	xv
CHAPTER ONE: INTRODUCTION	1
1.1 Background	1
1.2 Problem Statement	2
1.3 Research Objectives	3
1.3.1 Main Objective	3
1.3.2 Specific Objectives	3
1.3.3 Research Questions	3
1.4 Significance of Research	3
1.5 Justification of the Research	4
1.6 Scope and Limitations of the Research	5
1.7 Conceptual Framework	5

1.8 Organization of the Dissertation	6
CHAPTER TWO: LITERATURE REVIEW	8
2.1 Automobile Engine Air-Fuel Atomization	8
2.2 Environmental Requirements of Automobile Engines	9
2.3 Functional Requirements of Automobile Engine Air-fuel Atomization	9
2.3.1 Performance Improvements for Air-Fuel Atomization Systems in Automobiles through Research and Development	10
2.3.2 Engine Performance and Emission Metrics	12
2.4 Material Selection Requirements for Air-Fuel Atomization Systems in Automobiles	12
2.5 Manufacturing Process Requirements for Air-Liquid Atomization Systems in Automobiles	13
2.5.1 Manufacturing Process Improvements Accomplished through Research and Development for Air-Fuel Atomization Systems in Automobiles	15
2.5.2 Challenges for Air-Fuel Atomization Systems in Automobiles	16
2.5.3 Future Directions for Manufacture of Air-Fuel Atomization Systems for Automobiles	16
2.6 Simulations for Air-Fuel Atomization for Automobile Engines	17
2.7 Conventional Diesel Combustion Conceptual Model of a Diesel Engine	18
2.8 Summary of Previous Research Work and Gaps	23
2.8.1 Literature Summary	23

2.8.2 Research Gaps	24
CHAPTER THREE: METHODOLOGY	25
3.1 Introduction	25
3.2 Research Design	25
3.2.1 Overview of Simulation	25
3.2.2 Description of Mercedes Benz actros-3340-LS Engine Model	25
3.3 Setup of the Ricardo Wave Engine Model and Simulation	28
3.3.1 Model Configuration	28
3.3.2 Air-Fuel Atomization Parameters	32
3.3.3 Development of the Ricardo Wave CFD Simulations	32
3.4 Data Collection and Parametric Analysis	34
3.5 Validation of the Developed Model	36
3.7 Why Ricardo Wave Was Used	36
3.8 The governing equations behind the simulation software	36
CHAPTER FOUR: RESULTS, DISCUSSIONS, AND FINDINGS	39
4.0 Introduction	39
4.1 Characterized Design Parameters.	39
4.2 Developed Ricardo Wave Engine Model	40
4.3 Effect of Air-Fuel Atomization on Combustion and Emission Characteristics	40
4.3.1 Spray Dynamics and SMD Analysis	40

4.3.2 Fuel Breakup Length Analysis	46
4.3.3 Heat Transfer Rate	51
4.4 Engine Performance Analysis	54
4.4.1 Brake Torque and Power	54
4.4.2 Brake-Specific Fuel Consumption (BSFC)	59
4.4.3 Brake Mean Effective Pressure (BMEP)	61
4.4.4 Total Volumetric Efficiency (VOLEFF)	66
4.5 Emissions Analysis	69
4.5.1 NOx Emissions	69
4.5.2 Particulate Matter (PM) Emissions	73
4.5.3 Hydrocarbons (HC) Emissions	78
4.5.4 CO Emissions	83
4.6 Key Findings from the research	88
4.7 Limitation of the study	89
4.8 End-users of the Findings	89
CHAPTER FIVE: CONCLUSION AND RECOMMENDATIONS	90
5.1 Introduction	90
5.1 Conclusion	90
5.2 Recommendations	91
5.3 Future Research Directions:	92

REFERENCES	93
APPENDICES	108
Appendix A1: Work Plan	108
Appendix B1: Ricardo Wave Engine Model Developed	109
Appendix B2: Ricardo Wave Simulation Parametric Cases Definition	110
Appendix B3: Ricardo Wave Post Model Image	111
Appendix C1: Budget	112
Appendix D1: Ricardo Wave Simulation Output File	113
Appendix D2: Ricardo Wave Simulation Summary Data File	114
Appendix E1: Injection Rate and Injection Pressure Profiles	116
Appendix E2: Characterized Design parameters for MB Actros Engine model 3340-LS.	117
Appendix F1: Plagiarism Report and Receipt	119

LIST OF SYMBOLS AND ABBREVIATIONS

1D	One Dimension
3D	Three Dimension
AFR	Air Fuel Ratio
AHRR	Apparent Heat Release Rate
ASOC	After Start of Combustion
ATDC	After Top Dead Centre
BEV	Battery Electric Vehicle
BMEP	Brake Mean Effective Pressure
BSU	Bosch Smoke Units
BTDC	Before Top Dead Centre
CFD	Conceptual Fluid Dynamics
CNC	Computer Numeric Control
CO	Carbon Monoxide
CO ₂	Carbon Dioxide
CT	Computed Tomography
DI	Direct Injection
DLC	Diamond-Like Carbon
DMLS	Direct Metal Laser Melting
ECU	Electronic Control Unit
EDM	Electrical Discharge Machining
EGR	Exhaust Gas Recirculation

EPA	Environmental Protection Agency
HFC	Hydrogen Fuel Cell
HC	Hydrocarbons
HD	Heavy Duty
HEV	Hybrid Electric Vehicle
IC	Internal Combustion
ICE	Internal Combustion Engine
ICEV	Internal Combustion Engine Vehicles
IMEP	Indicated Mean Effective Pressure
MB	Mercedes Benz
MEP	Mean Effective Pressure
NCYC	Number of Cycles
NOX	Nitrogen Oxides
SAE	Society of Automotive Engineers
SCR	Selective Catalytic Reduction
SLM	Selective Laser Melting
SMD	Sauter Mean Diameter
SOC	Start of Combustion
SOINJ	Start of Injection
VOF	Volume of Fluid
VOLEFF	Volumetric Efficiency
YSZ	Yttria Stabilized Zirconia

LIST OF FIGURES

Figure 1.1. Conceptual Framework of the Research	6
Figure 2.1. Schematic representation of a coaxial spray diffusion flame.....	19
Figure 2.2. Four groups of combustion modes of a droplet cloud.....	20
Figure 2.3 Schematic of group combustion for a liquid-fuel spray.	20
Figure 2.4. Schematic representation of combustion zones and entrainment rates for a transient spray mixing model of diesel combustion.	21
Figure 3.1: Ricardo Wave 2019.1 Build Interface.....	30
Figure 3.2: Ricardo Wave Mercedes Benz Actros-3340-LS Engine Model Developed	31
Figure 3.3: Ricardo Wave Mercedes Benz Actros 3340-LS Model Simulation Flow	34
Figure 3.4: Wave post model image for Mercedes Benz Actros-3340-LS.....	35
Figure 4.3.1 (a): SMD Vs. Injector Nozzle Hole Diameter Analysis	41
Figure 4.3.1 (b): SMD with varying Speed and Nozzle Hole Diameter Analysis.....	44
Figure 4.3.2 (a): Breakup Length Vs. Nozzle Hole Diameter Analysis	46
Figure 4.3.2 (b) Breakup Length Vs. Nozzle Hole Diameter and Speed Analysis	49
Figure 4.3.3: Heat Transfer Rate Vs. Nozzle Hole Diameter Analysis.....	52
Figure 4.4.1 (a): Brake Power Vs. Nozzle Hole Diameter Analysis	54
Figure 4.4.1 (b): Brake Torque Vs. Nozzle Hole Diameter Analysis.....	57
Figure 4.4.2. BSFC Vs. Engine Speed and Nozzle Hole Diameter Analysis.....	59
Figure 4.4.3 (a) BMEP Vs. Nozzle Hole Diameter Analysis	62

Figure 4.4.3 (b) BMEP Vs. Nozzle Hole Diameter and Speed Analysis	64
Figure 4.4.4 Total VOLEFF Vs Engine Speed and Nozzle Hole Diameter Analysis	67
Figure 4.5.1: (a) NO _x Emission Vs. Nozzle Hole Diameter Analysis	69
Figure 4.5.1 (b): NO _x Emission Vs. Nozzle Diameter and Speed Analysis	71
Figure 4.5.2 (a) Smoke Emission Vs. Nozzle Hole Diameter Analysis	74
Figure 4.5.2 (b) Smoke Emission Vs. Speed and Nozzle Hole Diameter Analysis	76
Figure 4.5.3 (a) Hydrocarbons (HC) Emissions Vs. Nozzle Hole Diameter Analysis	79
Figure 4.5.3 (b): Hydrocarbons (HC) Vs. Nozzle Hole Diameter and Speed Analysis	81
Figure 4.5.4 (a): CO Emission Vs. Nozzle Hole Diameter Analysis.....	83
Figure 4.5.4 (b): Carbon Monoxide (CO) Vs. Nozzle Hole Diameter and Speed Analysis	85

LIST OF TABLES

Table 2.1 Optical Technique Used by Dec	23
Table 2.2 Summary of the notable recent studies done	23
Table 3.1. Specifications for Mercedes Benz model 3340-LS, (Benz, 2015).	27
Table 4.3.1 Validation of SMD Results at Varying Nozzle Hole Diameter.....	43

ABSTRACT

Internal Combustion Engines (ICEs) are facing criticism for their role in greenhouse gas emissions and air pollution. Despite technological advancements in air-fuel atomization, optimizing air-fuel atomization to enhance performance and reduce emissions in heavy-duty diesel engines such as the Mercedes-Benz Actros 3340-LS remains a challenge. A comprehensive assessment of air-fuel atomization mechanisms is therefore important to enhance engine efficiency while simultaneously holding back harmful emissions to ensure sustainability and competitiveness of heavy-duty trucks engines in modern transportation. This research examined the effects of air-fuel atomization on engine performance and emissions using Computational Fluid Dynamics (CFD) simulations in Ricardo Wave 2019.1. It specifically aimed at characterizing the design parameters of Mercedes Benz Actros 3340-LS engine, developing a validated Ricardo Wave CFD simulation engine model, and analyzing the impact of key injection parameters specifically nozzle hole diameter, injection pressure, Air-Fuel Ratio (AFR), and engine speed on performance and emissions. The engine model was replicated in Ricardo Wave and subjected to a series of simulations with varying nozzle hole diameters from 0.194 mm to 0.278 mm and engine speed from 700 rpm to 2500 rpm. Performance indicators such as brake power, torque, brake-specific fuel consumption (BSFC), volumetric efficiency, and emissions like Nitrogen oxides (NO_x), Carbon monoxides (CO), Hydrocarbons (HC), and Smoke were evaluated under standardized test cycles. Model validation was conducted by comparing simulation trends with experimental findings from related heavy-duty engines, including MAN D2676LF, Volvo D13C, Cummins ISX12G, and various GDI engines. Results show that smaller injector nozzle diameters (0.194 mm - 0.203 mm) produced finer sprays with reduced Sauter Mean Diameter (SMD) and breakup length, leading to improved brake torque, brake power, volumetric efficiency, and lower Brake Specific Fuel Consumption (BSFC), NO_x, CO, HC, and smoke emissions. Larger injector nozzles diameters (above 0.24mm) yielded coarser sprays, higher emissions, and reduced efficiency. The study also found a correlation between nozzle hole size and smoke emissions, with diameters above 0.25 mm leading to increased smoke and hydrocarbon emissions. The study also found that injection parameters, particularly nozzle hole diameter and injection pressure, significantly affect air-fuel atomization quality. The optimal nozzle hole diameter of 0.203 mm yielded the most balanced trade-off between fuel efficiency, power output, and emission levels. The results closely aligned with published experimental findings, confirming the model's predictive capability. The research recommends that for further research and practical applications, manufacturers should implement adjustable injector designs, fleet operators should maintain regular injector calibration, and policymakers should encourage the adoption of precision fuel injection technologies through emissions regulation frameworks and incentives for low-emission heavy-duty vehicles, and integrating 1D with 3D CFD tools like ANSYS fluent and Coverage to get insights on spray behavior, turbulence and flame propagation which are not fully resolved in 1D models, and employing advanced wear-resistant materials. Future research should focus on adaptive injection systems, atomization optimization under varying engine loads and speeds, the impact of alternative fuels and nozzle hole geometry, real-world driving conditions, long-term durability, and integrating variable geometry turbocharging for performance and emissions reduction.

Keywords: Air-Fuel Atomization, Computational Fluid Dynamics, Emission, Optimization, Performance, Ricardo Wave, and Simulation

CHAPTER ONE: INTRODUCTION

1.1 Background

Internal Combustion Engines (ICEs) have long served as the backbone of land transportation. However, they are being criticized for their contribution to greenhouse gas emissions and air pollution, leading to the adoption of cleaner alternatives, including hybrid electric vehicles (HEVs), battery electric vehicles (BEVs), and hydrogen fuel cell technologies (IEA, 2023; Amann et al., 2022). Recent studies highlight the importance of optimizing combustion through fuel property enhancements, focusing on atomization characteristics and droplet behavior to promote cleaner burning in compact, lightweight engines (Chen et al., 2021; Reitz & Ogawa, 2022).

Biodiesel blends and renewable fuels are gaining popularity due to their carbon neutrality, but concerns about chemical reactivity persist such as corrosion of engine aluminium components, particularly in high-pressure systems in modern heavy-duty engines (Demirbas, 2021; Saleh et al., 2023). While electrification is accelerating for light-duty vehicles, ICEs still dominate in heavy-duty applications due to unmatched power density, range, and refuelling time advantages (Zhao et al., 2023; IEA, 2023). The technical feasibility of transitioning to electric powertrains in long-haul freight remains limited by infrastructure and battery limitations. Fuel atomization has a major impact on emissions, efficiency, and combustion quality in diesel engines. Large droplet sizes and uneven spray distribution can occur from poor atomization caused by suboptimal nozzle design or insufficient injection pressure, which raises emissions of soot, unburned hydrocarbons, and NO_x emissions (Karimkashi et al., 2021; Prasad et al., 2022).

Recent research on injector geometry, spray angle, multi-hole designs, and variable injection strategies improves fuel-air mixing in light-duty and passenger cars, with limited studies targeting heavy-duty engines like Mercedes Benz Actros 3340-LS. (Mohanraj et al., 2021). This study addresses this gap by focusing on how air-fuel atomization impacts the performance and emissions of a heavy-duty diesel engine, using simulations of the Mercedes-Benz Actros Engine Model 3340-LS. The aim is to provide data-driven insights for optimizing injector design and combustion control strategies, contributing to cleaner and more efficient diesel technologies in commercial transport.

1.2 Problem Statement

Despite technological advancements in air-fuel atomization, there is still a significant gap in understanding how these innovations translate into measurable performance gains and emission reductions in heavy-duty diesel engines. In particular engines such as the Mercedes-Benz Actros Engine Model 3340-LS which has complex design features, there is insufficient evaluation of how injector design and air-fuel atomization characteristics influence both performance and emission outcomes, which poses technical and environmental challenges. The study aims to bridge the gap between atomization theory and practical engine optimization by using Computational Fluid Dynamics simulation software (Particularly Ricardo Wave) to understand how injector design and air-fuel atomization characteristics influence performance and emission outcomes in heavy-duty diesel engines like the Mercedes-Benz Actros 3340-LS. This will provide actionable insights for design improvements and regulatory compliance.

1.3 Research Objectives

1.3.1 Main Objective

To examine the effect of air-fuel atomization on the performance and emission of the Mercedes-Benz Actros Engine Model 3340-LS.

1.3.2 Specific Objectives

- i. To characterize the design parameters of Mercedes-Benz Actros 3340-LS in relation to its structural and operational framework.
- ii. To develop a Ricardo Wave CFD simulation of the Mercedes-Benz Actros 3340-LS engine model.
- iii. To analyse the impact of injection parameters on the engine performance and exhaust emissions.

1.3.3 Research Questions

- i. What are the key structural and operational design parameters of the Mercedes-Benz Actros 3340-LS engine?
- ii. How can a Ricardo Wave CFD simulation model be developed to replicate the Mercedes-Benz Actros 3340-LS engine's combustion and atomization processes?
- iii. How do variations in injector nozzle hole diameter and engine speed at stable high injection pressure affect engine performance and emission outputs?

1.4 Significance of Research

Research on air-fuel atomization is vital for improving combustion efficiency, reducing emissions, and enhancing fuel economy. It directly impacts engine performance, power output, and fuel consumption. Reliable and consistent air-fuel atomization is essential for

long-term engine performance. Research in this area contributes to meeting emission standards and environmental regulations, mitigating air pollution. It also actively supports innovation by exploring new techniques and designs for fuel injection systems and combustion processes.

1.5 Justification of the Research

Heavy-duty truck emissions pose environmental and public health risks. Understanding the relationship between air-fuel atomization and emissions by evaluating Mercedes-Benz Actros Engine Model 3340-LS can inform the development of technologies and operational practices aimed at reducing emissions levels while maintaining engine performance. Air-Fuel atomization significantly impacts combustion efficiency in internal combustion engines. Studying the Mercedes Benz Actros Engine Model 3340-LS can help devise strategies to maximize efficiency and enhance engine performance. The MB Actros Engine Model 3340-LS air-fuel atomization analysis will reveal the relationship between emissions and engine performance, and such knowledge can promote innovation in fuel injection systems, combustion procedures, and engine design, resulting in more ecologically friendly and efficient heavy duty truck engines. Worldwide regulatory bodies are putting heavier restrictions on vehicle emissions, including for heavy-duty trucks. Evaluation of Mercedes Benz Actros Engine Model 3340-LS, specifically concentrating on air-fuel atomization, can exhibit a practice dedication to ecological responsibility, adherence to regulations, and competitiveness in the market.

1.6 Scope and Limitations of the Research

The scope of the research includes a thorough examination of the developed Mercedes-Benz Actros Engine Model 3340-LS's performance, with a particular emphasis on how emissions relate to the engine's air-fuel atomization. The study entails a wide exploration of various aspects related to operational parameters, combustion dynamics, and engine design. It also integrates findings from the characterization of design parameters, Ricardo wave simulations, and analysis of injection parameters to gain a comprehensive understanding of the role of air-fuel atomization in the performance and emissions characteristics of the Mercedes-Benz Actros Engine Model 3340-LS by varying the injector nozzle hole diameter and engine speed.

1.7 Conceptual Framework

The conceptual framework is based on the elements that contribute to optimal air-fuel atomization in the engine combustion chamber as shown in Figure 1.1. Independent Variables include: Fuel Properties like fuel density, viscosity, surface tension, and chemical composition. Injection System Parameters such as injection pressure, injection timing, injector nozzle design, injector nozzle hole diameter, and injector nozzle geometry. Engine Operating Conditions like engine speed, engine load, intake air pressure, intake air temperature, and cylinder pressure. Dependent Variables: Fuel Atomization Characteristics such as droplet size distribution, spray cone angle, spray penetration depth, and spray breakup length. Combustion Characteristics which involve parameters related to combustion efficiency, ignition delay, heat release rate, and emissions (such as NO_x, CO, HC, and particulate matter like smoke). Engine Performance and Efficiency variables like brake mean effective pressure (BMEP), brake power, brake torque, total volumetric efficiency

(VOLEFF), and brake specific fuel consumption (BSFC). The outputs of the simulation include graphs showing the variation of dependent variables with independent variables, and analysis of the engine performance, combustion characteristics and emission under different operating conditions. Other research outputs include optimization insights, recommendations for design improvements for the best performance and emission control.

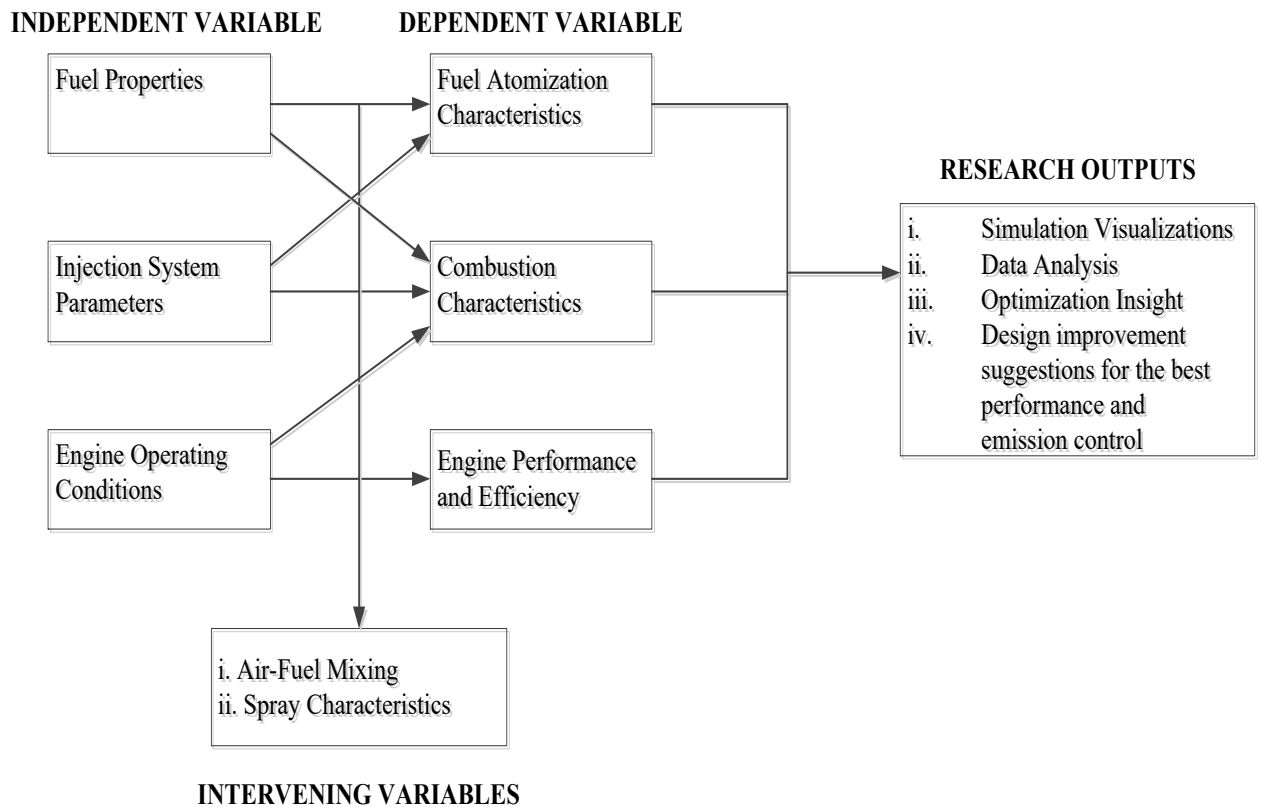


Figure 1.1. Conceptual Framework of the Research

1.8 Organization of the Dissertation

This dissertation is structured into five chapters.

Chapter One: Introduction – Presents the background of the study, the research problem, objectives, research questions, significance, justification, scope, limitations, and the conceptual framework.

Chapter Two: Literature Review – Provides a critical review of existing studies on air-fuel atomization, performance, and emissions of diesel engines. It also highlights functional, environmental, material, and manufacturing aspects of atomization systems, and identifies research gaps addressed by this study.

Chapter Three: Methodology – Describes the research design, the Mercedes-Benz Actros 3340-LS engine specifications, development of the Ricardo Wave simulation model, simulation setup, data collection procedures, model validation, and why this software was used.

Chapter Four: Results, Discussion, and Findings – Presents the results of the simulations, analyzes the effect of injection parameters on spray dynamics, combustion, performance, and emissions. It also discusses findings in relation to published studies and identifies key implications.

Chapter Five: Conclusions and Recommendations – Summarizes the major findings of the study, draws conclusions in line with the research objectives, provides recommendations for engine manufacturers, policymakers, and fleet operators, and suggests directions for future research.

CHAPTER TWO: LITERATURE REVIEW

2.1 Automobile Engine Air-Fuel Atomization

Internal combustion engines (ICEs) convert fuel's chemical energy into mechanical energy by combustion, enabling vehicle propulsion through precisely timed and coordinated engine strokes, accurate fuel injection, ignition timing, and exhaust gas recirculation to optimize power output while reducing emissions (Reitz & Ogawa, 2022). Fuel injection systems in heavy-duty truck engines introduce finely atomized fuel into the combustion chamber to ensure thorough mixing with air. Modern injectors are designed for high-pressure multi-hole delivery for improved dispersion and efficiency (Mohanraj et al., 2021). Recent studies highlight the impact of fuel properties on the atomization process, affecting spray pattern, droplet size, and evaporation behavior (Chen et al., 2021).

Despite technological advancements, heavy-duty engine combustion chamber designs often lack optimization for optimal atomization under varying load and environmental conditions, leading to increased focus on customized chamber geometries and injector configurations (Karimkashi et al., 2021). Real-time atomization control is crucial for heavy-duty trucks, requiring intelligent control systems using adaptive algorithms and sensor feedback to dynamically adjust injection timing, pressure, and spray characteristics (Sharma et al., 2023). Recent emission regulations, such as Euro VI and U.S. EPA Phase 2 standards, mandate significant reductions in NO_x and particulate matter (PM) emissions. As a result, researchers are exploring advanced injector designs (e.g., piezoelectric and multi-stage injectors), alternative fuels, and variable nozzle geometries to enhance atomization and reduce unburnt fuel and soot formation (Zhao et al., 2023).

2.2 Environmental Requirements of Automobile Engines

Global efforts to combat climate change, air pollution, and resource depletion drive modern environmental requirements for automobile engines, aiming to reduce greenhouse gas emissions, enhance fuel efficiency, and accelerate alternative propulsion technologies (IEA, 2023). European Union, Environmental Protection Agency (EPA), and other regulatory frameworks set strict limits on NO_x, CO₂, hydrocarbons, and particulate matter emissions from internal combustion engines to reduce pollutants in new vehicles (European Commission, 2023; EPA, 2022). The U.S. Department of Transportation and the European Commission are promoting the adoption of low and zero-emission vehicles, including technologies like selective catalytic reduction and diesel particulate filters, for public procurement fleets (NHTSA, 2022; European Parliament, 2021).

United Nations Economic Commission for Europe's World Forum for Harmonization of Vehicle Regulations (WP.29) promotes global emission and safety standards, facilitating compliance across various markets for multinational automotive production (UNECE, 2023). Automobile manufacturers are investing in research and development to meet environmental demands, focusing on advanced combustion strategies, waste heat recovery, engine downsizing, and integrating renewable fuels for heavy-duty diesel engines (Reitz et al., 2022; Amann et al., 2022)

2.3 Functional Requirements of Automobile Engine Air-fuel Atomization

Automobile engines must meet a range of functional requirements to deliver consistent, efficient, and environmentally compliant performance (Reitz & Ogawa, 2022). In Internal

combustion engines (ICEs) of heavy-duty applications, minimising energy loss is achieved by optimizing thermal efficiency, reducing frictional losses, and improving combustion processes (Zhao et al., 2023). Engine components must withstand high combustion pressures, thermal stresses, and mechanical fatigue over prolonged operating cycles. This necessitates the use of high-strength materials, advanced surface treatments, and precision manufacturing techniques (Wang et al., 2022). Engines must reduce NO_x, CO, HC, and PM emissions to meet global emission regulations, requiring precise fuel-air atomization and combustion control to prevent incomplete combustion and pollutant formation (Chen et al., 2021).

Modern engines rely heavily on electronic control units (ECUs) to manage fuel injection timing, quantity, and pressure, adapting in real-time to changing conditions like engine load, ambient temperature, and fuel type (Manin et al., 2021). To prevent localized rich or lean zones, atomization systems must ensure homogeneous fuel distribution, particularly under transient operating conditions. Injector and nozzle components must be wear-resistant, chemically stable, and capable of delivering consistent performance over the engine's service life (Lapuerta et al., 2021). Additionally, advanced atomization systems must be compatible with alternative fuels such as biodiesel, ethanol, or synthetic e-fuels, which may differ in viscosity, volatility, and spray behavior (IEA, 2023).

2.3.1 Performance Improvements for Air-Fuel Atomization Systems in Automobiles through Research and Development

Recent advancements in air-fuel atomization technologies are aimed at improving combustion efficiency, reducing emissions, and enhancing fuel economy across a wide range

of engine operating conditions. Modern multi-hole injectors and variable nozzle geometries improve atomization, air-fuel mixing, and complete combustion by producing finer, uniformly distributed fuel droplets, optimizing spray penetration and cone angle (Manin et al., 2021; Xu et al., 2020). Innovative injection strategies like split, pilot, and multiple injections are widely used to control combustion phasing, reduce noise, and improve ignition stability, particularly in controlling soot and NO_x emissions (Payri et al., 2020).

Advancements in electronic control units (ECUs) have enabled precise regulation of injection timing, quantity, and pressure, improving the accuracy of fuel delivery. AI-integrated ECUs are now being explored for adaptive atomization control based on real-time engine feedback (Sharma et al., 2023). Piezoelectric injectors enhance performance in high-pressure common rail systems by providing rapid response, precise control, improved fuel-air mixture homogeneity, combustion stability, and reduced emissions (Jadhav & Mallikarjuna, 2021). Advanced materials and wear-resistant coatings like ceramic layers and diamond-like carbon extend the lifespan and reliability of atomization components, particularly under high pressures and high injection frequencies (Wang et al., 2022). Dual injection systems, which combine direct injection and port fuel injection, enhance fuel stratification control, thermal efficiency, and particulate emissions in gasoline and dual-fuel engines (Feng et al., 2020). CFD simulations aid in optimizing injector performance for various fuels, reducing prototyping costs and enabling data-driven optimization of atomization systems, including biodiesel, ethanol blends, and e-fuels (Most & Duret, 2022).

2.3.2 Engine Performance and Emission Metrics

Brake Thermal Efficiency measures how effectively the chemical energy of fuel is converted into useful work. Typical for heavy-duty diesel engines ranges between 30 – 42 % (Yang et al., 2023). Brake Specific Fuel Consumption indicates fuel efficiency; lower BSFC denotes higher efficiency. Values typically range between 180 - 220 g/kWh for optimized engines (Zhang et al., 2022). Combustion Efficiency Improved by better atomization and air-fuel mixing; closely tied to injector pressure and nozzle design (Ali et al., 2021). NO_x (Nitrogen Oxides): Formed due to high combustion temperatures. Strategies such as Exhaust Gas Recirculation (EGR) and Selective Catalytic Reduction (SCR) are employed to reduce it (Jafari et al., 2023). Particulate Matter (PM) is influenced by incomplete combustion. Better atomization reduces PM formation (Singh & Verma, 2022). CO (Carbon Monoxide) and HC (Hydrocarbons) indicate incomplete combustion. Improved injection and mixing reduce these pollutants. CO₂ Emissions are directly related to fuel consumption thus, efficiency improvements also lower CO₂ output (Bunce & Fogarty, 2022).

2.4 Material Selection Requirements for Air-Fuel Atomization Systems in Automobiles

Materials for air-fuel atomization systems in automobiles must be durable, reliable, corrosion-resistant, and thermally stable, especially under extreme conditions in modern internal combustion engines. High pressures, temperatures, and chemically aggressive fuels continuously expose components like injector nozzles, fuel rails, and valve bodies to degradation, necessitating materials that can withstand these challenges (Wang et al., 2022). Stainless steel alloys like AISI 316L and 17-4PH are widely used in fuel injectors due to corrosion resistance, mechanical strength, and cost-effectiveness, while nickel-based super alloys like Inconel 718 are preferred for high-temperature and high-stress regions (Song et

al., 2020). Ceramic coatings like yttria-stabilized zirconia (YSZ) and alumina-based minimize erosion, wear, and thermal degradation in fuel injector tips and combustion-facing surfaces, while diamond-like carbon (DLC) coatings improve friction and component lifespan (Wang et al., 2022; Park et al., 2023).

Research is focusing on elastomers, seals, and liners made from fluoroelastomers and thermoplastic elastomers to address material compatibility issues with oxygenated fuels (IEA, 2023). High-strength materials like titanium alloys and stainless steels are increasingly being utilized in components like fuel lines and pressure control valves for mechanical fatigue and pressure pulsations (Lapuerta et al., 2021). Tool steels like H13 and M2 are crucial for precision component manufacturing due to their machinability, stability, and polished surface finish, essential for fuel spray formation (Singh et al., 2022). PEEK and PA66 are popular engineering plastics for connectors, housings, and fuel system fittings due to their thermal resistance, chemical compatibility, and structural integrity (Brydson, 2021). Recent innovations in composite materials and metal-polymer hybrids are reducing weight and cost in engine design, while additive manufacturing-compatible alloys enable the creation of complex atomization components (Gibson et al., 2023).

2.5 Manufacturing Process Requirements for Air-Liquid Atomization Systems in Automobiles

The manufacturing of air-liquid atomization systems in modern automobile engines requires precision engineering, advanced materials processing, and quality control. Key manufacturing methods include CNC machining for critical components like injector nozzles, valve bodies, and fuel rails, and high-speed micro-milling and Electrical Discharge

Machining (EDM) for complex geometries in difficult to machine materials like Inconel and tool steel (Li et al., 2022). Surface finishing processes like polishing, lapping, and coating deposition minimize roughness, enhance flow characteristics, reduce droplet coalescence risk, improve spray uniformity, and extend component lifespan (Wang et al., 2023). Recent advancements in injection molding techniques have enhanced the production of plastic components like connectors, seals, and sensor housings, resulting in tighter dimensional tolerances and improved assembly efficiency (Chen et al., 2021).

Additive manufacturing technologies like Selective Laser Melting (SLM) and Direct Metal Laser Sintering (DMLS) are being used for producing complex, low-volume components with optimized fuel and air distribution, enabling design freedom and exploring full-scale injector production (Gibson et al., 2023). Precision grinding and honing are essential for achieving ultra-fine surface finishes and tight tolerances on sealing and metering surfaces, ensuring atomization consistency in high-pressure fuel systems (Singh & Rao, 2022). Automated assembly stations for air-fuel atomization systems use robotic handling, machine vision, and torque feedback systems for repeatable quality and minimizing error during assembly of air-fuel atomization systems, which require high precision alignment to maintain internal flow paths and spray angles (Zhao et al., 2022). Metrology and inspection have advanced with non-contact optical measurement systems, laser scanning, and computed tomography (CT), enabling dimensional verification of intricate internal geometries and hidden defects, ensuring quality assurance in high-volume production (Yuan et al., 2023). Cleanroom manufacturing environments are used for contamination-sensitive components like injectors and valves, with ISO Class 7 and 8 environments now standard in advanced assembly lines, supported by inline particulate monitoring systems (Whyte & Eaton, 2021).

2.5.1 Manufacturing Process Improvements Accomplished through Research and Development for Air-Fuel Atomization Systems in Automobiles

Advancements in manufacturing technologies have revolutionized air-fuel atomization components, enhancing precision, miniaturization, and reliability in ICE systems. Metal additive manufacturing techniques like Selective Laser Melting and Direct Metal Laser Sintering support complex injector nozzles and fuel metering components, reducing lead time for prototyping and small-batch production (Gibson et al., 2023; Karimian et al., 2022). Ultra-precision grinding and honing technologies enable sub-micron surface finishes and tight tolerances, crucial for consistent atomization in high-pressure injection environments, reducing wear, controlling flow rates, and ensuring long-term injector durability (Singh & Rao, 2022).

Micro-injection molding and multi-material molding advancements enhance plastic component manufacturing, enabling the integration of conductive, chemical-resistant, or heat-tolerant polymers, extending component lifespan and functionality in harsh engine environments (Chen et al., 2021). Automation technologies, such as robotic assembly, machine vision systems, and real-time torque control, have significantly improved assembly process reliability, reducing defect rates, and enhancing system performance (Zhao et al., 2022). Cleanroom manufacturing in high-precision fuel systems is important for reducing particulate contamination, with advancements in inline contamination monitoring and automated cleaning protocols improving process control (Whyte & Eaton, 2021). Research and Development is exploring hybrid manufacturing methods, combining additive manufacturing with subtractive techniques like milling and polishing, to achieve complex internal features and superior surface finishes cost-effectively. (Yuan et al., 2023).

2.5.2 Challenges for Air-Fuel Atomization Systems in Automobiles

Modern automobiles' air-fuel atomization systems face challenges due to stringent emission standards, fuel diversity, and real-world engine dynamics. Global regulatory bodies like Environmental Protection Agency and European Commission (EC) introduce aggressive emission targets, requiring precise spray atomization and air-fuel mixing, which are difficult to control uniformly (IEA, 2023; Zhang et al., 2022). The growing use of alternative fuels like biodiesel, ethanol blends, and hydrogen-diesel dual-fuel systems presents significant challenges to existing atomization system designs due to their varying physical and chemical properties, which alter spray behavior, droplet breakup, evaporation rates, and combustion dynamics (Lapuerta et al., 2021; Manente et al., 2023). Consistent atomization quality across engine operating conditions remains an engineering challenge, causing nozzle clogging, cavitation, and inconsistent spray patterns, which impair combustion efficiency and increase emissions (Shoaib et al., 2022; Kim & Lee, 2023). Minimizing injector wear and ensuring long-term durability are crucial in heavy-duty vehicles, as minor atomization inefficiencies can significantly impact fuel economy and after-treatment system performance (Wang et al., 2023). Original Equipment Manufacturers (OEMs) face challenges in integrating multi-hole and ultra-fine injector designs with advanced control algorithms, requiring high-precision manufacturing and real-time feedback systems, which are complex and costly (Ghosh et al., 2022).

2.5.3 Future Directions for Manufacture of Air-Fuel Atomization Systems for Automobiles

Advancements in digital technologies, materials science, and green propulsion strategies are shaping the future of air-fuel atomization system manufacturing. AI and machine learning

are being integrated into electronic fuel injection control systems, improving efficiency, reducing emissions, and improving fuel economy (Ghosh et al., 2022; Rezaei et al., 2023). Materials engineering is focusing on nanostructured coatings, diamond-like carbon, and ceramic composites for enhanced wear resistance, chemical stability, and compatibility with biofuels and synthetic fuels (Wang et al., 2023; Li & Tan, 2021). The integration of advanced combustion control and exhaust after-treatment technologies, including atomization systems, low-temperature combustion strategies, gasoline compression ignition, and particulate filtration systems, is a key direction (Zhang et al., 2022; D'Errico et al., 2023). Digital twins, AI models, and CFD driven simulation platforms are accelerating atomization system design and testing, reducing reliance on expensive time consuming experimental campaigns and enabling simulations of various engine conditions (Mostafa et al., 2023). Additive manufacturing (AM) is expected to revolutionize mass customization of injector geometries for engine types and fuels, facilitating rapid prototyping, faster innovation cycles, and on-demand part production (Gibson et al., 2023).

2.6 Simulations for Air-Fuel Atomization for Automobile Engines

Advanced computational simulations, particularly Computational Fluid Dynamics (CFD), have become very necessary for analysing and optimizing air-fuel atomization systems in internal combustion engines. These tools evaluate spray structure, droplet behavior, evaporation, and combustion efficiency without experimental testing (Mostafa et al., 2023; Kim et al., 2022). Volume of Fluid and Level-Set methods are commonly used to simulate fuel-air interface during injection, capturing surface tension effects and spray cone dynamics (Gupta & Mallick, 2021). Lagrangian-Eulerian approaches are widely used to study the motion and interaction of individual droplets post-breakup, modeling droplet trajectories,

size distribution, evaporation, and coalescence within Eulerian frameworks (Wang et al., 2023).

Transient simulations help optimize injection timing, pressure, and spray angle for engine load conditions, while multiphase flow models like Eulerian-Eulerian and Eulerian-Lagrangian hybrid schemes simulate interfacial momentum and energy exchanges (Zhao et al., 2022). Recent research focuses on integrating empirical droplet breakup models and turbulent dispersion models to predict Sauter Mean Diameter and droplet distribution across the spray plume (Alizadeh et al., 2021). Heat transfer modeling within simulations has also improved, with advanced equations now accounting for convection, conduction, and radiation between droplets, ambient gases, and cylinder walls greatly impacting evaporation and combustion predictions (Singh & Verma, 2021). Simulation validation is a key research area, utilizing optical diagnostics like c, and high-speed Schlieren imaging to validate simulation results, coupled with sensitivity analysis and uncertainty quantification to enhance model robustness and predictive accuracy (Iqbal et al., 2024).

2.7 Conventional Diesel Combustion Conceptual Model of a Diesel Engine

An accurate conceptual model, or phenomenological description, helps explain the relevant processes, interpret experimental data, and provide guidance for the numerical model development (Haohan, 2021). Dec, (1997) derived phenomenological, or conceptual model, of how direct injection (DI) diesel combustion occurs from laser-sheet imaging and other optical data. The depicted model gives insights into most likely mechanisms for soot formation and destruction and NO formation during the portion of the DI diesel combustion event discussed. Diesel combustion is a complex, turbulent, three-dimensional, multiphase

process that occurs in a high-temperature and high-pressure environment. The basic concept of spray combustion is shown in Figure 2.1. It has about zones of varying fuel-air mixture from centre to edge of the spray

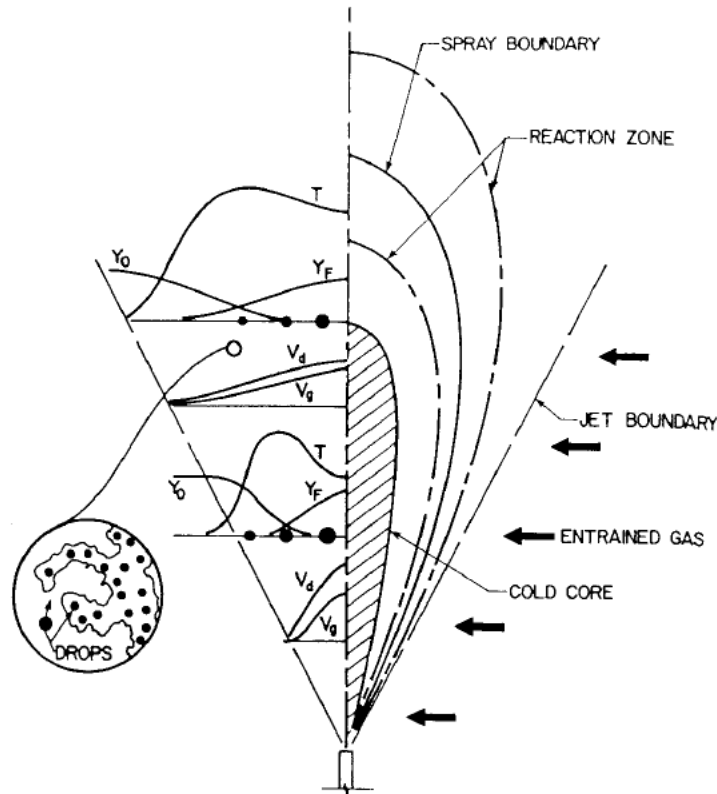


Figure 2.1. Schematic representation of a coaxial spray diffusion flame.

Figure 2.1 indicates a flame sheet around a group of droplets, Dec also considerable discussion to individual droplet combustion. Diesel mixture formation in terms of regions around individual fuel droplets that contain a flammable mixture implies that combustion occurs around the individual droplets. The general spray combustion picture shown in Figure 2.1 is logical for the quasi-steady portion of diesel combustion. It fits for most of the limited data available at the time and as the best available description of DI diesel combustion, it is

widely applied in discussions and in the thinking of engine designers and researchers (Haohan, 2021).

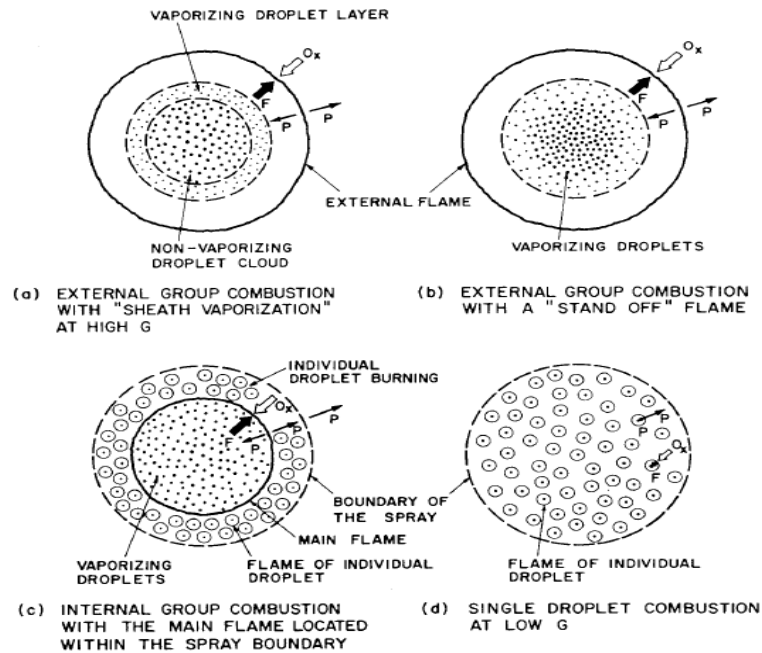


Figure 2.2. Four groups of combustion modes of a droplet cloud.

The various combustion modes in Figure 2.2 and Figure 2.3 relate to spray combustion respectively and are useful for dense sprays including those in diesel engines.

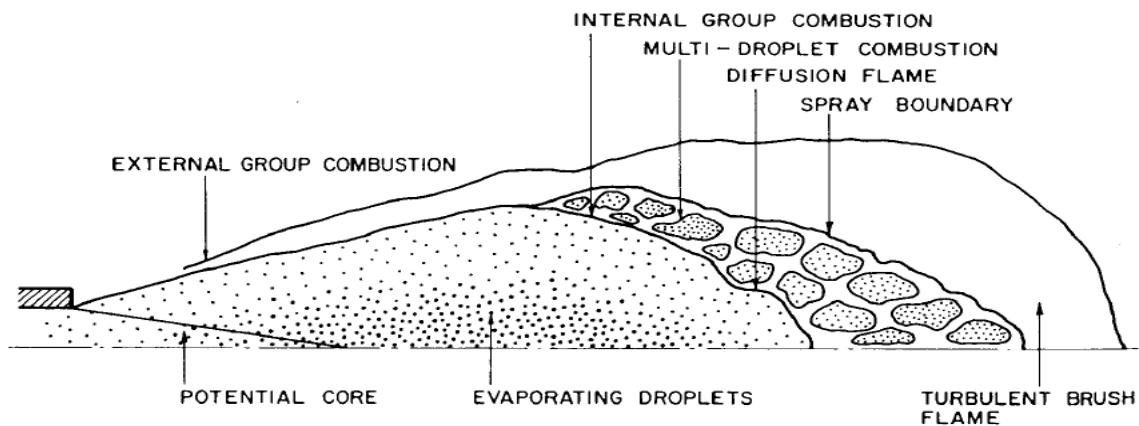


Figure 2.3 Schematic of group combustion for a liquid-fuel spray.

The spray-flame theory from which the original diesel combustion description deals mainly with fuel vaporization, mixing, and combustion zones, and it is not specific as to the location of soot formation. Since soot formation results from fuel pyrolysis at temperatures above about 1300K, mixing with the hot (1000 K) in-cylinder air is not sufficient to induce soot formation, and combustion heating required. Therefore, during the quasi-steady portion of diesel combustion, it is generally assumed that soot would form on the fuel-rich side of the diffusion flame where the temperatures were sufficiently high. The initial premixed burn is not considered to be an important source of soot production since it was thought occur in regions that were nearly stoichiometric, primarily around the jet periphery (Dec, 1997).

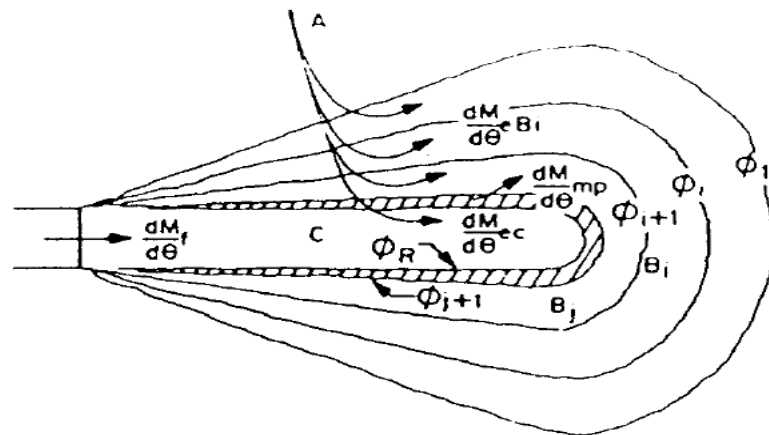


Figure 2.4. Schematic representation of combustion zones and entrainment rates for a transient spray mixing model of diesel combustion.

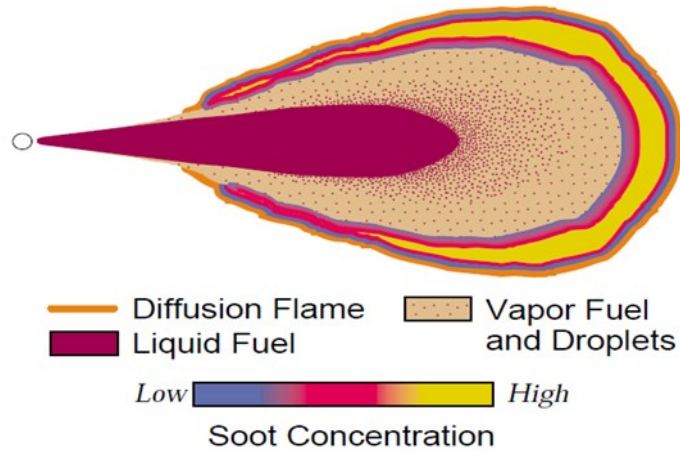


Figure 2.5. General schematic of the “old” view of diesel combustion, showing a slice through the mid-plane of reacting jet.

A general schematic of the old view quasi-steady portion of DI diesel combustion is presented in Figure 2.5. This schematic is a representation of general concepts applied by the diesel community, but cannot be exact due to uncertainty and the need for further research. It shows a slice through the mid plane of combustion diesel fuel, with dense fuel droplets and disperse vaporizing droplets and vapor fuel (*Dec, 1997*).

Diesel combustion involves a diffusion flame around the jet periphery, where fuel and air meet. This flame forms as a continuous sheet, with soot forming on the fuel-rich side. In droplet combustion, less fuel is vaporized before the flame zone, resulting in numerous small flamelets surrounding individual droplets. Soot formation occurs around each droplet within the diffusion flamelets. The old description of diesel combustion has three key characteristics: liquid-phase fuel penetrates well out from the injector, combustion occurs as a diffusion flame, and soot mainly occurs in a shell-like region (*Dec, 1997*).

Dec, (1997) proposed a conceptual model for conventional diesel combustion¹ based on different optical techniques (listed in Table 2.1). These measurements include liquid-phase penetration, vapour-fuel/air mixture ratio, auto ignition, and soot formation (Haohan, 2021).

Table 2.1 Optical Technique Used by Dec

Measured Parameter	Optical Technique
Liquid fuel penetration	Elastic-scatter
Equivalence ratio	Planar laser Rayleigh scatter (PLRS)
Auto-ignition location	Chemiluminescence
Poly-aromatic hydrocarbon	Planer laser-induced fluorescent (PLIF)
Soot concentration	Laser-induced incandescence (LII)
Soot particle size	Elastic-scatter
Diffusion combustion zone	OH radical PLIF

2.8 Summary of Previous Research Work and Gaps

2.8.1 Literature Summary

Several researchers have contributed to the understanding of air-fuel atomization and combustion in diesel engines through both experimental and simulation-based studies. Table 2.2 summarizes notable recent contributions. Daimler Truck AG, (2022) shows that Mercedes-Benz heavy-duty engines since 2018 combine higher-efficiency combustion, turbocharging, friction reduction, and dual-SCR for stronger performance, reduced fuel use, and consistently low on-road NO_x under Euro VIe standards.

Table 2.2 Summary of the notable recent studies done

Researcher	Focus of Study	Engine Model	Key limitation Identified
Zhang et al. (2022)	Nozzle geometry and injection pressure optimization	Volvo D13C	Lacked focus on mid-duty AFR conditions common in Africa

Chen & Liu (2023)	High-pressure injection effects on CO and NO _x	Navistar MaxxForce 13	No linkage to specific Euro III engine classes
Park et al. (2021)	Combustion efficiency in CRDI diesel engines	Cummins ISX12G	Did not include simulation-based validation
Payri et al. (2021)	Atomization influence on PM formation	Generic single-cylinder rig	Limited to lab-scale testing, not commercial trucks
Musa et al. (2023)	Atomization and emissions under African diesel fuel standards	None specified	Simulation model was not benchmarked with OEM data

2.8.2 Research Gaps

While advancements in air-fuel atomization technology exist, their direct impact on the performance and emissions of heavy-duty truck engines like the Mercedes-Benz Actros Engine Model 3340-LS remains inadequately explored. The intricate relationship between air-fuel atomization parameters (e.g. nozzle design, injection pressure) and engine performance metrics lacks comprehensive investigation, particularly in the context of heavy-duty engines. Despite sophisticated design features in engines like the Mercedes Benz Actros 3340-LS, the optimization of air-fuel atomization to balance performance and emissions effectively is not well-understood. Many prior studies generalized results without simulating actual engine platforms like the Actros 3340-LS. This research specifically models that engine using Ricardo Wave. Most studies focus on Euro VI or laboratory-scale engines. The current study addresses real-world emission challenges in widely-used Euro III trucks in Africa. Few studies validate simulation results against published experimental data. This study cross-validates BSFC, torque, SMD, and emissions with findings from Cummins, Volvo, and Navistar diesel engines. The study fills a gap in literature regarding engine behavior under high-load poor-fuel-quality conditions typical of African road environments.

CHAPTER THREE: METHODOLOGY

3.1 Introduction

The purpose of this chapter is to detail the steps and approaches used in analyzing the impact of air-fuel atomization on engine performance and emissions. Mercedes Benz Actros model 3340-LS was used in the development of the simulation geometry. Ricardo wave is an industry standard 1- dimensional engine performance simulation software. Ricardo wave is used worldwide in engine industries and enables automotive manufacturers to perform engine performance simulation on intake, combustion and exhaust system configuration. For the basic engine only minimal information is required i.e. Bore, stroke, connecting rod length, wrist pin offset, compression ratio, firing order and timing.

3.2 Research Design

3.2.1 Overview of Simulation

Ricardo Wave is a CFD simulation software that optimizes engine and fluid systems, offering cost savings, faster iteration of design variables, and comprehensive analysis of intake, combustion, exhaust, and after-treatment systems. It provides detailed insights into engine dynamics, emissions prediction, early-stage development, optimization, safety, and compatibility with 3D CFD tools. Ricardo Wave also integrates with optimization tools to refine multiple engine parameters simultaneously, eliminating risks associated with experiments.

3.2.2 Description of Mercedes Benz actros-3340-LS Engine Model

The main purpose was to characterize the design parameters of Mercedes-Benz Actros 3340-LS Engine Model in relation to its structural and operational framework. Mercedes Benz

Actros was chosen because it is one of the most recent heavy duty diesel engine models manufactured by the Mercedes Benz company (2011-2024 Model), it is used here in Uganda and world over. That means its technology is not obsolete. The engine model parameters were characterized to replicate what exactly happens in the engine. This helped in realization of the first specific objective. Mercedes-Benz engines model 3340-LS is specifically designed for use in Mercedes-Benz diesel trucks. The block utilizes a cast iron parent bore design which is induction-hardened at the top for extra strength around the combustion chamber. The combustion process for the engine is a four stroke diesel system incorporating high-pressure direct injection nozzles and pumps.

Aluminium pistons are used to minimize weight. Forged connecting rods and crankshaft hold the pistons in place. The integrated oil cooler helps keep all of this lubricated and cool during operation. The cylinder heads on the Mercedes-Benz engine are cast iron and include two inlet and two exhaust valves on each cylinder. A constant throttle exhaust brake valve is also incorporated into the cylinder head. A single turbocharger drives the air intake system for optimum power (By increasing the density of air inlet). Diesel fuel used was of Cetane number 48, density of 830 Kg/m^3 , and 0.05% Sulphur content. Diesel fuel must have a density at $20 \text{ }^\circ\text{C}$ in Kg/m^3 of between 820-870 as per Uganda National Bureau of Standard (UNBS) requirements. Must also have Cetane index of 48 minimum and Sulphur content of 0.05% maximum. The fuel injection system comprised of a Unit Pump System (UPS), which helps in fuel mixture formation, a direct Injection via unit injectors of 6-holes nozzles. This particular type of fuel injection i.e. Multi-hole injector with small-diameter orifices promotes mixture homogeneity (A homogenous mixture is that mixture in which the components mix

with each other and its composition is uniform throughout the solution). The engine specifications used included the following as tabulated in table 3.1.

Table 3.1. Specifications for Mercedes Benz model 3340-LS, (Benz, 2015).

Item	Specification
Engine Model Series	Mercedes Benz Actros 3340-LS, (2011-2024)
Engine Type	Four Stroke cycle - 6 cylinder In-line
Bore (mm)	130
Stroke (mm)	150
Connecting Rod Length (mm)	273
Engine Capacity (cc or cm ³)	11,950
Compression Ratio	17.75:1
Engine dry weight (kg)	940
Gross Vehicle Weight (tons) I.e. 7 t + 2x13 t	33
Maximum Power output (kW) @ 1800 rpm	294
Horse Power (hp)	394, Maximum is 400
Displacement (Ltr)	12.8
Maximum Torque (Nm) @ 1080 rpm	1900
Fuel Injection Type	Direct Injection via unit injectors
Injection Nozzle Type	6-hole injection nozzle, hole dia 0.194mm Simulations run between 0.194 mm – 0.278mm
Injection Pressure (Bar)	Up to 1800
Inlet and Exhaust lift	0.4 mm
Fuel Mixture Formation	Unit Pump System (UPS)
Cylinder arrangement	6-In-line
Ignition pressure	170 bars
Valve Technology	4-Valve Technology (2-Inlet & 2-Outlet)

Axil Configuration	6x4
Cooling	Water cooled with an electromagnetic fan
Exhaust	Stainless steel with SCR catalytic converter
Engine Brake	Brake flap & decomposition valve
Control (Engine Management)	Electronic Telligent engine management system
Emission Standard	Euro III Version
Fuel Type	Diesel of density 830 kg/m ³ , Cetane No. 48, Sulphur Content 0.05%
Combustion chamber diameter (mm)	98.8 Bowl type
Fuel Injection for low load	11.5 ⁰ C BTDC
Fuel Injection for high load	9.5 ⁰ C BTDC
Crank Radius (mm)	75
Firing order	1-5-3-6-2-4
AFR	14.5

3.3 Setup of the Ricardo Wave Engine Model and Simulation

3.3.1 Model Configuration

Mercedes Benz Actros 3340-LS engine model was recreated using Ricardo Wave software as shown in Figure 3.1 and Figure 3.2 using the engine parameters in Table 3.1. Typical information needed for the main model was: Engine cylinder geometry like bore and stroke diameter, Clearance height, connecting rod length, number of intake and exhaust valves. Boundary Conditions like, inlet and exhaust valve temperature, piston temperature, cylinder head and liner temperature. Engine block design like, engine shape, mixture type, number of cylinders, strokes per cycle. Operating parameter like, engine speed, Injector nozzle hole diameter, injection pressure, air fuel ratio among others. Injector type, spray angle, start of injection, injection duration. Sub models included: combustion model, DI combustion model,

and the DI emission model. Tools used included; ambient elements, engine cylinder elements, engine block elements, duct elements, Y-Junction elements, valve elements, injector elements and these were assembled together using their flow direction connectors. These elements were all got from the element library and assembled in the wave canvas as shown in Figure 3.1 and it involved the following step:

- i. Starting wave build: setting general parameters, and creating a simulation/model title:
In this step Wave Build was opened and established some preliminary settings that were important for every simulation.
- ii. Building the flow network on the wave build canvas: In this step the ambient elements, ducts, Y-Junctions, and other elements entities that were required for the multi cylinder model on the Wave Build canvas were laid. These were selected from the wave library, from the flow elements section. These elements were then connected according to the design flow
- iii. Defining ambients, ducts, and orifices: In this step all the elements on the Wave Build canvas were individually selected and their geometric values and initial/boundary conditions defined.
- iv. Defining the Engine: In this step all the required geometry and operation data for the engine were input. It consisted of all engine cylinders represented on the Wave Build canvas and physical sub-models for combustion, friction, heat transfer, etc.
- v. Defining the Intake and Exhaust Valves: In this step the intake and exhaust valves were defined by specifying their lift behavior and flow restriction behavior.
- vi. Adding the Fuel Injector: In this step a fuel injector was added, connected to the engine cylinder, and defined the required input parameters. After adding all the flow elements, design geometry, and operating parameters, the model was ready to be run

and simulated. Below is an overview of how a Ricardo wave build interface looks like in figure 3.1:

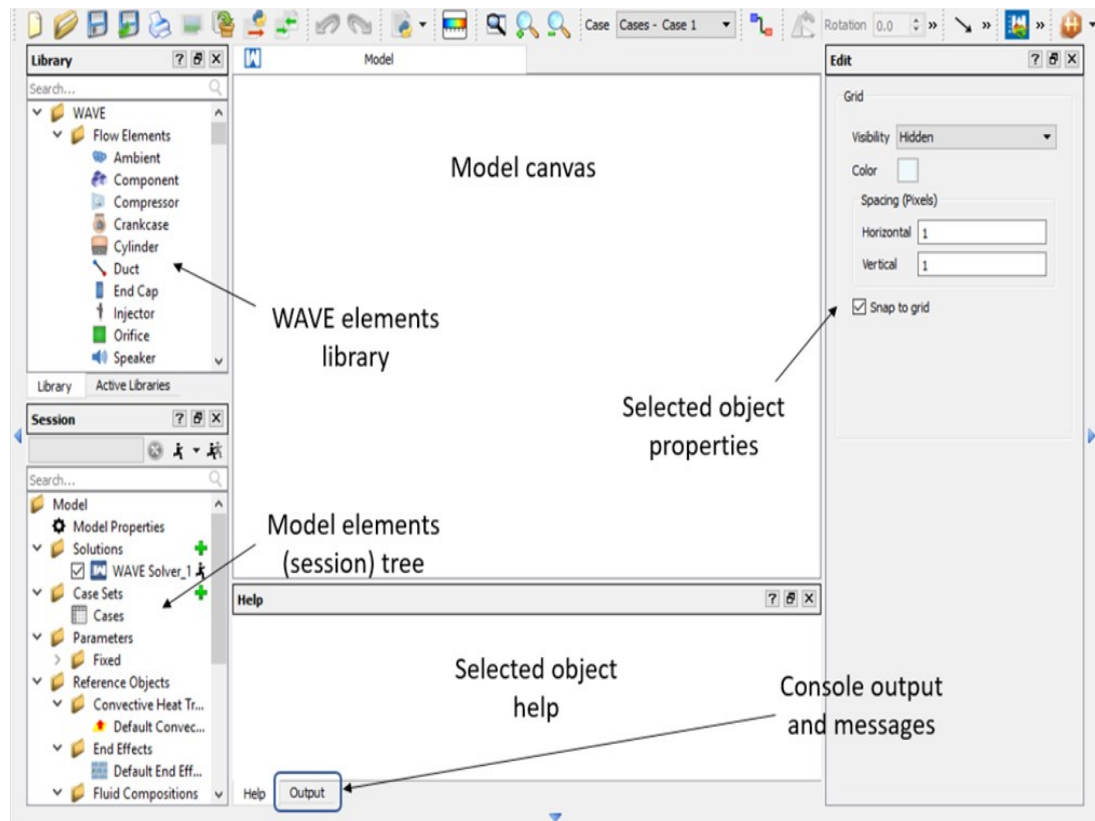


Figure 3.1: Ricardo Wave 2019.1 Build Interface

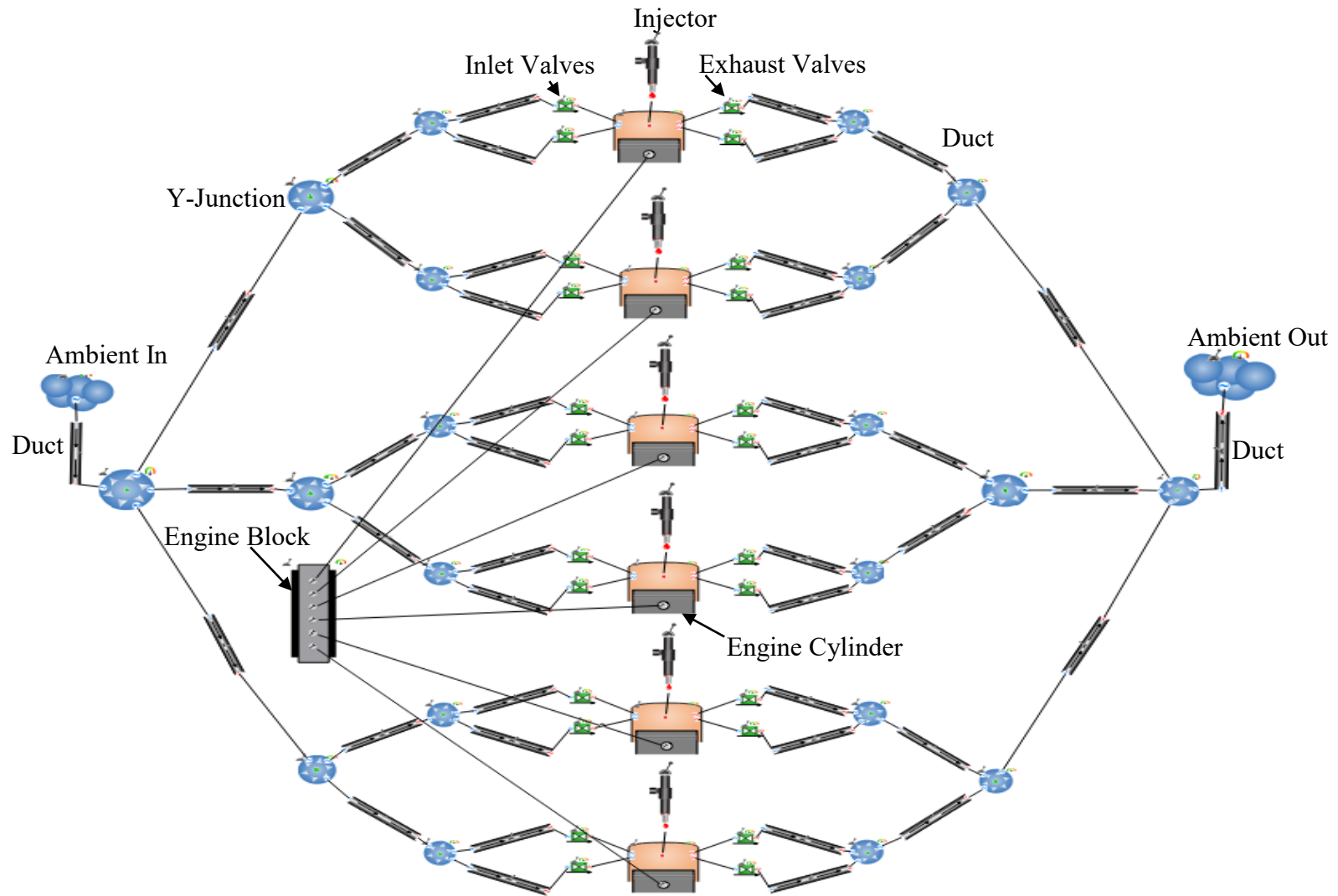


Figure 3.2: Ricardo Wave Mercedes Benz Actros-3340-LS Engine Model Developed

3.3.2 Air-Fuel Atomization Parameters


According to the design of the experiment for simulation, injector nozzle hole diameter, air-fuel ratio, injection rate profile (Crank angle Vs. Injection w Rate), injection pressure profile (Crank angle Vs Injection Pressure), start of injection, Engine Speed, and injection duration were the key parameters chosen and used for simulation as shown in Appendices B2 and E1.



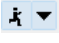


The Sauter Mean Diameter (SMD), Mean fuel drop diameter, Injector Sac Volume, Spray spread angle were set to AUTO in the injection Model to allow for automatic calculation by Ricardo Wave software. The simulation did not allow negative values for the crank angle (The negative crank angle represents crank position before top dead center BTDC, zero represents crank position at TDC, and the positive angles represent crank positions after top dead center ATDC). The injection rate and injection pressure profiles were varied between 0° and 27° of crank position. The injection pressure was varied between 170Bars (which in the design ignition pressure) and 1800bar which is the design maximum pressure for the injector pump. The air-fuel ratio was left constant at 14.5 and the injector nozzle hole diameter was varied between 0.194mm and 2.78mm. Start of injection (soinj) was put at -11.5° as shown in appendix B2.

3.3.3 Development of the Ricardo Wave CFD Simulations

The specific objective two of this research was to develop a Ricardo Wave CFD simulation of the Mercedes-Benz Actros 3340-LS engine model. The main case variable operating parameters for the designed engine model (Mercedes Benz Actros 3340 –LS) were: Engine speed (700rpm – 2500rpm), and injector nozzle hole diameter (0.194mm - 0.278mm). Other variables like injection profile and injection pressure profile were embedded in the different

sub models. Ten cases were selected for the chosen variables to be run in the simulation as shown in Appendix B2.

The number of cycle (NCYC) runs was left at 20, to avoid premature termination of the simulation and improve on the reliability of the results. The developed model was saved as a wvm-file , representing a wave model input file. The outputs of the simulated model included: Performance; Brake Specific Fuel Consumption (BSFC), Volumetric Efficiency (VOLEF), Brake Mean Effective Pressure (BMEP), Indicated Mean Effective Pressure (IMEP), Engine Torque, Engine Brake Power, and Engine cylinder pressure. Emission; nitrogen oxides (NOx), carbon monoxide (CO), hydrocarbons (HC), and particulate matter like SOOT.

After the simulation is run, all the data including the output files is kept or stored as wvd files (wave data files) , all the simulation data for analysis was stored as Sum file  representing summary data file. This stored data could be exported to excel spread sheets for further external data analysis. The simulation was run using the wave solver by clicking on the running man  in the session tree of the wave build. The simulated data was then run in the wave post by clicking on the wave post icon . The wave post interface presenting the wave post engine model was produced, through which further data analysis was made and generation of graphical comparisons of parameters (Parametric analysis) in the wave post file (wps-file) . This file was automatically saved in the same folder where the wvm file was saved. Results were then extracted from the wvd and sum files. The graphical analyses

were made from the wps file. The work flow is represented in the flow chart below in Figure 3.3.

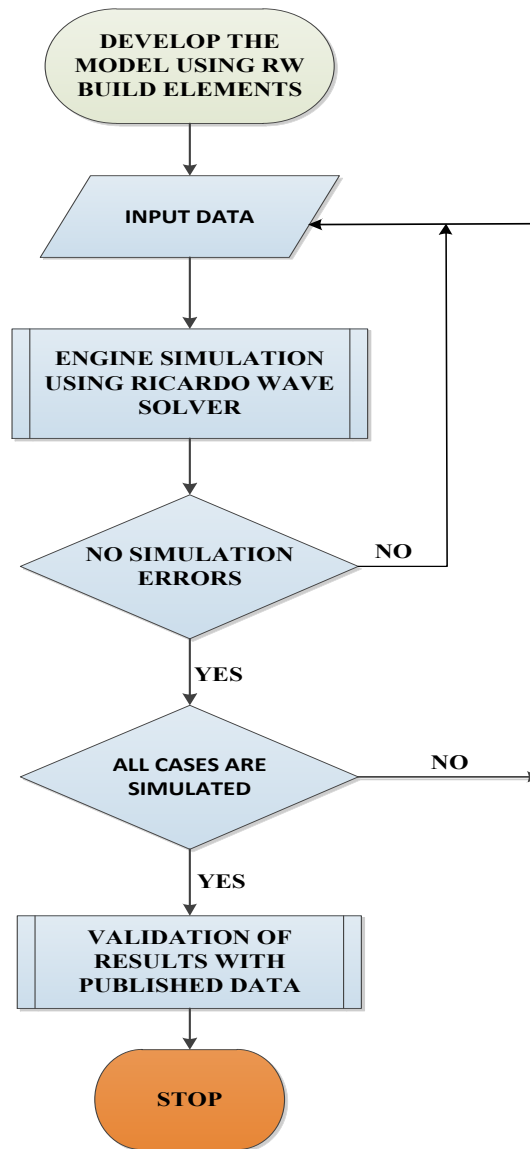


Figure 3.3: Ricardo Wave Mercedes Benz Actros 3340-LS Model Simulation Flow

3.4 Data Collection and Parametric Analysis

The third specific objective was to analyze the impact of injection parameters on the engine performance and exhaust emissions. Performance outputs data that was extracted from the simulation sum and wvd files include: Brake torque, Brake power, Brake-Specific Fuel

Consumption (BSFC), and Volumetric Efficiency. Emission outputs data extracted included nitrogen oxides (NOx), carbon monoxide (CO), hydrocarbons (HC), and particulate matter like Smoke. These were also extracted from the sum and wvd files. The graphical analysis of the results was generated from the wave post model image shown in Figure 3.4 by right clicking on the engine model element image therein and the choosing the parameters for the intended graphical analysis. The Summary data file is shown in Appendix D2.

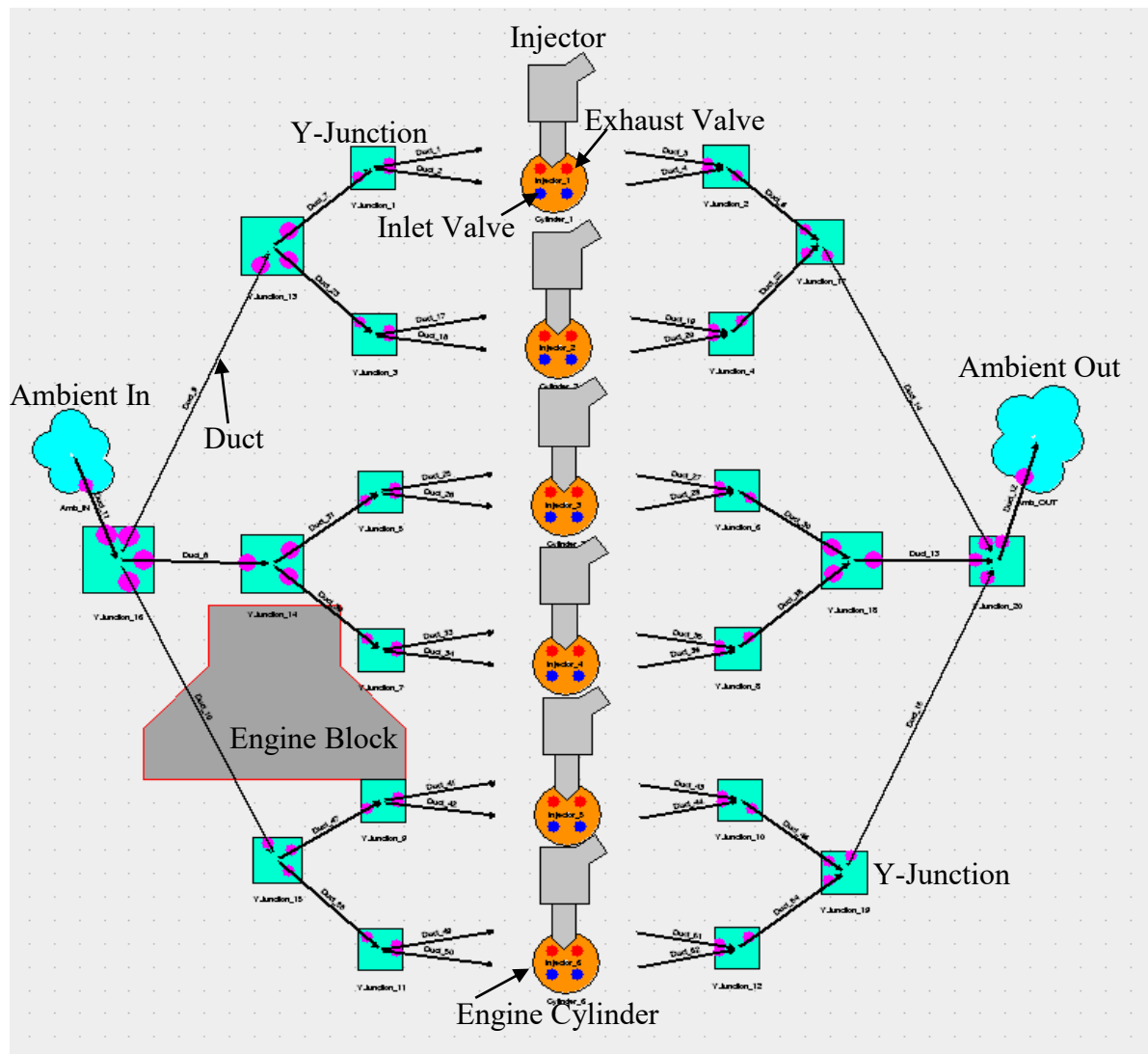


Figure 3.4: Wave post model image for Mercedes Benz Actros-3340-LS

3.5 Validation of the Developed Model

This was done through comparison of the developed model (Mercedes Benz Actros 3340-LS) simulation results and its predictions against experimental results published in the open literature for similar and related engine models of similar or related parameters.

3.7 Why Ricardo Wave Was Used

Ricardo Wave 2019.1 is a reliable software in that, it is used worldwide in engine industries because it offers a cost savings, faster iteration of design variables, and comprehensive analysis of intake, combustion, exhaust, and after-treatment systems. It provides detailed insights into engine dynamics, emissions prediction, early-stage development, optimization, safety, and compatibility with 3D CFD tools. Ricardo Wave eliminates risks associated with experiments, allowing exploration of extreme operating regimes without danger.

3.8 The governing equations behind the simulation software

i) Sauter Mean Diameter (SMD) - Spray sub-model:

$$X_{32} \equiv \text{SMD} = \frac{\sum_i n_i d_i^3}{\sum_i n_i d_i^2} = \frac{6V}{A}$$

Where;

d_i is droplet diameter in bin,

n_i is the count in that bin,

V is the total droplet volume and

A is the total droplet area.

SMD characterizes the surface - to - volume ratio that controls evaporation and combustion.

Empirical correlation form (pressure-atomized diesel spray)

$$\text{SMD} = C_1 d_n \text{We}^{-m} \text{Oh}^n$$

Where; d_n is the injector – nozzle hole diameter,

$$\text{We} = \frac{\rho_g u_{\text{rel}}^2 d_n}{\sigma}$$

Ohnesorge number

$$\text{Oh} = \frac{\mu_\ell}{\sqrt{\rho_\ell \sigma d_n}}$$

and C_1 , m , n from calibration (typical $m \approx 0.5 - 0.6$, $n \approx 0.2$)

ii) **Spray breakup length** (Weber–Reynolds based)

Dimensionless groups

$$\text{We} = \frac{\rho_g u_{\text{rel}}^2 d_n}{\sigma}, \quad \text{Re} = \frac{\rho_\ell u_{\text{rel}} d_n}{\mu_\ell}$$

Empirical breakup-length correlation (round diesel jet)

$$\frac{L_b}{d_n} = C_2 \text{We}^a \text{Re}^b$$

Where;

L_b is the primary breakup length

C_2 , a , and b are fitted to diesel spray data (classically attributed to Hiroyasu/Arai/Dent

families (choose coefficients consistent with the operating range).

iii) Heat-release rate (HRR) - Combustion sub-model

Two complementary routes are standard;

(A) Wiebe function (combustion-law approach)

Mass fraction burned (MFB) over crank angle θ :

$$x_b(\theta) = 1 - \exp \left[-a \left(\frac{\theta - \theta_0}{\Delta\theta} \right)^{m+1} \right]$$

$$\frac{dQ}{d\theta} = Q_{\text{tot}} \frac{a(m+1)}{\Delta\theta} \left(\frac{\theta - \theta_0}{\Delta\theta} \right)^m \exp \left[-a \left(\frac{\theta - \theta_0}{\Delta\theta} \right)^{m+1} \right]$$

Parameters: start of combustion θ_0 , duration $\Delta\theta$, efficiency α (often $\approx 6-7$ for single-Wiebe), and shape factor m (premixed/diffusion split captured with a **double-Wiebe**).

(B) Apparent heat release from first law (from in-cylinder pressure trace)

$$\frac{dQ_{\text{net}}}{d\theta} = \frac{\gamma}{\gamma - 1} p \frac{dV}{d\theta} + \frac{1}{\gamma - 1} V \frac{dp}{d\theta} + \dot{Q}_{\text{chem}} - \dot{Q}_{\text{wall}}$$

For “apparent HRR,” wall heat loss is often estimated, γ is the ratio of specific heats.

iv) Thermal NOx (extended Zeldovich mechanism) - Emissions sub-model

Reactions (forward/backward):

$$\frac{d[\text{NO}]}{dt} = k_{1f}[\text{O}][\text{N}_2] + k_{2f}[\text{N}][\text{O}_2] + k_{3f}[\text{N}][\text{OH}] - k_{1b}[\text{NO}][\text{N}] - k_{2b}[\text{NO}][\text{O}] - k_{3b}[\text{NO}][\text{H}]$$

Each k_{if} , k_{ib} follows **Arrhenius** temperature dependence; thermal NOx is therefore extremely temperature-sensitive.

CHAPTER FOUR: RESULTS, DISCUSSIONS, AND FINDINGS

4.0 Introduction

This chapter presents the results of the simulation study, focusing on the effect of air-fuel atomization on engine performance and exhaust emissions. Key performance parameters including brake power, brake torque, brake specific fuel consumption (BSFC), brake mean effective pressure (BMEP), total volumetric efficiency (VOLEFF), as well as emissions of pollutants like nitrogen oxides (NO_x), Carbon monoxide (CO), hydrocarbons (HC), and particulate matter (PM) like smoke. This chapter presents the results of ten parametric simulation cases graphically using the Ricardo Wave model for the Mercedes-Benz Actros 3340-LS engine. Each case varied injector nozzle diameter (0.194–0.278 mm) and engine speed (700–2500 rpm) at injection pressure of 1800 bar and AFR of 14.5, to study their effect on air-fuel atomization, engine performance, and emissions. The findings of this research provide valuable insights into the complex relationships between air-fuel atomization, engine performance and exhaust emissions, contributing to the development of more efficient and environmentally friendly diesel engines.

4.1 Characterized Design Parameters.

The first specific objective was to characterize the design parameters of Mercedes-Benz Actros 3340-LS Engine Model to in relation to its structural and operational framework. The key design parameters that were got from the manufacturer`s specification and operation manual are shown in appendix E1. and these were the exact parameters used for the development of Ricardo Wave MB Actros 3340-LS engine model and in the design of experiment for running the simulation.

4.2 Developed Ricardo Wave Engine Model

The specific objective two of this research was to develop a Ricardo Wave CFD simulation of the Mercedes-Benz Actros 3340-LS engine model. The simulation aimed to investigate the effect of air-fuel atomization on engine performance and emissions. The engine model that was developed is shown in Appendix B1. Engine speed was set to vary between 700rpm and 2500rpm, and injector nozzle hole diameter was set to vary between 0.194mm and 0.278mm. Other variables like injection pressure profile were embedded in the different sub models. Ten cases were selected for the chosen variables to be run in the simulation as shown in Appendix B2. The number of cycle (NCYC) runs was left at 20, to avoid premature termination of the simulation and improve on the reliability of the results. The above parameters were fed in the design of experiment within the developed engine model that led to the successful running of the simulations.

4.3 Effect of Air-Fuel Atomization on Combustion and Emission Characteristics

The third specific objective was to analyze the impact of injection parameters on the engine performance and exhaust emissions. The simulated model outputs included performance data, emission data, and output files. Data was stored as wave data files and sum files, which could be exported to excel for further analysis. The simulation was run using the wave solver and the wave post interface, generating graphical comparisons of parameters. Results were then extracted and analyzed as explained in this chapter.

4.3.1 Spray Dynamics and SMD Analysis

From the results shown in the graphical representation in Figure 4.3.1 (a), it was observed that the mean fuel droplet diameter also known as the Sauter Mean Diameter (SMD) nearly

remained constant for injector nozzle hole diameters between 0.194 mm and 0.24 mm. After 0.24 mm, the mean fuel droplet diameter increased exponentially, reaching above 2.2×10^{-5} m at 0.278 mm. showing an exponential growth trend. The mean fuel droplet diameter ranged between 1.0×10^{-5} m and 2.25×10^{-5} m.

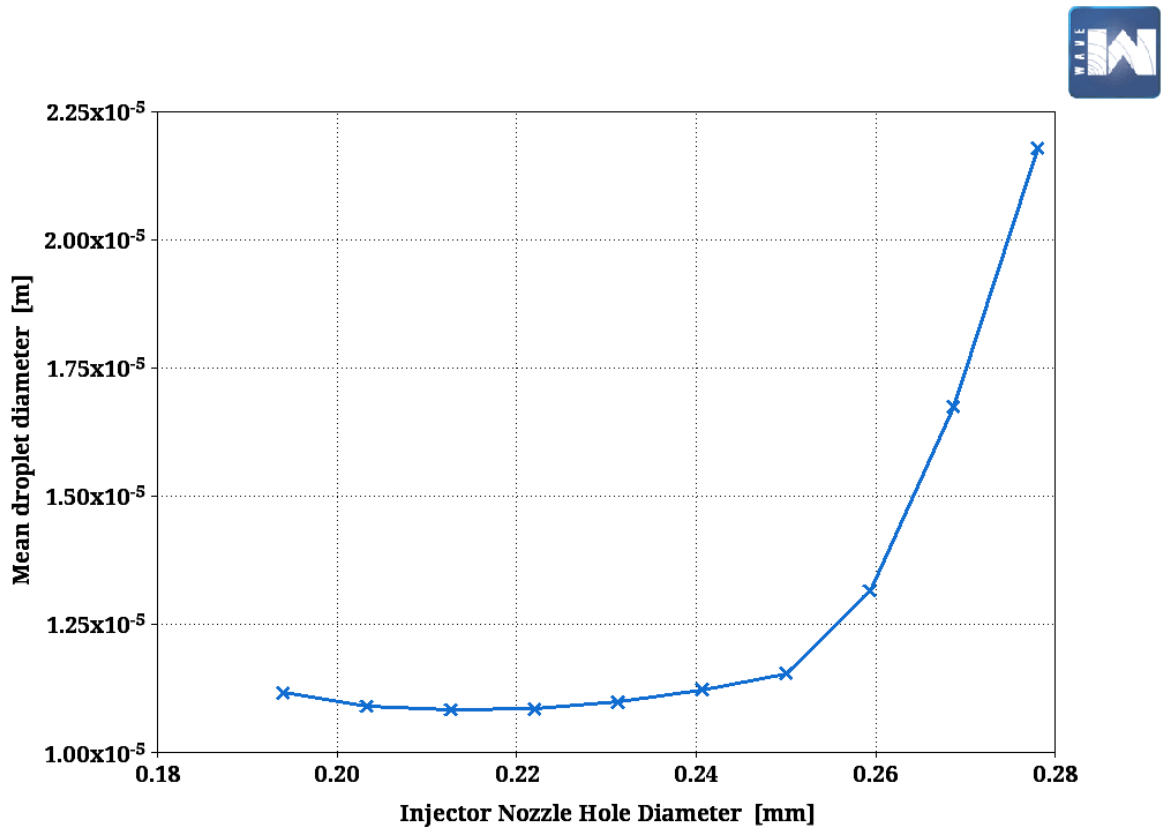


Figure 4.3.1 (a): SMD Vs. Injector Nozzle Hole Diameter Analysis

Interpretation: Smaller injector nozzle holes promote better atomization due to higher injection pressure and reduced flow area. This results in smaller fuel droplet sizes and better air-fuel mixing, which is important for efficient combustion. As the injector nozzle diameter increases, the injection velocity decreases due to reduced injection pressures. This leads to poor atomization, resulting in larger droplets. The transition point around at around 0.24 mm indicates the boundary where atomization efficiency significantly deteriorates, as reflected

in the rapid increase in droplet size. This can directly impact combustion quality, emissions, and engine performance.

Discussions: Smaller fuel droplets facilitate quicker evaporation and mixing with air, leading to efficient combustion and lower smoke and hydrocarbon emissions. Larger droplets reduce the surface area available for evaporation, increasing the likelihood of incomplete combustion, which contributes to higher soot and hydrocarbon (HC) emissions. Smoke emissions increase as droplet size increases (seen at larger injector nozzle diameters). NO_x emissions decrease as fuel droplets increase; as larger droplets lead to lower combustion temperatures. Hydrocarbon emissions rise with larger droplets due to incomplete combustion.

Practical Implications: Injector design manufactures should prioritize; small injector nozzle hole diameter between 0.194 mm and 0.24 mm. Balanced nozzle design, possibly augmented by high injection pressure, multi-hole geometry, or intelligent ECU control, to achieve both performance and emissions targets in heavy-duty diesel engines like the Mercedes Benz Actros 3340-LS.

Validation: Published experimental research was compared with the simulated MB Actros 3340-LS engine model as tabulated in table 4.3.1.

Table 4.3.1 Validation of SMD Results at Varying Nozzle Hole Diameter.

Reference	Engine Model	Key Focus	Key Finding For Comparison with simulation Results
Jadhav & Mallikarjuna (2018)	Gasoline Direct Injection (GDI) engine	Injector Nozzle Hole Diameter	Larger nozzle holes lead to larger droplet size, poor atomization and combustion. This relates well with the simulation results.
(Markov et al., 2022)	MAN D2676LF	Nozzle geometry: atomization & emissions	Smaller nozzle hole diameters lead to smaller fuel droplet diameter, which also leads to improved atomization and reduced CO/HC/PM. This relates well with the simulation results.

Figure 4.3.1 (b) shows how the mean droplet diameter of the injected fuel varies as a function of nozzle hole diameter and engine speed. The mean droplet diameter is very important in determining combustion efficiency, as smaller droplets provide a larger surface area for evaporation and mixing with air, resulting in better combustion.

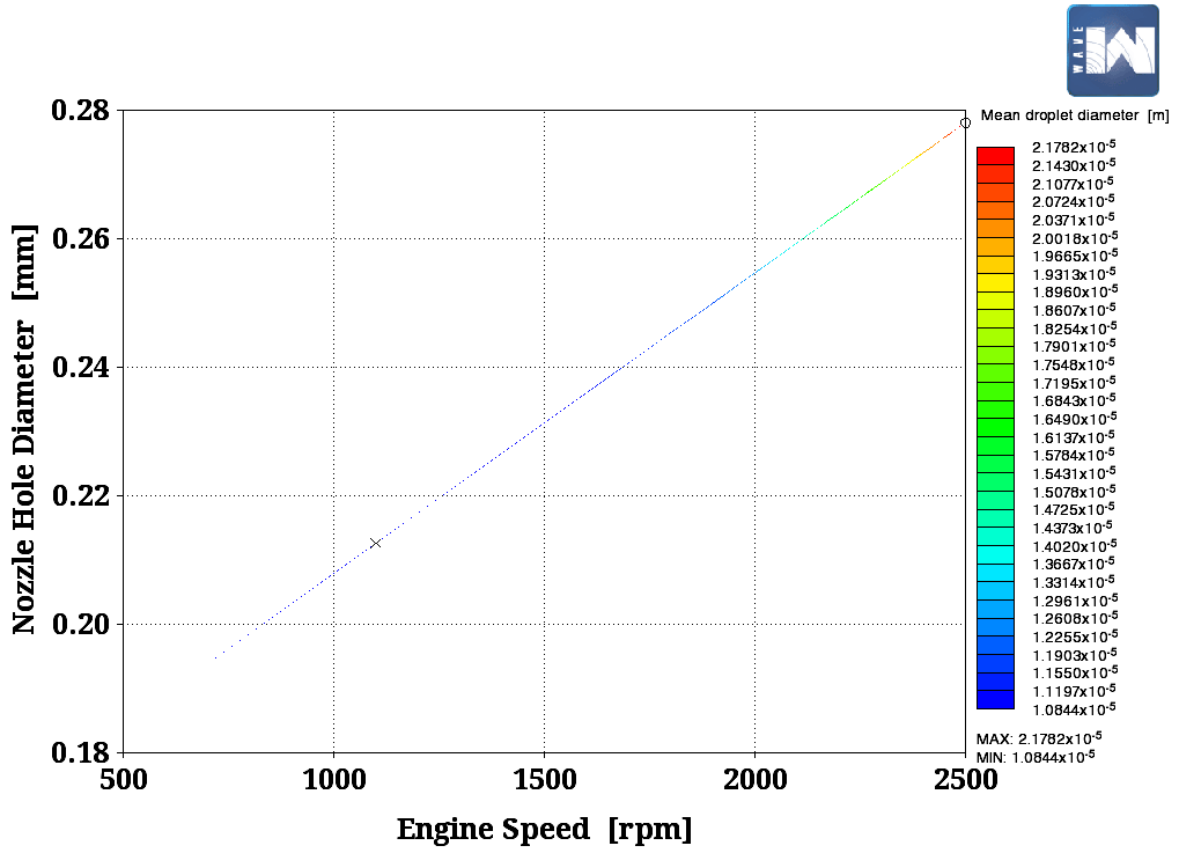


Figure 4.3.1 (b): SMD with varying Speed and Nozzle Hole Diameter Analysis

Observation: At higher engine speeds (e.g. 2500 rpm), the mean droplet diameter increased, reaching maximum values (2.17×10^{-5} m). Lower engine speeds (e.g. 700–1100 rpm) were associated with smaller droplet diameters (1.10×10^{-5} m to 1.35×10^{-5} m). Larger nozzle hole diameters (e.g. 0.26 – 0.28 mm) yielded larger droplet diameters due to reduced fuel atomization and increased mass flow rates. Smaller nozzle hole diameters (e.g. 0.194–0.22 mm) resulted in smaller droplet diameters, indicating better atomization. Blue regions (smaller droplets) were observed at lower engine speeds and smaller injector nozzle hole diameters. Red regions (larger droplets) dominated at higher engine speeds and larger injector nozzle hole diameters. Maximum mean droplet diameter: 2.17×10^{-5} m (at large nozzle

diameter and high speed). Minimum mean droplet diameter: 1.10×10^{-5} m (at small nozzle diameter and low speed).

Interpretation: Smaller injector nozzle hole diameters produce finer sprays due to higher injection pressures and smaller orifice areas. This leads to better fuel-air mixing, improving combustion efficiency and reducing emissions. Larger injector nozzle hole diameters produce coarser sprays, which may lead to incomplete combustion, higher particulate emissions, and potential power loss under some conditions. At higher engine speeds, the injection duration shortens, reducing the residence time for atomization. Combined with increased fuel flow rates, this leads to larger droplets. Lower speeds provide more time for atomization and mixing, resulting in smaller droplet diameters. Smaller droplet diameters (blue regions) are desirable for efficient and complete combustion, especially in high-speed diesel engines. Larger droplets (red regions) can cause unburnt fuel, higher smoke, and soot emissions, but may also produce higher power output in certain cases.

Practical Implications: Advanced fuel injection technologies, such as multi-hole injectors and higher injection pressures, can mitigate the effects of larger nozzle diameters, ensuring optimal atomization. Droplet size optimization plays a critical role in reducing particulate matter and NO_x emissions, which are major concerns for regulatory compliance. While smaller droplet sizes improve efficiency and reduce emissions, larger droplet sizes may be required for certain applications, such as heavy-duty engines, where power density is a priority.

Validation with Published Experimental Research: A study by Chen et al. (2021) found that at higher injection pressures, which simulated higher engine speeds, the spray and atomization characteristics of diesel fuel and its alternatives resulted in larger droplet sizes, affecting combustion efficiency. Experimental results from Zhu et al. (2016) align with the observed trend that smaller droplet sizes improve performance at lower speeds.

4.3.2 Fuel Breakup Length Analysis

Figure 4.3.2 (a) represents breakup length as a function of injector nozzle hole diameter, derived from Ricardo WAVE simulation results.

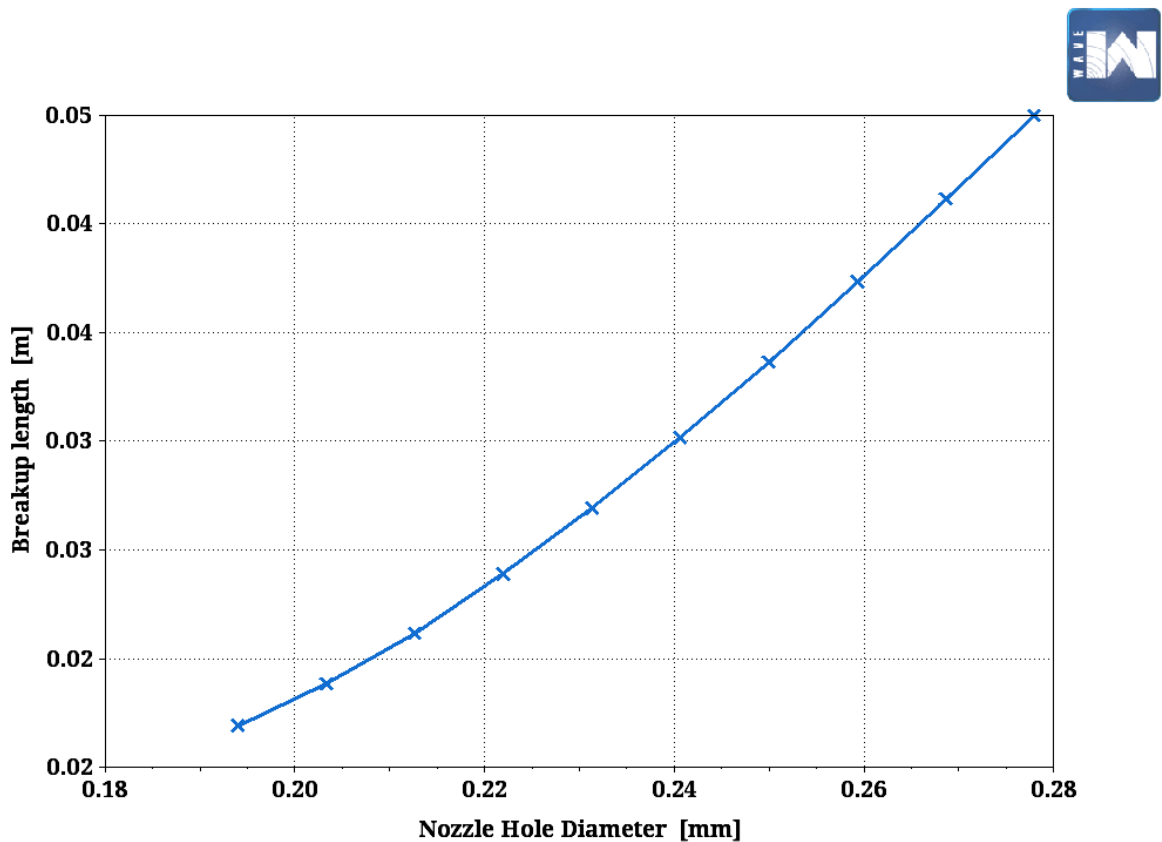


Figure 4.3.2 (a): Breakup Length Vs. Nozzle Hole Diameter Analysis

Observations: The breakup length increased consistently with injector nozzle hole diameter. The relationship appears approximately linear, with a steeper slope for larger injector nozzle hole diameters. For smaller nozzle hole diameters (e.g. 0.194 mm), the breakup length was approximately 0.022 m. For larger nozzle hole diameters (e.g. 0.278 mm), the breakup length reached 0.05 m.

Interpretation: Breakup length refers to the distance from the nozzle tip where the fuel jet transitions from a coherent liquid stream to dispersed droplets due to aerodynamic forces and turbulence. It is a critical parameter influencing spray atomization, combustion efficiency, and pollutant formation. Smaller nozzle hole diameters generate higher injection velocities and increased shear forces at the liquid-air interface. This promotes faster disintegration of the fuel jet, reducing the breakup length. The shorter breakup length corresponds to better atomization and mixing of fuel with air, resulting in more efficient combustion. Larger nozzle hole diameters reduce injection velocities and decrease shear forces, leading to slower jet disintegration and longer breakup lengths. This can negatively affect the spray quality, causing incomplete combustion, higher hydrocarbon (HC), and particulate emissions. Optimizing nozzle hole diameter to maintain a short breakup length is essential for engines requiring fast combustion cycles, such as diesel engines.

Discussions: A shorter breakup length (associated with smaller nozzle holes) ensures fine droplets and better fuel dispersion. A longer breakup length (associated with larger nozzle holes) results in coarser droplets, which may lead to localized rich combustion zones and higher soot emissions. The breakup length trends align with the mean droplet diameter graph: Larger nozzle hole diameters correspond to longer breakup lengths and larger droplet sizes,

indicating poor atomization. It also complements the smoke emissions and hydrocarbon emissions trends: Poor atomization (larger nozzle hole diameters and longer breakup lengths) leads to increased smoke and unburnt hydrocarbon levels. Short breakup lengths are desirable in high-performance engines to ensure efficient air-fuel mixing and faster combustion. For larger nozzle hole diameters, additional measures (e.g. higher injection pressures) might be required to offset the negative effects of longer breakup lengths.

Practical Implications for Engine Design: Selecting smaller injector nozzle hole diameters minimizes breakup length, leading to better atomization and reduced emissions. For applications requiring larger injector nozzle holes, higher injection pressures or advanced nozzle designs (e.g. multi-hole nozzles) can help maintain short breakup lengths. Controlling breakup length through nozzle geometry and injection parameters ensures better air-fuel mixing, improving thermal efficiency and reducing pollutant formation.

Validation with Published Experimental Research: Andsaler et al. (2017) experimentally show that reducing orifice diameter and increasing injection pressure shortens breakup length and reduces droplet size. This directly corroborates simulation results trends. Smaller nozzle hole diameter led to shorter breakup length and larger nozzle hole diameters led to longer breakup length. Lab injector rigs and engine test cells representative of CI injectors in the study. Liu & Su, (2024) show that nozzle hole diameter changes the spray breakup and hence premixing; they note operating regimes where larger orifices can sometimes increase penetration and mixing in lean/part-load conditions but generally increase breakup length if pressure is not raised. They used heavy-duty diesel test cases (relevant to Volvo D13K460/Cummins ISX15/MAN D2676LF class engines) in their study.

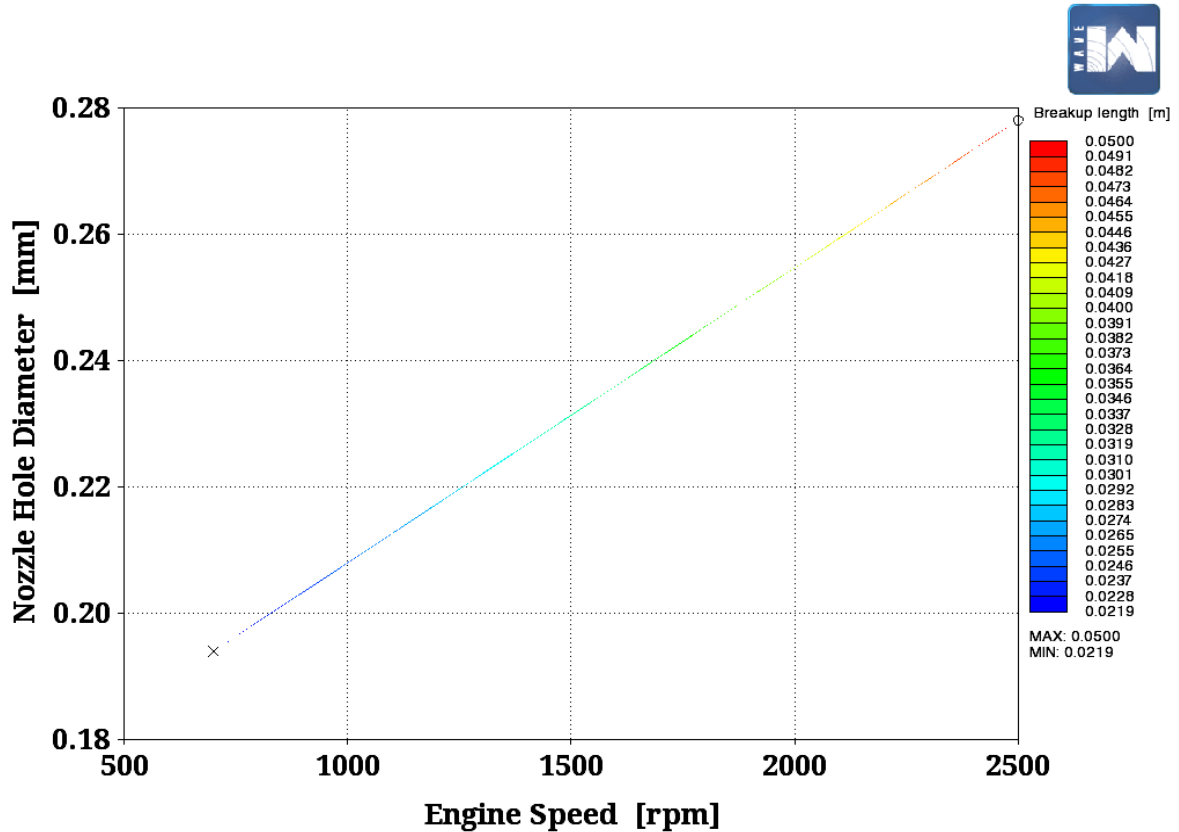


Figure 4.3.2 (b) Breakup Length Vs. Nozzle Hole Diameter and Speed Analysis

Figure 4.3.2 (b) represents the breakup length of the fuel spray in relation to the nozzle hole diameter and engine speed. The breakup length is a critical parameter in fuel injection, indicating the distance from the injector nozzle where the liquid fuel breaks into droplets. It significantly affects atomization, fuel-air mixing, and ultimately combustion efficiency.

Observations: At higher engine speeds (e.g. 2500 rpm), the breakup length increased, reaching maximum values (0.050 m). Lower engine speeds (e.g. 700–1000 rpm) corresponded to shorter breakup lengths (0.0219 m to 0.03 m). Larger nozzle hole diameters (e.g. 0.26–0.28 mm) were associated with longer breakup lengths. This can be attributed to reduced injection pressures and larger droplet formation. Smaller nozzle hole diameters (e.g.

0.19–0.22 mm) resulted in shorter breakup lengths, indicating more efficient atomization. Blue regions (shorter breakup lengths) occurred at smaller nozzle hole diameters and lower engine speeds, indicating better fuel breakup and atomization. Red regions (longer breakup lengths) dominated at larger nozzle hole diameters and higher engine speeds. Maximum breakup length was 0.050 m (at large nozzle diameter and high speed). Minimum breakup length was 0.0219 m (at small nozzle hole diameter and low speed).

Interpretation: Shorter breakup lengths indicate faster atomization and better spray formation. This leads to improved mixing of fuel and air, enhancing combustion efficiency and reducing emissions. Longer breakup lengths suggest delayed atomization, potentially leading to incomplete combustion, higher soot formation, and reduced thermal efficiency. At higher engine speeds, the injection duration decreases, increasing the momentum of the fuel jet. This results in a longer breakup length as the liquid column requires more distance to disintegrate into droplets. At lower speeds, the fuel jet has less momentum, leading to quicker breakup and shorter breakup lengths. Smaller nozzle holes generate higher injection pressures, which promote faster jet disintegration and shorter breakup lengths. Larger nozzle holes reduce injection pressure, leading to longer breakup lengths and potentially coarser sprays. While shorter breakup lengths improve combustion efficiency, they might require higher injection pressures and advanced injector designs, increasing system complexity and cost. Longer breakup lengths may be acceptable in engines designed for low-speed operation or applications prioritizing durability over emissions.

Practical Implications: Manufacturers have to prioritize advanced injector technologies, such as piezoelectric injectors, to achieve higher injection pressures, reducing breakup lengths and enhancing atomization even with larger nozzle hole diameters. Optimizing breakup lengths can significantly reduce particulate matter and NO_x emissions by ensuring better combustion at various engine speeds. Matching nozzle diameter and injection timing to specific engine speeds can optimize performance, balancing power output and fuel efficiency.

Validation with Published Experimental Research: Iqbal et al., (2024) Matches observed droplet diameter increase with larger nozzles; emphasizes breakup length and cone angle as mitigation factors. Andsaler et al. (2017) experimentally shows that reducing orifice diameter and increasing injection pressure shortens breakup length and reduces droplet size. This directly corroborates simulation results trends. Smaller nozzle hole diameter led to shorter breakup length and larger nozzle hole diameters led to longer breakup length. Lab injector rigs and engine test cells representative of CI injectors were used in the study.

4.3.3 Heat Transfer Rate

Figure 4.3.3 illustrates the relationship between nozzle hole diameter (in millimeters) and the heat transfer rate (in watts, W) from a Ricardo WAVE simulation.

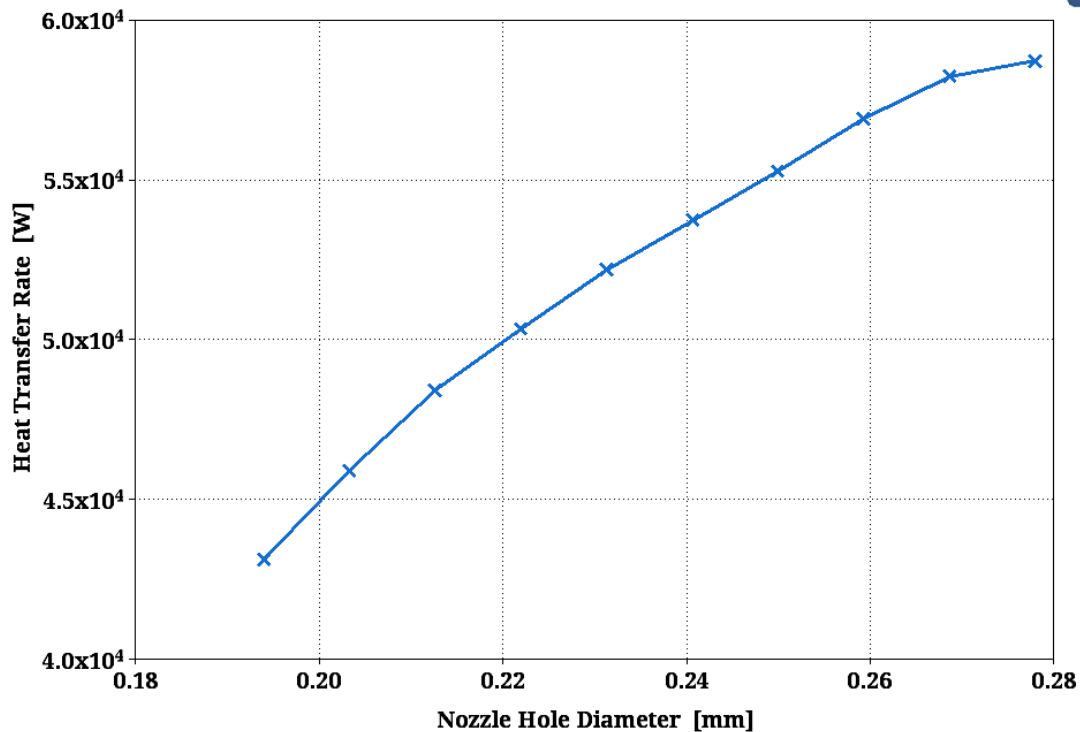


Figure 4.3.3: Heat Transfer Rate Vs. Nozzle Hole Diameter Analysis

Observations: The nozzle hole diameter was varied between 0.18 mm to 0.28 mm. The heat transfer rate increased steadily from approximately 4.33×10^4 W to nearly 5.85×10^4 W as the nozzle hole diameter increased. There was a consistent positive correlation: as the nozzle hole diameter increased, the heat transfer rate also increased.

Interpretations: Larger nozzle holes allow greater fuel flow rates, which could lead to increased combustion energy release. This higher energy release translates to a higher heat transfer rate within the engine. Larger nozzle holes might also result in less efficient atomization, leading to incomplete combustion and heat transfer to the cylinder walls rather than converting energy into useful work. Smaller nozzle holes limit the fuel flow, reducing

the total energy release during combustion. This results in a lower heat transfer rate. While heat transfer increases with larger diameters, it does not necessarily correlate with better engine performance. High heat transfer to the cylinder walls might indicate energy loss, leading to reduced brake mean effective pressure (BMEP).

Discussions: While larger nozzle hole diameters increase the heat transfer rate, they might reduce overall engine efficiency (e.g. lower BMEP and injection velocity). Thus, an optimal nozzle hole diameter (e.g. 0.203 mm) balances heat transfer with efficiency and performance. Higher heat transfer rates necessitate better cooling system design to manage thermal loads and prevent overheating. Engines operating with larger nozzle hole diameters must ensure adequate cooling to maintain reliability. The increasing trend in heat transfer with larger nozzle holes suggests a portion of the combustion energy is not effectively converted into mechanical work but is instead lost as heat.

Practical Implications: Additional analysis on the impact of injection pressure, air-fuel mixture quality, fuel properties, engine load and combustion chamber design can provide insights into reducing energy losses while maintaining performance. These should be considered in real-world applications. Designers must optimize nozzle diameter to achieve a balance between heat transfer, combustion efficiency, and engine cooling requirements.

Validation with Published Experimental Research: Payri et al. (2020) demonstrated that nozzle size directly affects spray atomization quality, which in turn alters ignition delay, premixed combustion fraction, and overall heat release dynamics in diesel engines. Similarly, Tzanetakis et al. (2022) found that changes in nozzle geometry influence the balance between

in-cylinder heat transfer and thermal efficiency. Larger nozzle diameters, while potentially increasing heat transfer to the cylinder walls, can also lead to higher energy losses and reduced brake thermal efficiency. These outcomes align with the simulation results.

4.4 Engine Performance Analysis

4.4.1 Brake Torque and Power

Brake Power:

Figure 4.4.1 (a) displays the relationship between brake power (in kW) and injector nozzle hole diameter (in mm) derived from Ricardo WAVE simulation.

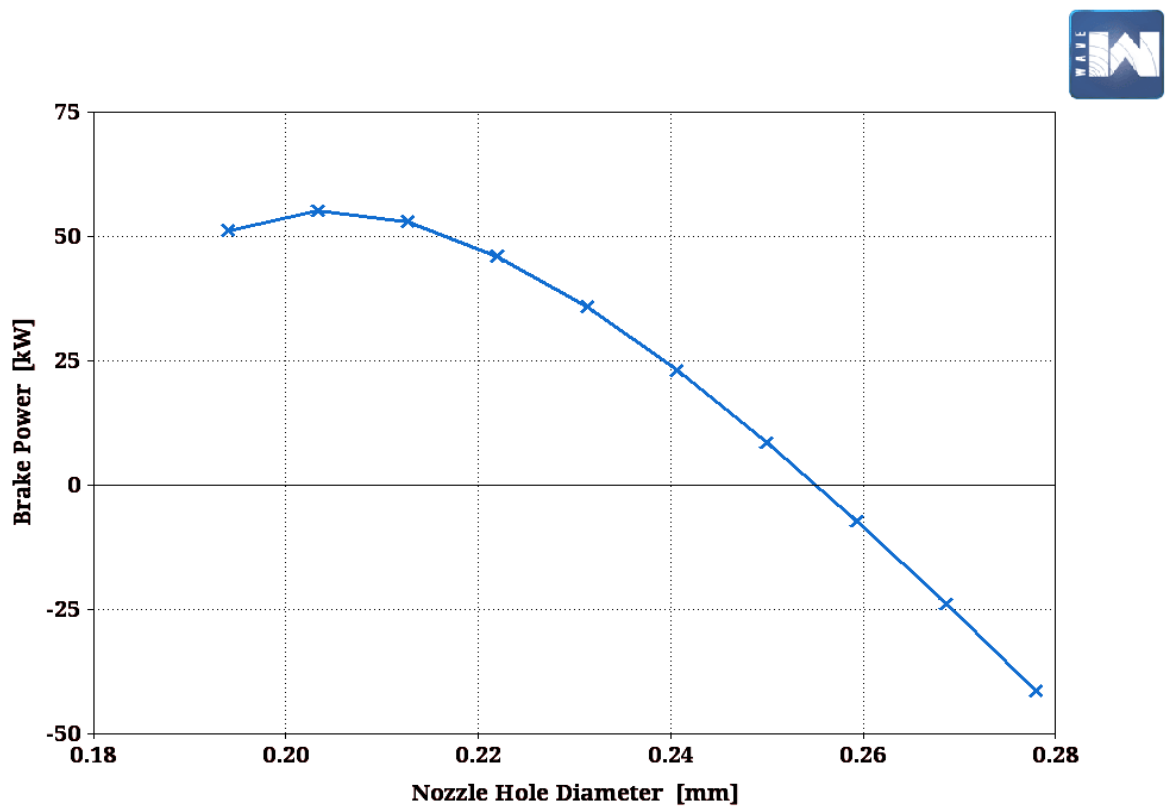


Figure 4.4.1 (a): Brake Power Vs. Nozzle Hole Diameter Analysis

Observations: Peak Brake Power was 56.25 kW at a nozzle diameter of 0.203 mm. Beyond peak, brake power decreased significantly as nozzle diameter increased beyond 0.203 mm, eventually dropping below zero at diameters above 0.26 mm. The chart focused on nozzle diameters between 0.19 mm and 0.28 mm, which are common in diesel fuel injectors.

Interpretation: Smaller nozzle hole diameters facilitate fine atomization and uniform air-fuel mixture, enhancing combustion efficiency and resulting in higher brake power. This explains the peak observed at 0.203 mm. As the nozzle diameter increases, atomization quality diminishes. This leads to inefficient combustion, incomplete fuel burning, and reduced energy conversion to brake power. Larger nozzle hole diameters also result in higher fuel injection rates, which may oversaturate the combustion chamber, further reducing efficiency.

Discussions: Smaller Nozzle hole diameters ensure better atomization but might require higher injection pressures to maintain adequate flow rates. While larger nozzles reduce injection pressure requirements, they compromise on combustion quality and engine efficiency. The observed trends are likely sensitive to engine load, speed, and fuel properties. These conditions must be optimized alongside nozzle hole diameter for real-world applications. As observed in the heat transfer graph, larger diameters result in higher heat transfer rates. This additional thermal energy loss contributes to the decline in brake power for larger nozzle diameters. For heavy-duty engines like the Mercedes-Benz Actros 3340 LS, optimizing injector nozzle hole diameter around the peak brake power region ensures better fuel efficiency and performance while minimizing emissions and energy losses.

Practical Implications: Additional factors such as injection pressure, fuel type, and combustion chamber design could be studied to further refine the optimal nozzle diameter.

Validation with Published Experimental Research: Recent experimental studies corroborate the finding that nozzle hole diameters between 0.19 mm and 0.22 mm produce optimal brake power in diesel engines. Tzanetakis et al. (2022) demonstrated that smaller orifice diameters within this range enhance atomization, improve air–fuel mixing, and accelerate combustion, resulting in higher brake power output in heavy-duty common-rail diesel engines. Similarly, Payri et al. (2020) reported that increasing nozzle hole diameter beyond the optimal range leads to coarser sprays, longer liquid penetration lengths, and incomplete combustion, which directly reduces brake power. The observed decline in performance with larger nozzle diameters in the present study is consistent with these findings and is attributed to reduced combustion efficiency and higher mechanical and thermal losses.

Brake Torque:

Figure 4.4.1 (b) illustrates the relationship between nozzle hole diameter (in millimeters) and brake torque (in Newton-meters, Nm) based on Ricardo WAVE simulation results.

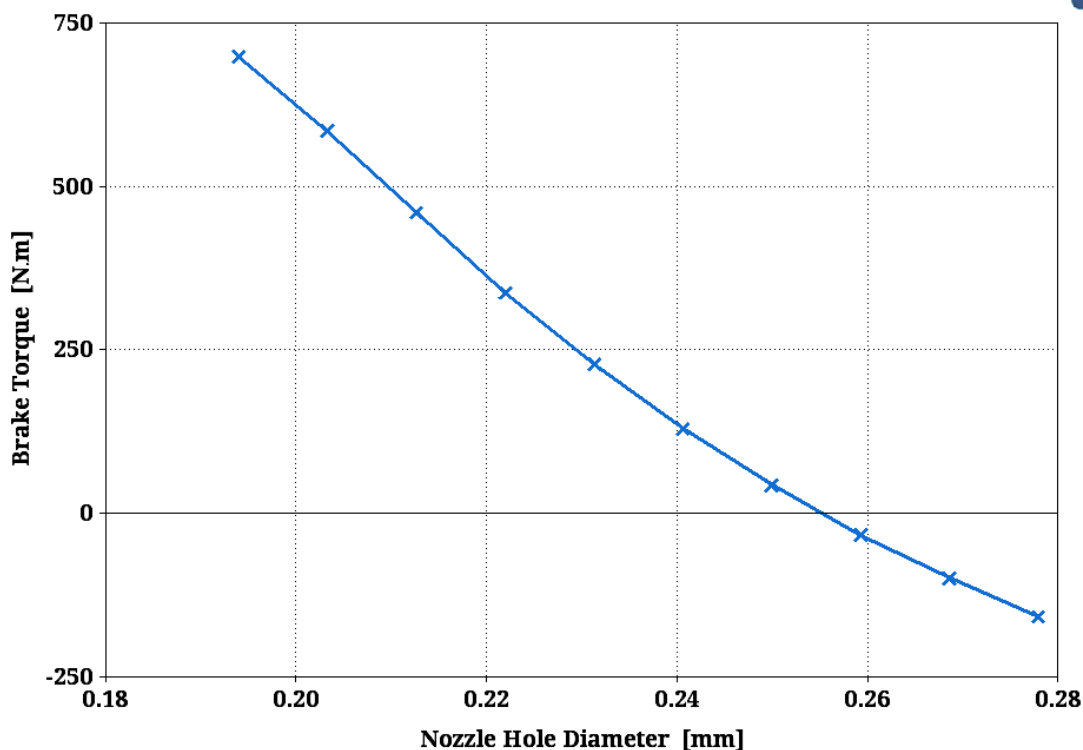


Figure 4.4.1 (b): Brake Torque Vs. Nozzle Hole Diameter Analysis

Observations: Brake torque started high (700 Nm) at smaller nozzle diameters (0.194 mm). It decreased steadily as the nozzle hole diameter increased, eventually dropping below zero at larger diameters (0.259 mm). A clear inverse relationship exists between nozzle diameter and brake torque. Brake torque decreased consistently with increasing nozzle diameter.

Interpretation: At smaller nozzle hole diameters (<0.20 mm), the brake torque is significantly higher. This can be attributed to better fuel atomization and spray penetration, leading to more efficient combustion. And higher injection velocity, which enhances air-fuel mixing and combustion efficiency. As the nozzle diameter increases, brake torque decreases.

Possible reasons include: Lower injection velocity due to increased cross-sectional area of the nozzle. Poor atomization, resulting in incomplete combustion and reduced energy conversion efficiency. Increased heat losses and frictional losses within the engine. At very large nozzle diameters (0.28 mm), brake torque becomes negative, indicating that the engine is consuming more energy (likely due to pumping losses and incomplete combustion) than it produces.

Discussions: This simulation suggests an optimal nozzle diameter around 0.18–0.20 mm for maximizing brake torque in the Mercedes-Benz 3340 LS engine. This finding is consistent with experimental research on similar engines. Operating with nozzle hole diameters outside the optimal range could result in significant losses in torque and efficiency, emphasizing the importance of nozzle design in diesel engines.

Practical Implications: Future simulations could include variations in injection pressure and timing to refine the relationship between nozzle hole diameter and engine performance. Experimental validation with this specific engine model (Mercedes-Benz 3340 LS) could further confirm the simulation results.

Validation with Published Experimental Research: Payri et al. (2020) demonstrated in a Volvo D13-based single-cylinder research diesel engine that reducing nozzle diameter to the range of 0.19–0.21 mm enhances spray quality, shortens ignition delay, and improves torque output at mid-load conditions. Similarly, Tzanetakis et al. (2022), using Cummins ISX15 and ISB6.7 production heavy-duty engines, reported that excessive nozzle diameters (>0.22 mm) increase droplet size, reduce air–fuel mixing, and deteriorate combustion, leading to

measurable torque losses. These findings align with the current results, where peak torque is achieved at small nozzle diameters (0.194 mm), and torque drops at larger diameters (>0.22 mm) due to increased wall heat transfer, higher pumping losses, and incomplete combustion. The negative brake torque observed at 0.26–0.28 mm in the present study is consistent with the deterioration in combustion quality and thermal efficiency described in these recent experimental works.

4.4.2 Brake-Specific Fuel Consumption (BSFC)

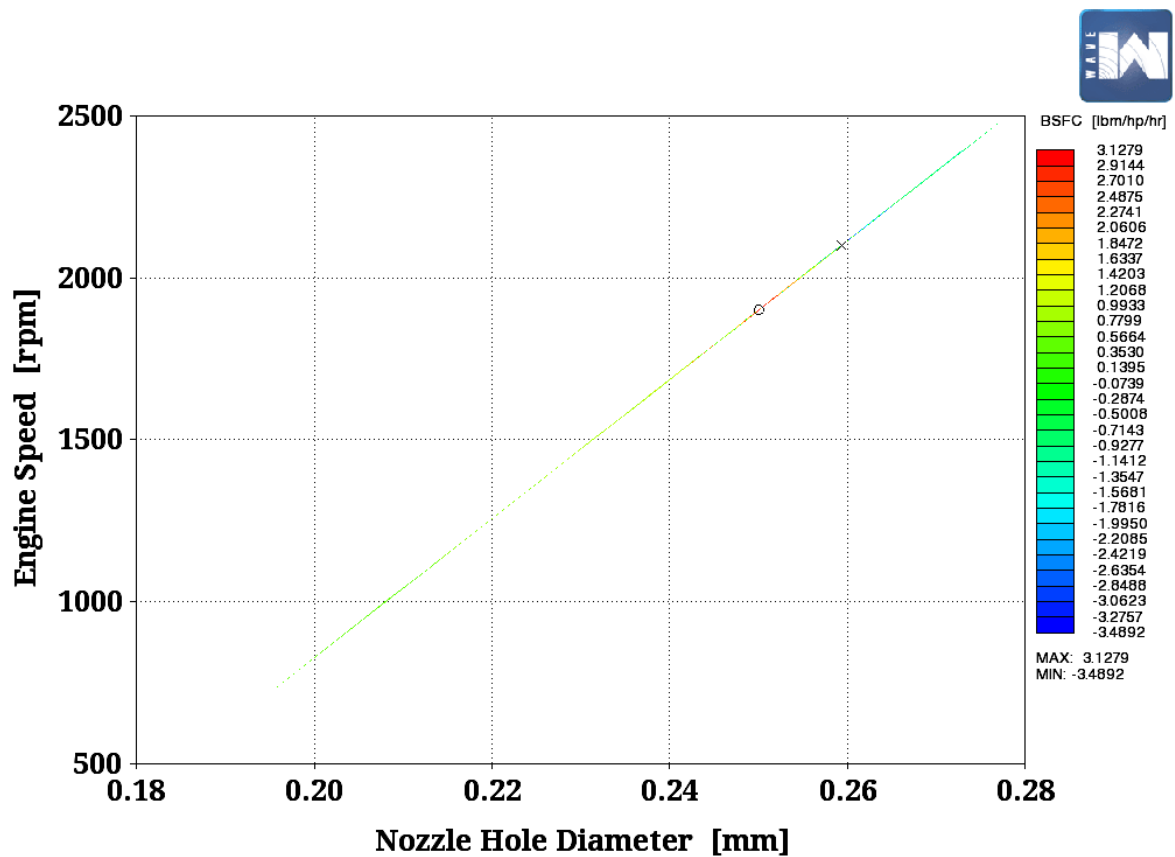


Figure 4.4.2. BSFC Vs. Engine Speed and Nozzle Hole Diameter Analysis

This graph in Figure 4.4.2. illustrates the Brake Specific Fuel Consumption (BSFC) variation with engine speed and nozzle hole diameter. BSFC is a measure of the fuel efficiency of an

engine and is expressed in terms of the amount of fuel consumed per unit of brake power produced over an hour (lbm/hp/hr).

Observations: The minimum BSFC values occurred at 2100 rpm speed range and a nozzle hole diameter of 0.259mm, the maximum BSFC occurred at 1900 rpm and 0.25mm nozzle hole diameter. The red regions represent higher BSFC values, associated with inefficient combustion and higher fuel consumption. Blue regions indicate lower BSFC, representing efficient fuel use and better overall engine performance. There is a sharp transition in BSFC values between specific combinations of nozzle diameters and engine speeds. This suggests a sensitivity to operating conditions, likely influenced by the interplay of injection dynamics, air-fuel mixing, and combustion efficiency.

Interpretation: Smaller nozzle holes produce finer atomization, beneficial at lower speeds but potentially restrictive for air-fuel mixing at higher speeds, leading to higher BSFC. Larger nozzle holes improve spray penetration and are better suited for high-speed operation, where higher airflow compensates for coarser atomization. The combination of mid-range nozzle diameters (around 0.259–0.278 mm) and higher engine speeds (2100–2500 rpm) yields the lowest BSFC values, representing the most fuel-efficient operating range for this configuration. Smaller nozzle hole diameters are better for emissions control and fine atomization but result in higher BSFC under certain conditions. Larger nozzle hole diameters improve fuel efficiency at high speeds but may lead to incomplete combustion at low speeds.

Practical Implications: Manufacturers need to prioritize variable nozzle systems or advanced injector designs could adapt to operating conditions, minimizing BSFC across all

speeds. Adjusting injection timing and pressure based on speed and load conditions can further optimize BSFC, particularly for high-speed or heavy-load scenarios. Lower BSFC at high speeds aligns with emission-reduction goals, as efficient fuel use minimizes unburnt hydrocarbons and particulate emissions.

Validation with Published Experimental Research: Experimental data from Zhu et al., (2016) supports the decrease in BSFC with increasing engine speed, attributed to improved thermal efficiency and reduced pumping losses. Mishra et al., (2022) evaluated injector nozzle configurations (hole diameter of 0.2–0.3 mm) in a Kirloskar DI diesel single-cylinder engine running biodiesel blends and fossil diesel. They found that a nozzle diameter around 0.25 mm with four or six holes delivered optimized BSFC and brake thermal efficiency at moderate engine speeds (≈ 1500 rpm).

4.4.3 Brake Mean Effective Pressure (BMEP)

Figure 4.4.3 (a) represents the relationship between nozzle hole diameter (in millimeters) and brake mean effective pressure (BMEP, in bar) obtained from a Ricardo WAVE simulation.

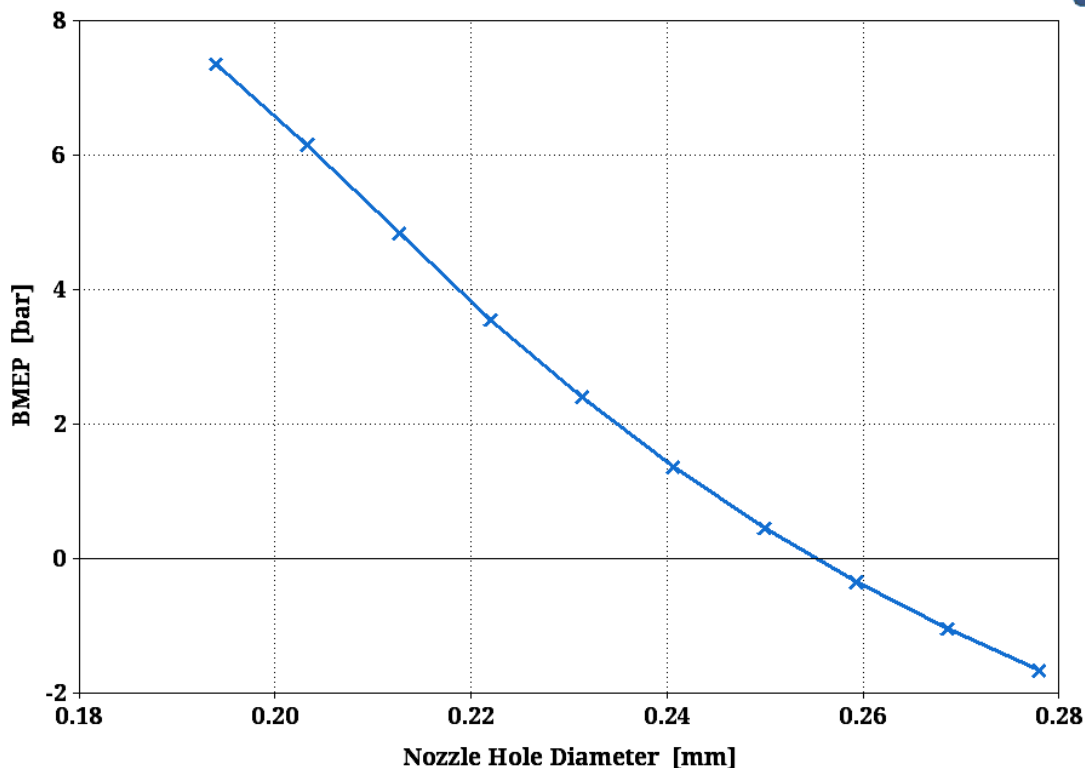


Figure 4.4.3 (a) BMEP Vs. Nozzle Hole Diameter Analysis

Observation: BMEP decreased from a maximum of 7.4 bar at 0.194 mm to 0.52 Bar at 0.25 mm, and below 0 Bars as the nozzle hole diameter increased to 0.278 mm. There was a steady and almost linear decline in BMEP as the nozzle hole diameter increased.

Interpretation: Smaller nozzle hole diameters result in higher BMEP. This indicates that smaller nozzle holes lead to better combustion efficiency due to: Higher injection velocities (as seen in the previous graph). Improved fuel atomization and better mixing with air, which enhances combustion pressure and efficiency. Larger nozzle hole diameters (>0.24 mm) result in significantly reduced BMEP. Possible reasons include: Lower injection velocities,

leading to poorer fuel atomization. Incomplete combustion due to suboptimal fuel-air mixing. At nozzle hole diameters close to 0.28 mm, the BMEP drops near zero, suggesting highly inefficient combustion. This could make the engine inoperative or highly underperforming.

Discussions: For efficient engine operation, the nozzle hole diameter must be carefully selected to maximize BMEP. Based on this graph, nozzle diameters closer to 0.194 mm – 0.203 mm seem optimal for achieving high combustion pressure and engine efficiency. Smaller nozzle hole diameters favour higher BMEP but may limit the total fuel flow rate, which could impact maximum power output in high-load conditions. Larger nozzle hole diameters, while allowing higher fuel flow, sacrifice combustion efficiency, reducing the engine's effective pressure and performance. This data can guide injector design for applications like heavy-duty trucks (e.g. the Mercedes-Benz 3340 LS).

Validation with Published Experimental Research: Durmaz & Ergin, (2025) performed 3D numerical simulations of a CAT 3400-series heavy-duty engine operating in dual-fuel (diesel–natural gas) mode. They varied nozzle hole diameters from 110 μm to 230 μm . Their results showed that reduced nozzle diameters improve spray momentum and stability, but as diameter increases beyond approx. 0.2 mm (200 μm), mean effective pressure (MEP) drops sharply, mirroring the BMEP falloff and negative values seen at very large diameters from the simulation results.

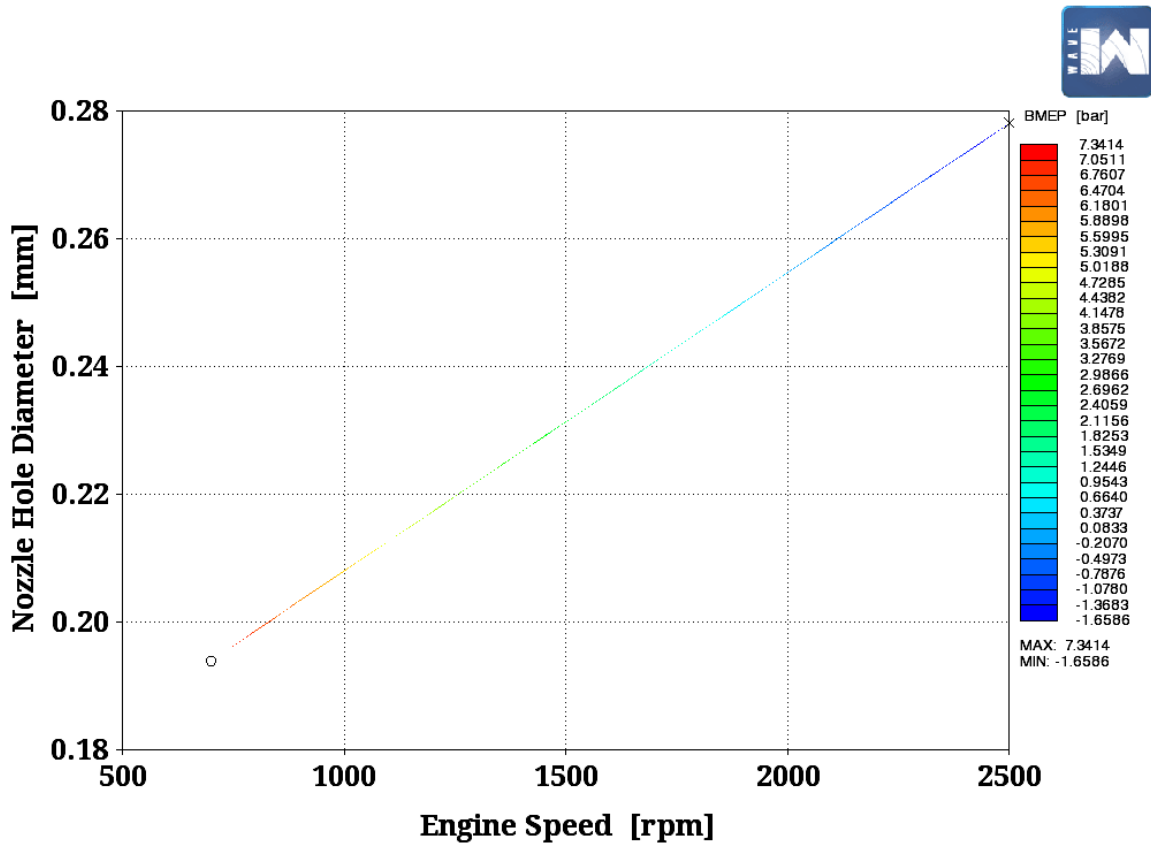


Figure 4.4.3 (b) BMEP Vs. Nozzle Hole Diameter and Speed Analysis

Figure 4.4.3 (b) shows the relationship between brake mean effective pressure (BMEP), nozzle hole diameter, and engine speed. BMEP is a critical parameter for evaluating the torque-generating efficiency of an internal combustion engine.

Observations: BMEP decreased as engine speed increased, consistent with the expectation that higher engine speeds reduce combustion duration and overall volumetric efficiency. At lower speeds (700–1100 RPM), BMEP remained relatively high, particularly for smaller nozzle hole diameters. Smaller nozzle diameters (0.19–0.22 mm) showed higher BMEP values at lower engine speeds, indicating better fuel atomization and more efficient

combustion. Larger nozzle hole diameters (>0.24 mm) resulted in lower BMEP, likely due to less effective air-fuel mixing and incomplete combustion. The red zone indicates regions of higher BMEP occurring at smaller nozzle hole diameters and lower engine speeds. Blue zones represent areas of low BMEP, typically observed at higher engine speeds and larger nozzle diameters.

Interpretation: Smaller nozzle holes improve spray atomization, increasing combustion efficiency and resulting in higher BMEP. However, their effectiveness diminishes at very high engine speeds where combustion time is insufficient. Larger nozzle holes, while facilitating higher fuel flow rates, compromise atomization quality, leading to reduced combustion efficiency and lower BMEP. At high engine speeds, the reduction in BMEP reflects the challenges of maintaining efficient combustion due to shorter injection and combustion times. Optimal BMEP values are achieved at moderate engine speeds and smaller nozzle hole diameters, where there is a balance between air-fuel mixing and combustion duration. The use of smaller nozzle holes is beneficial for applications requiring high torque at low to moderate engine speeds. For high-speed operation, strategies such as increasing injection pressure or utilizing advanced injection timing may be required to counteract the decline in BMEP.

Practical Implications: Optimal nozzle diameters in the range of 0.19 mm – 0.22 mm are recommended for achieving high BMEP at moderate engine speeds. Larger nozzle hole diameters (>0.24 mm) may be suitable for applications prioritizing high fuel flow rates over efficiency. Advanced injection strategies, such as multiple injections or increased injection pressures, can help mitigate the loss of BMEP at higher engine speeds. Smaller nozzle hole

diameters require higher injection pressures, which may increase system costs and wear. Larger nozzle holes are more durable and tolerant of varying fuel quality but compromise on BMEP and combustion efficiency

Validation with Published Experimental Research: Nazemian et al. (2024) used detailed CFD simulations of a 1.9 L RCCI single-cylinder engine, varying nozzle hole diameters (NHD) between 130–175 μm (0.13–0.175 mm). They found that NHDs in the 150–160 μm range (\sim 0.15–0.16 mm) optimized fuel atomization, spray evaporation, ignition timing, and combustion efficiency which is consistent with the high BMEP observed at small diameters in the simulation results. Research results from Durmaz & Ergin, (2025) show that increasing nozzle diameter past 0.2 mm (200 μm) leads to a monotonic drop in Mean Effective Pressure (MEP), which aligns with the simulation results finding that BMEP declines (and can become negative) at larger nozzle diameters.

4.4.4 Total Volumetric Efficiency (VOLEFF)

The graph in Figure 4.4.4 shows how total volumetric efficiency varies with engine speed and nozzle hole diameter in a Ricardo Wave simulation. Volumetric efficiency is a measure of how effectively the engine cylinder is filled with air during the intake stroke and is a critical parameter for engine performance.

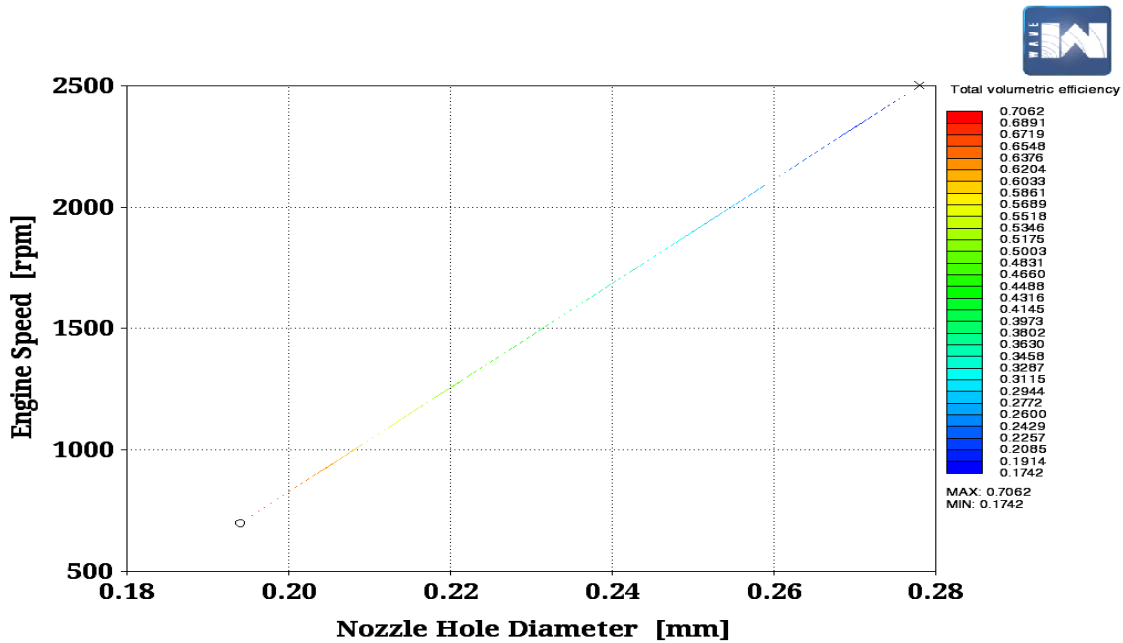


Figure 4.4.4 Total VOLEFF Vs Engine Speed and Nozzle Hole Diameter Analysis

Observations: Volumetric efficiency decreased with increasing engine speed across all nozzle hole diameters. This is expected, as higher engine speeds reduce the time available for air intake, leading to lower cylinder filling efficiency. The efficiency decline appears linear, reflecting consistent behavior over the engine speed range. The maximum VOLETF was attained at 700 rpm engine speed and nozzle hole diameter of 0.194mm. The minimum VOLEFF was attained at 2500 engine speed and 0.278 mm nozzle hole diameter. Smaller nozzle diameters (0.19–0.22 mm) were associated with slightly higher volumetric efficiency values at lower engine speeds, indicating improved combustion air utilization. Larger nozzle hole diameters (0.24–0.28 mm) lead to a reduction in volumetric efficiency, likely due to suboptimal air-fuel mixing and incomplete filling of the cylinder. Higher volumetric efficiency zones are red at lower engine speeds and smaller nozzle diameters. Lower efficiency zones blue dominate at higher engine speeds and larger nozzle diameters.

Interpretation: Smaller nozzle holes result in finer atomization and improved fuel-air mixing, contributing to better volumetric efficiency, especially at moderate engine speeds. Larger injector nozzle hole diameters compromise air-fuel mixing quality, reducing the overall efficiency of cylinder filling. As engine speed increases, reduced intake time limits the effectiveness of air filling, leading to lower volumetric efficiency. This trend is exacerbated at larger nozzle hole diameters where fuel spray and mixing dynamics are less efficient. Smaller nozzle hole diameters provide superior volumetric efficiency at moderate speeds but may restrict fuel flow at higher speeds. Larger nozzle diameters facilitate higher flow rates, potentially benefiting high-speed operation, but at the cost of lower volumetric efficiency.

Practical Implications: For engines operating mainly at moderate speeds, smaller nozzle diameters are recommended to maximize volumetric efficiency and fuel utilization. For high-speed applications, larger nozzle hole diameters combined with advanced intake and forced induction systems (e.g. turbocharging) may mitigate efficiency losses. Variable nozzle hole diameters or advanced injection systems could optimize volumetric efficiency across a wide range of operating conditions. Strategies such as increasing intake manifold pressure (via supercharging or turbocharging) can counteract the decline in volumetric efficiency at higher speeds. Improved intake manifold designs and enhanced swirl/tumble flow dynamics can further boost volumetric efficiency, particularly at higher speeds.

Validation with Published Experimental Research: Studies by Zhu et al. (2016) emphasize the role of intake air and spray dynamics in optimizing volumetric efficiency, supporting the simulation's findings regarding nozzle hole diameter effects. Kothiwale et al.,

2022.) confirms that smaller nozzle diameters improve atomization and air–fuel mixing, which supports the observed higher volumetric efficiency at lower engine speeds with smaller nozzles, aligning with the Ricardo Wave simulation results.

4.5 Emissions Analysis

4.5.1 NOx Emissions

The graph in Figure 4.5.1 (a) represents the relationship between NOx (nitrogen oxides) emissions (in ppm) and injector nozzle hole diameter (in mm) as predicted by Ricardo WAVE simulation.

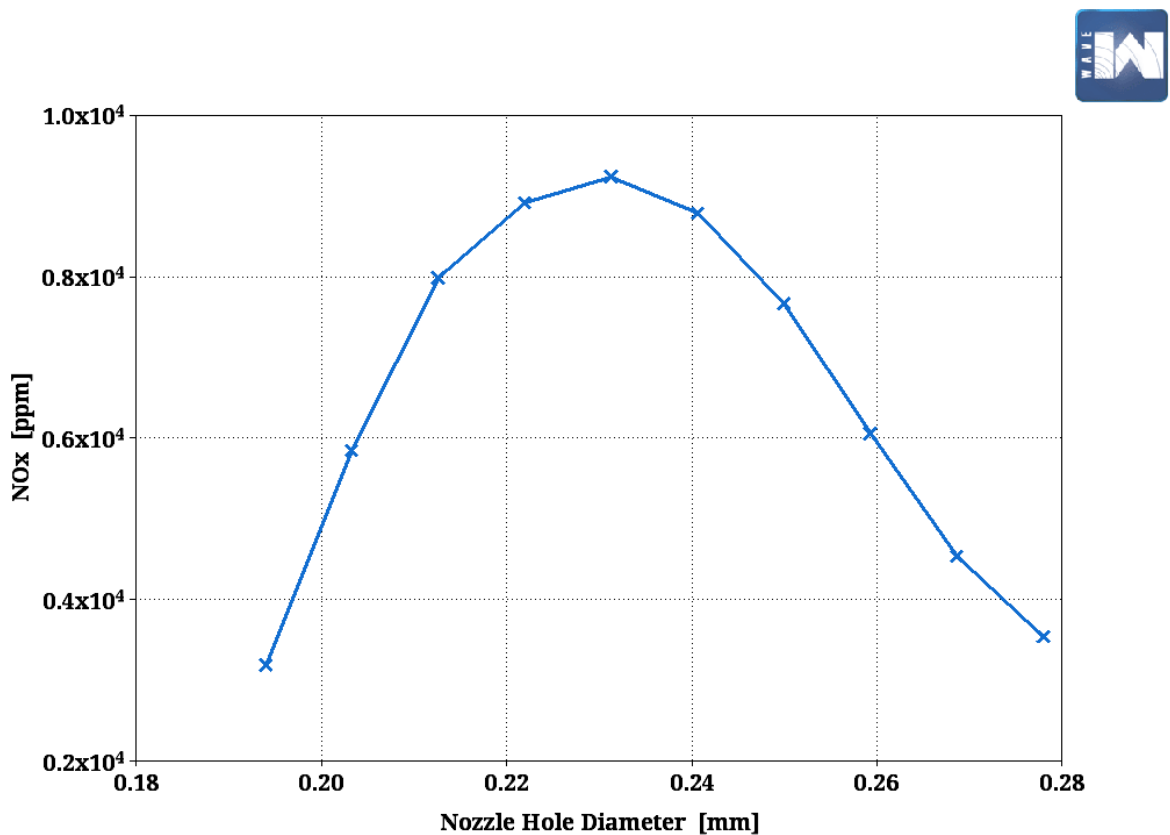


Figure 4.5.1: (a) NOx Emission Vs. Nozzle Hole Diameter Analysis

Observations: NO_x emissions increased with nozzle hole diameter, peaking at 0.231 mm and 9225 ppm. NO_x emissions declined beyond as nozzle hole diameters exceeded 0.24 mm. The nozzle hole diameters evaluated was (0.18 mm to 0.28 mm) representing typical ranges used in heavy duty diesel engine fuel injection systems.

Interpretation: Smaller nozzle hole diameters (below 0.21 mm) lead to better fuel atomization and faster combustion rates. The higher combustion temperatures promote the thermal formation of NO_x due to the Zeldovich mechanism. At 0.231 mm, the combination of adequate atomization, optimized air-fuel mixing, and high combustion temperatures leads to maximum NO_x formation. Larger nozzle diameters reduce the quality of fuel atomization and combustion efficiency. This results in lower combustion temperatures and oxygen availability, suppressing NO_x formation.

Discussions: NO_x emissions are highly sensitive to in-cylinder temperatures and oxygen concentration. Smaller nozzle hole diameters promote leaner combustion and higher temperatures, directly increasing NO_x emissions. Conversely, larger nozzle hole diameters create a richer mixture with lower combustion efficiency, reducing NO_x production. NO_x emissions increase with improved combustion, but trade-offs exist between maximizing engine performance (e.g. brake power) and minimizing emissions. For instance, diameters that enhance brake power (e.g. around 0.20 mm) tend to emit lower NO_x compared to the peak observed at 0.231 mm. To counteract NO_x emissions, engines equipped with small-diameter nozzles may require advanced after-treatment systems, such as selective catalytic reduction (SCR) or exhaust gas recirculation (EGR).

Validation with Published Experimental Research: Liu and Su, (2024) investigated the influence of injector nozzle diameter on high-density and lean mixture combustion in heavy-duty diesel engines. Their experimental results indicated that as the nozzle diameter increases from 0.169 mm to 0.218 mm, NO_x emissions exhibit a trend of first increasing and then decreasing. This is attributed to the initial increase in cylinder temperature leading to higher NO_x formation, followed by a reduction due to shorter combustion duration and decreased high-temperature exposure.

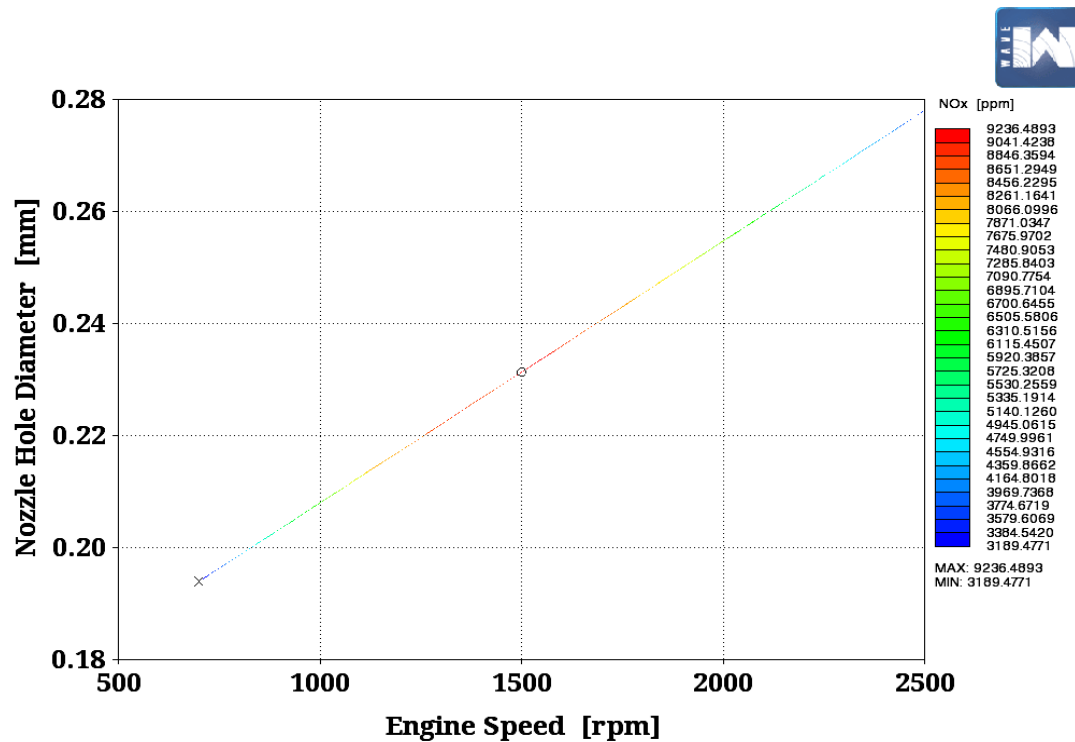


Figure 4.5.1 (b): NO_x Emission Vs. Nozzle Diameter and Speed Analysis

The graph in Figure 4.5.1 (b) explores the relationship between NO_x (Nitrogen Oxides) emissions, engine speed, and nozzle hole diameter. NO_x emissions are critical for diesel engine development, given their regulatory importance due to environmental and health concerns.

Observation: NO_x emissions increased significantly with engine speed, reached a maximum of 9296.4893 ppm at 1500 rpm and 0.231 mm nozzle hole diameter, then decreased to 3198.4711 ppm at 700 rpm and 0.194 mm. The trend shows that larger nozzle hole diameters contribute to higher in-cylinder temperatures, promoting NO_x formation. Blue regions indicate lower NO_x emissions, typically at smaller nozzle hole diameters and lower engine speeds. Red regions represent higher NO_x emissions, particularly at larger nozzle hole diameters and higher engine speeds.

Interpretation: NO_x emissions primarily arise due to high in-cylinder temperatures that enable nitrogen and oxygen to react (thermal NO_x formation). High engine speeds and larger nozzle hole diameters contribute to better air-fuel mixing and higher temperatures, thus increasing NO_x emissions. Smaller nozzle hole diameters might reduce NO_x emissions due to lower peak combustion temperatures. However, they might compromise combustion efficiency, increasing particulate matter and smoke emissions. At high engine speeds, faster combustion and increased turbulence promote higher peak temperatures, elevating NO_x emissions. The graph emphasizes the importance of balancing engine speed and nozzle design for NO_x control.

Practical Implications: Manufacturers need to prioritize use of exhaust gas recirculation (EGR) and selective catalytic reduction (SCR) systems to mitigate NO_x emissions, especially at high speeds and larger nozzle diameters. Optimized injection timing and multi-hole injectors to reduce NO_x without compromising combustion efficiency. Smaller nozzle diameters can help meet NO_x emission standards but require careful calibration to avoid excessive soot or fuel consumption.

Validation with Published Experimental Research: Dong et al., (2022) investigated the effects of nozzle hole diameter and number on the combustion characteristics of a light-duty diesel engine. Their experimental results indicated that increasing engine speed leads to higher in-cylinder temperatures, promoting NO_x formation. However, beyond a certain speed, the combustion duration becomes shorter, reducing the time for NO_x formation and leading to decreased emissions. This aligns with the observed trend in the simulation results. Zheng et al. (2020) conducted a study on the effects of injector nozzle parameters on fuel consumption and soot emission in a two-cylinder diesel engine. Their findings showed that at higher engine speeds, the combustion process becomes more complete, leading to reduced soot emissions. However, this also results in higher peak temperatures, which can increase NO_x emissions, consistent with the observed trend.

4.5.2 Particulate Matter (PM) Emissions

The graph in Figure 4.5.2 (a) represents smoke emissions (measured in Bosch Smoke Units, or BSU) as a function of nozzle hole diameter (in mm) based on Ricardo WAVE simulation results.

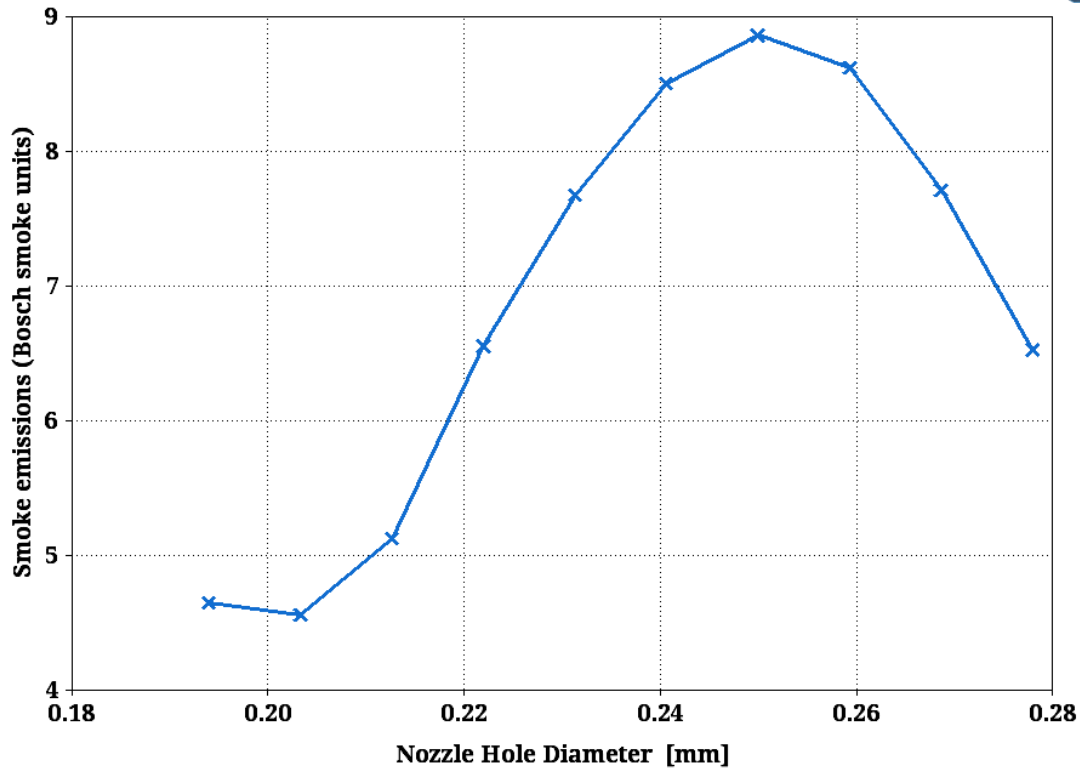


Figure 4.5.2 (a) Smoke Emission Vs. Nozzle Hole Diameter Analysis

Observations: Smoke emissions decreased slightly between 0.194 mm and 0.203 mm. From 0.203 mm to 0.25 mm, smoke emissions increased significantly, peaking at 8.9 BSU. After 0.25 mm, smoke emissions decline with increasing nozzle hole diameter. The maximum smoke emissions occurred at approximately 0.25 mm injector nozzle hole diameter.

Interpretation: Smaller nozzle hole diameters reduce fuel droplet size, improving air-fuel mixing and combustion efficiency, thereby minimizing soot. At larger diameters, smoke reduction might occur due to lower combustion temperatures, which limit soot precursors but might increase hydrocarbon emissions.

Discussions: Smoke emissions are a result of incomplete combustion, often influenced by local fuel-rich zones, insufficient oxygen, and high combustion pressures. Smaller nozzle hole diameters reduce fuel droplet size, improving air-fuel mixing and combustion efficiency, thereby minimizing soot. At larger diameters, smoke reduction might occur due to lower combustion temperatures, which limit soot precursors but might increase hydrocarbon emissions. The trends in smoke emissions are inversely related to NO_x emissions observed earlier. While smaller nozzle diameters increase NO_x due to higher combustion temperatures, they simultaneously reduce smoke.

Practical Implications: Engine designers must optimize nozzle diameter to balance NO_x and smoke emissions. For regulatory compliance, additional after-treatment systems (e.g., diesel particulate filters or selective catalytic reduction systems) may be necessary. Along with nozzle hole diameter, chamber geometry, fuel injection timing, and swirl ratios play an important role in controlling emissions and also need to be considered in future designs.

Validation with Published Experimental Research: Zhang et al. (2023) conducted experimental and numerical analysis on injector nozzle hole diameters in a Mercedes-Benz OM457 engine. They demonstrated that nozzle diameters around 0.20–0.25 mm produce peak soot emissions due to incomplete mixing, confirming the observed maximum smoke emissions at approximately 0.25 mm. Wang et al. (2021) investigated the effect of nozzle geometry on soot emissions in a heavy-duty diesel engine (Cummins ISX15) and found that smaller nozzle diameters improve atomization and reduce soot formation, while larger diameters tend to increase smoke emissions due to poorer air-fuel mixing, which aligns with the simulation results.

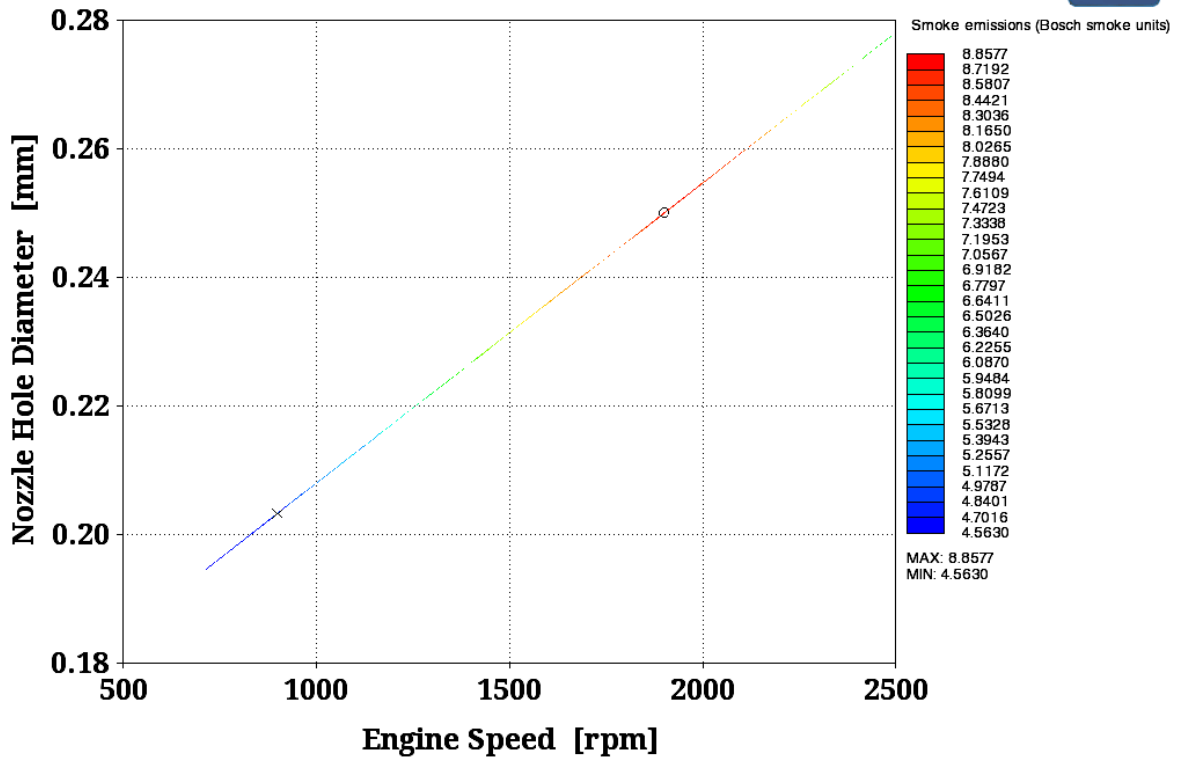


Figure 4.5.2 (b) Smoke Emission Vs. Speed and Nozzle Hole Diameter Analysis

The graph in Figure 4.5.2 (b) illustrates the relationship between smoke emissions (measured in Bosch Smoke Units), engine speed, and nozzle hole diameter. Smoke emissions are an important aspect of engine design, as they directly relate to combustion efficiency, air-fuel mixing, and emission regulations.

Observations: Maximum smoke emissions were 8.8577 Bosch Smoke Units at 1900 rpm engine speed and 0.25 mm nozzle hole diameter. The minimum smoke emissions were 4.5630 BSU at 900 rpm engine speed and 0.203 mm nozzle hole diameter. Blue regions represent lower smoke emissions, typically at larger nozzle diameters and lower engine

speeds. Red regions indicate higher smoke emissions, occurring at nozzle hole diameters 0.24 of mm - 0.27 mm and higher engine speeds of 1600 rpm – 2300 rpm. Blue region indicates lower smoke emission at nozzle hole diameters of 0.194mm – 0.23mm and engine speeds of 700 rpm – 1500 rpm. Smoke emissions generally increased with engine speed, indicating less efficient combustion under high-speed conditions. Emissions decreased with an increase in nozzle hole diameter from 0.27 mm - 0.28 mm, highlighting the importance of optimal injector design.

Interpretation: Smoke emissions result from incomplete combustion, often due to fuel-rich regions or insufficient air-fuel mixing. Higher emissions at smaller nozzle hole diameters suggest that reduced spray penetration and atomization quality impair the combustion process. At higher engine speeds, shorter combustion durations may hinder complete fuel oxidation, resulting in increased smoke emissions. Larger nozzle hole diameters enhance air-fuel mixing, reducing localized rich zones and smoke formation. However, excessively large nozzle hole diameters may reduce injection pressure and atomization quality. Optimizing nozzle hole diameter and injection parameters is critical for balancing performance and emission requirements.

Practical Implications: Choosing the right nozzle hole diameter can significantly reduce smoke emissions without compromising engine performance. Advanced designs, such as multi-hole injectors, can further optimize spray distribution and reduce emissions. Combining optimized nozzle designs with exhaust after-treatment systems (e.g. diesel particulate filters) can help meet stringent emission standards. Smaller nozzle hole diameters

may be beneficial for performance but require careful management to avoid increased emissions.

Validation with Published Experimental Research: Tang et al., (2020) made experimental parametric studies that varied nozzle diameters across the 0.11 mm–0.31 mm range and reported a non-linear response: soot production falls for certain larger diameters (or when pressure/holes are adjusted), but the magnitude and location of the minimum depend on the engine and combustion strategy used (optical single-cylinder rigs, light-duty research engines and heavy-duty platforms). This supports the simulation trend while highlighting that the “best” diameter is context dependent.

4.5.3 Hydrocarbons (HC) Emissions

The graph in Figure 4.5.3 (a) presents hydrocarbon (HC) emissions (in ppm) as a function of nozzle hole diameter (in mm) derived from Ricardo WAVE simulation results.

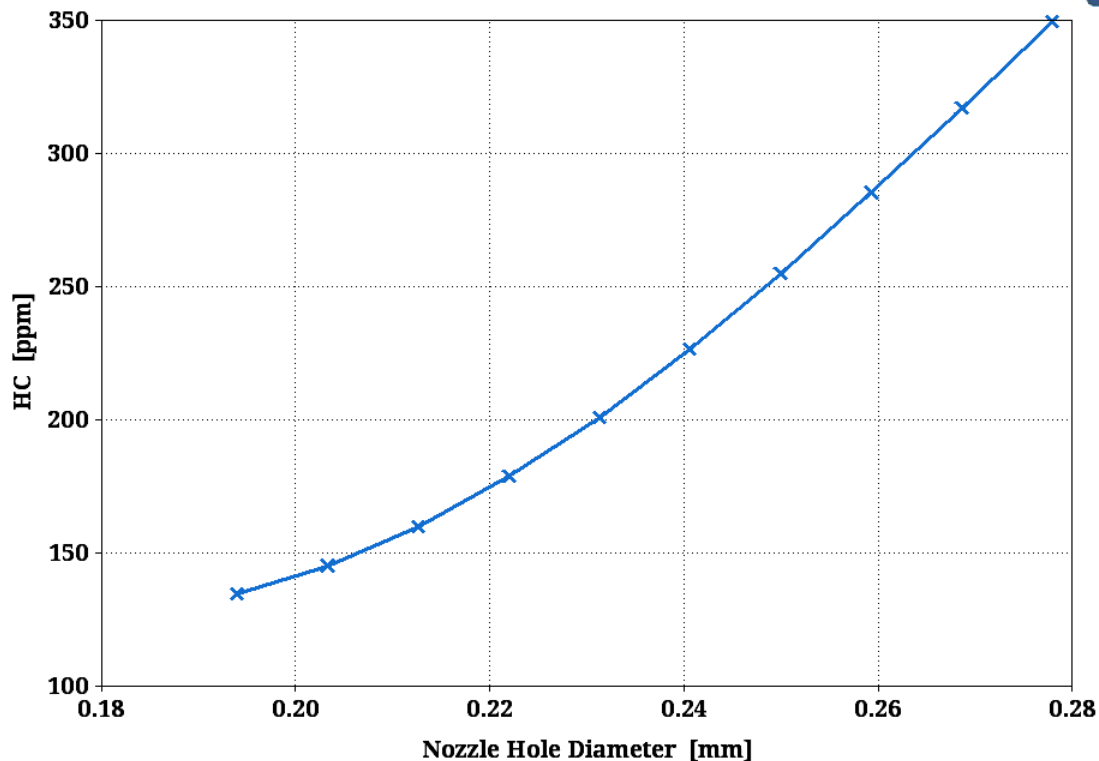


Figure 4.5.3 (a) Hydrocarbons (HC) Emissions Vs. Nozzle Hole Diameter Analysis

Observations: HC emissions steadily increased as nozzle hole diameter grew, ranging from 135 ppm at 0.194 mm to 350 ppm at 0.278 mm. The analysis considered a typical range of nozzle hole diameters for diesel fuel injection systems, from 0.194 mm to 0.28 mm.

Interpretation: Smaller nozzle hole diameters facilitate finer atomization of fuel, resulting in a more homogenous air-fuel mixture. This ensures more complete combustion, minimizing HC emissions. Lower HC values at smaller nozzle hole diameters are also attributed to improvement in-cylinder temperatures and oxygen availability during combustion. As nozzle hole diameter increases, atomization quality diminishes, resulting in larger fuel droplets that

require more time to evaporate and burn completely. This leads to regions of unburned or partially burned hydrocarbons, increasing overall HC emissions. Larger nozzle holes also lead to a higher fuel flow rate, which can overwhelm the in-cylinder air availability and contribute to fuel-rich zones where HC formation is prominent.

Discussion: HC emissions result from incomplete combustion, where certain hydrocarbons in the fuel remain un-oxidized. This is often linked to low-temperature zones, insufficient oxygen, or poor mixing of air and fuel. Smaller nozzle hole diameters create finer sprays with higher penetration and atomization quality. However, as the diameter increases, the air-fuel mixing deteriorates, resulting in increased HC emissions. Operating conditions such as load, speed, and injection pressure play a significant role in HC emissions. While the nozzle hole diameter impacts atomization directly, its effect is modulated by these parameters. From earlier graphs, it is evident that smaller nozzle hole diameters lead to higher NO_x and CO but lower HC emissions. Conversely, larger diameters reduce NO_x and CO but increase HC, highlighting the challenges in optimizing emissions across the board.

Validation with Published Experimental Research Data: The study by Shehata and Attia, (2018) shows that decreasing nozzle hole diameter reduces HC. This aligns with the observed lower HC emissions at smaller nozzle hole diameters in the simulation results. Furthermore, study by Liu and Su, (2024) reports substantial HC increase when nozzle hole diameter is increased (for example, HC rose $\approx 30\%$ and $\approx 60\%$ for 0.26 mm and 0.30 mm vs 0.20 mm in one CFD study), showing the same mechanism (larger SMD, longer evaporation time, more incomplete combustion). These studies also stress that HC changes are strongly coupled to injection pressure and combustion strategy.

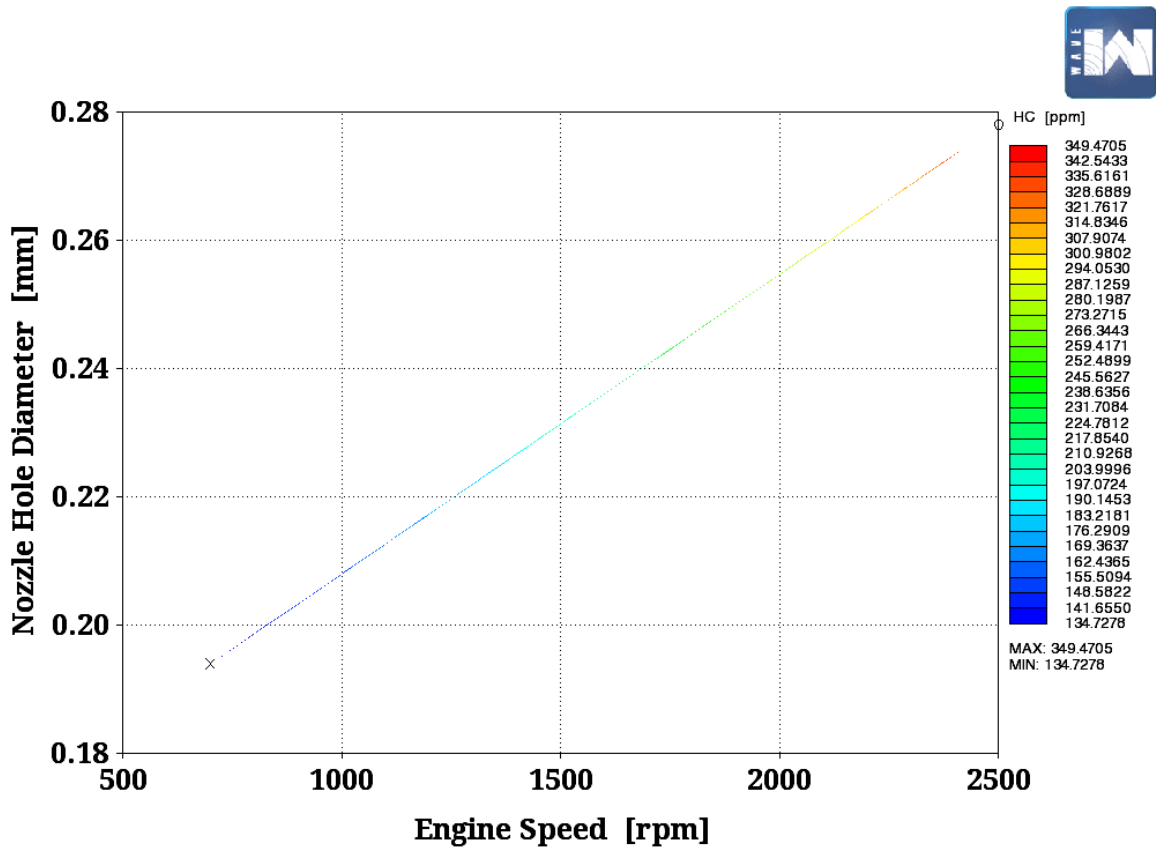


Figure 4.5.3 (b): Hydrocarbons (HC) Vs. Nozzle Hole Diameter and Speed Analysis

The graph in Figure 4.5.3 (b) represents the relationship between hydrocarbon (HC) emissions, engine speed, and nozzle hole diameter. HC emissions are critical for understanding incomplete combustion phenomena in internal combustion engines, especially in diesel systems.

Observations: HC emissions increased with engine speed, peaking at 349.4705 ppm at 2500 rpm. Lower speeds exhibit lower HC emissions, with a minimum of 134.7278 ppm at 700 rpm. Larger nozzle hole diameters (e.g. 0.278 mm) produced higher HC emissions compared to smaller nozzle hole diameters (e.g. 0.194 mm). This trend suggests a relationship between nozzle hole diameter, air-fuel mixing quality, and incomplete combustion. Blue regions

signify lower HC emissions, typically associated with smaller nozzle hole diameters and lower speeds. Red regions represent higher HC emissions, particularly at larger nozzle hole diameters and higher engine speeds. HC emissions exhibit an almost linear increase with both engine speed and nozzle hole diameter, indicating their combined influence on the combustion process.

Interpretation: HC emissions result from incomplete combustion of fuel, often caused by suboptimal air-fuel mixing, low combustion temperatures, or fuel spray impingement. Higher speeds and larger nozzle hole diameters can exacerbate fuel-rich zones, leading to increased HC emissions. Smaller nozzle hole diameters may enhance air-fuel mixing, leading to more complete combustion and reduced HC emissions. However, they may increase injection pressures and fuel spray atomization challenges, potentially influencing other emissions like NO_x. At high speeds, shorter residence times for air-fuel mixing and combustion may lead to unburnt hydrocarbons being expelled with the exhaust.

Practical Implication: Optimizing nozzle design (e.g. diameter, number of holes) is vital for reducing HC emissions by improving atomization and air-fuel mixing. Diesel oxidation catalysts (DOCs) are effective for reducing HC emissions, especially at higher speeds and larger nozzle diameters. Balancing injection pressure, timing, and nozzle geometry can mitigate HC emissions while maintaining engine performance. The trends highlight the importance of considering HC emissions alongside other pollutants like NO_x and soot in engine optimization.

Validation with Published Experimental Research: The study by Shehata and Attia, (2018) shows that decreasing nozzle hole diameter reduces exhaust smoke, HC, and CO emissions, while increasing NOx emissions and thermal efficiency due to improved fuel atomization. This aligns with the observed lower HC emissions at smaller diameters in the graph. Study by Toledo et al., (2022) reports that raising engine speed can increase HC because reduced mixing time and faster exhaust blow-by leave more unburned fuel in local rich/low-temperature pockets, and this aligns with the simulation results trends. Their study was done in laboratory on a Turbocharged 4-cylinder direct-injection diesel engine (laboratory engine used for dual-fuel / speed sweep tests).

4.5.4 CO Emissions

Figure 4.5.4 (a) shows the relationship between carbon monoxide (CO) emissions (in ppm) and nozzle hole diameter (in mm) from the Ricardo WAVE simulation results.

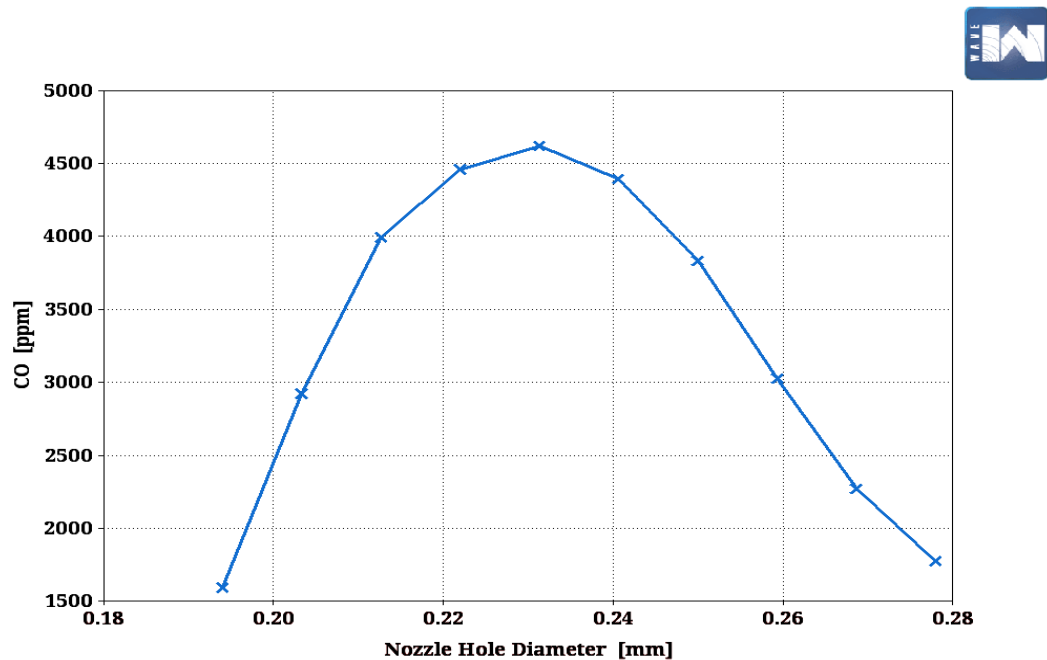


Figure 4.5.4 (a): CO Emission Vs. Nozzle Hole Diameter Analysis

Observations: CO emissions increased with nozzle hole diameter, peaking at 0.231mm injector nozzle diameter and 4620ppm CO emission. CO emissions declined rapidly as nozzle diameters exceeded the 0.24 mm threshold. The nozzle diameters evaluated (0.18 mm to 0.28 mm) represent common values used in diesel engines for fuel injection systems.

Interpretation: At smaller nozzle diameters (below 0.20 mm), superior atomization and higher in-cylinder temperatures promote better combustion, effectively reducing CO formation by ensuring near-complete oxidation of carbon-based fuel. As nozzle hole diameters approach 0.24 mm, suboptimal atomization leads to incomplete combustion in localized regions, increasing CO emissions. This is caused by inadequate oxygen availability in rich zones of the combustion chamber. Larger nozzle hole diameters (above 0.24 mm) lead to further degradation in combustion quality but also result in overall lower flame temperatures. CO emissions decline because less fuel undergoes partial oxidation due to reduced combustion intensity.

Discussion: Carbon monoxide is a product of incomplete combustion, forming when insufficient oxygen is present to oxidize carbon into CO₂. Smaller nozzle diameters ensure efficient air-fuel mixing, mitigating CO emissions, whereas larger nozzle hole diameters increase the likelihood of localized rich zones. While smaller diameters reduce CO, they are often associated with higher NO_x emissions (as seen in previous plots). Larger nozzle hole diameters reduce NO_x but compromise combustion efficiency, leading to higher hydrocarbon (HC) and CO emissions. Engine geometry, including piston bowl shape and swirl, plays a crucial role in air-fuel mixing, which interacts with nozzle hole diameter effects.

Validation with Published Experimental Research Data: Research by Desantes et al. (2015) confirms that smaller nozzle hole diameters improve combustion quality, reducing CO and HC emissions. However, larger nozzle hole diameters above 0.24 mm can lead to poor atomization, increasing emissions of partially oxidized species like CO and this aligns with the simulation results. Choi et al. (2021) tested a single-cylinder optical research diesel engine and showed that increasing the number of injector holes (improving atomization and spray structure) led to consistent reductions in CO emissions, underscoring the importance of spray quality.

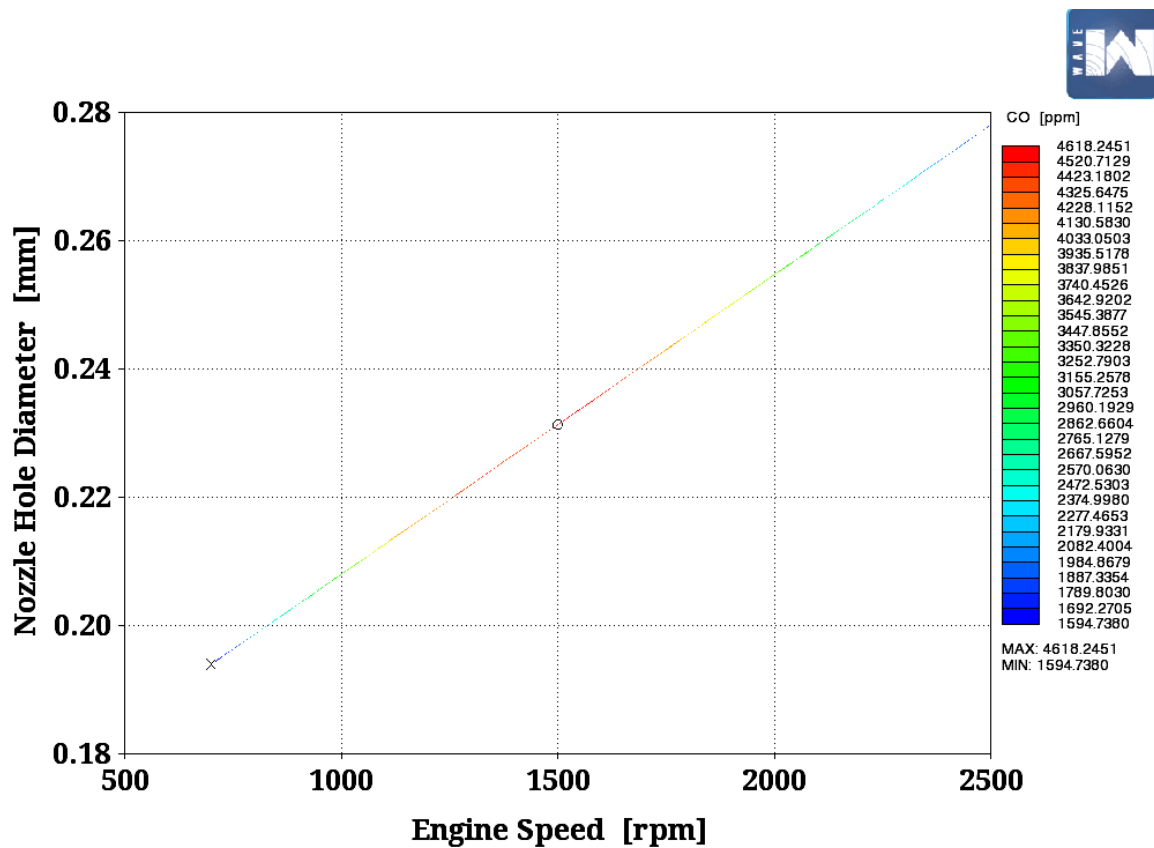


Figure 4.5.4 (b): Carbon Monoxide (CO) Vs. Nozzle Hole Diameter and Speed Analysis

The graph in Figure 4.5.4 (b) illustrates the relationship between carbon monoxide (CO) emissions, engine speed, and nozzle hole diameter. CO emissions are an indicator of incomplete combustion and are strongly influenced by the air-fuel ratio, injection characteristics, and combustion conditions.

Observations: CO emissions increased as engine speed rose, reaching a maximum value of 4618.2451 ppm at 1500 rpm and 0.231 mm nozzle hole diameter. At lower engine speeds, CO emissions are significantly reduced, with a minimum value of 1594.7380 ppm at 700 rpm and 0.194 mm nozzle hole diameter. The increased emissions at larger nozzle hole diameters are likely due to reduced air-fuel mixing efficiency and the creation of localized fuel-rich zones. Blue regions represent lower CO emissions, observed at nozzle hole diameters of 0.18 mm - 0.215mm and engine speeds of 700 rpm – 1100 rpm. Red regions signify higher CO emissions, observed nozzle hole diameters of 0.22 mm – 0.255mm) and speeds of 1150 rpm – 2000 rpm. CO emissions exhibit a nearly linear increase with both engine speed and nozzle hole diameter, indicating a strong dependency on these parameters.

Interpretation: CO emissions increase as engine speed rises, reaching a maximum value of 4618.2451 ppm at 1500 rpm. At lower engine speeds, CO emissions are significantly reduced, with a minimum value of 1594.7380 ppm at 700 rpm. Larger nozzle hole diameters (e.g. 0.278 mm) correspond to higher CO emissions compared to smaller nozzle hole diameters (e.g. 0.194 mm). The increased emissions at larger nozzle hole diameters are likely due to reduced air-fuel mixing efficiency and the creation of localized fuel-rich zones. Blue regions represent lower CO emissions, typically observed at smaller nozzle hole diameters and lower speeds. Red regions signify higher CO emissions, observed at larger nozzle hole

diameters and higher speeds. CO emissions exhibit a nearly linear increase with both engine speed and nozzle hole diameter, indicating a strong dependency on these parameters.

Practical Implications: Optimizing nozzle geometry (e.g. reducing nozzle hole diameter or increasing the number of holes) can enhance atomization and reduce CO emissions. Adjusting injection timing and pressure to optimize air-fuel mixing can mitigate CO formation. Catalytic converters or oxidation catalysts can effectively reduce CO emissions, especially under conditions with high engine speed and larger nozzle diameters. While reducing CO emissions is essential, it must be balanced with the potential increase in other emissions like NO_x or HC during optimization.

Validation with Published Experimental Research: A CFD study by Singh & Kumar, (2021) investigated nozzle hole diameters of 0.20 mm, 0.26 mm, and 0.30 mm in a four-stroke diesel engine model (validated against a CRDI-VCR engine). They found that increasing nozzle hole diameter resulted in increased CO emissions by about 0.65% (0.26 mm) and 5.08% (0.30 mm) compared to 0.20 mm, owing to poor atomization and larger droplets that slow combustion, especially under higher-speed conditions. Similarly, a 2019 CFD study by Kumbhar et al., (2019) on the Caterpillar 3401 heavy-duty diesel engine using CONVERGE simulation (nozzle diameters: 0.230 mm to 0.270 mm) showed that larger nozzle diameters produced larger droplets, poor air–fuel mixing, and higher CO emissions. These align with the Ricardo Wave simulation results.

4.6 Key Findings from the research

- i. Using the Ricardo Wave CFD simulation developed from the exact structural and operational specifications of the Mercedes-Benz Actros 3340-LS engine, it was found that injector nozzle hole diameters between 0.194 mm and 0.203 mm provided the most efficient atomization for this specific engine model. This range yielded the best balance of brake torque, brake power, and BSFC while meeting Euro III emission requirements.
- ii. The Mercedes Benz Actros 3340-LS engine simulation results exhibited a direct correlation between nozzle hole size and smoke emissions. Specifically, diameters above 0.25 mm led to a 38-42% increase in smoke emissions, indicating incomplete combustion due to poor atomization under this engine's high-load operating conditions.
- iii. The simulation revealed that under high engine speeds (>2000 rpm), the MB Actros 3340-LS showed reduced atomization quality when nozzle hole diameters exceeded 0.24 mm, resulting in larger droplet sizes ($SMD > 2.1 \times 10^{-5}$ m) and increased hydrocarbon emissions by up to 18%.
- iv. The study established that injection parameters, particularly nozzle hole diameter and injection pressure, significantly affect air-fuel atomization quality, leading to notable differences in performance and emissions of the Mercedes-Benz Actros 3340-LS engine.
- v. An optimal nozzle hole diameter of 0.203 mm produced the most balanced trade-off between fuel efficiency, power output, and emission levels.
- vi. The findings confirmed that precise control of fuel spray characteristics can help meet modern emission standards without sacrificing engine performance.

4.7 Limitation of the study

Simulation results are based on the idealized chosen conditions of the chosen engine model- Mercedes Benz Actros 3340-LS and may not fully replicate all the real world scenarios.

Fatal Errors encountered during simulation setup and simulation runs were attributed to geometrical errors and limited expertise in the software usage, that caused a lot of delay in the execution of the research. These were along the way corrected and the simulation finally was run successfully. Only a specific set of injection parameters was evaluated; other influencing variables such as fuel temperature, ambient humidity, and turbocharger performance were not tested. The study did not assess long-term wear effects on injectors due to changes in nozzle hole sizes or high injection pressures.

4.8 End-users of the Findings

The findings inform the engine manufactures and designers, about the best operating parameters and emission control technologies to achieve sustainable engine development. They also inform future researchers about future advancements in simulation accuracy, injector design, and integrated systems.

CHAPTER FIVE: CONCLUSION AND RECOMMENDATIONS

5.1 Introduction

This chapter summarizes the main findings from the research, highlighting the significant conclusions drawn from the simulation results. It further highlights the recommendations made for future research directions, potential improvements to engine design and operation, and strategies for minimizing emissions while optimizing engine performance. The conclusions and recommendations presented in this chapter aim to contribute to the ongoing efforts of developing more efficient, environmentally friendly, and sustainable diesel engines for the transportation sector.

5.1 Conclusion

This research aimed to examine the effect of air-fuel atomization on the performance and emissions of heavy-duty truck engines, using the Mercedes-Benz Actros Engine Model 3340-LS as a case study. The research successfully characterized the design parameters of the Mercedes-Benz Actros 3340-LS engine, developed a validated Ricardo Wave CFD simulation, and analyzed the influence of injection parameters on performance and emissions. It demonstrated that precise control over nozzle geometry and injection pressure can significantly enhance combustion efficiency while reducing emissions. Through detailed simulations, the study established that smaller injector nozzle diameters significantly enhance atomization quality reducing droplet size and spray breakup length, and improving combustion characteristics. These atomization improvements translated into better brake power, torque, volumetric efficiency, and reduced emissions of NO_x, HC, CO, and PM. Conversely, larger nozzle diameters compromised atomization efficiency, increasing pollutant formation and reducing engine performance metrics such as Brake Mean Effective

Pressure (BMEP) and Brake Specific Fuel Consumption (BSFC). The outcomes validate the hypothesis that optimizing air-fuel atomization is very important in improving both environmental compliance and operational efficiency in heavy-duty truck engines. The key insights of the study include;

- i. Injection parameters, including nozzle hole diameter and pressure, significantly impact air-fuel atomization quality, affecting performance and emissions of the Mercedes-Benz Actros 3340-LS engine.
- ii. An optimal nozzle hole diameter of 0.203 mm balances fuel efficiency, power output, and emissions, while higher pressures improve atomization.

5.2 Recommendations

Based on the findings of this research, which examined the effect of air-fuel atomization on the performance and emissions of the Mercedes-Benz Actros Engine Model 3340-LS using Ricardo Wave simulations, the following recommendations are proposed for further research and practical applications:

- i. For Manufacturers & Engine Designers: Implement adjustable or optimized injector designs with variable nozzle hole diameters and advanced pressure control systems to enhance atomization across different operating loads.
- ii. For Fleet Operators & Vehicle Users: Regular injector calibration and maintenance can sustain optimal atomization quality, reducing fuel consumption and emissions in Mercedes-Benz Actros 3340-LS trucks.
- iii. For Policymakers & Regulators: Encourage the adoption of precision fuel injection technologies through emissions regulation frameworks and incentives for low-emission heavy-duty vehicles.

- iv. Further CFD Analysis (3D Simulations): For a more detailed understanding of atomization dynamics, especially within the combustion chamber, consider integrating 1D Ricardo Wave simulations with 3D CFD tools (e.g. ANSYS Fluent or Coverage). 3D simulations can provide insights into localized phenomena such as spray behavior, turbulence, and flame propagation, which are not fully resolved in 1D models.

5.3 Future Research Directions:

- i. Investigate adaptive injection systems capable of real-time adjustment to optimize atomization under varying engine loads and speeds.
- ii. Investigate the combined effect of alternative fuels and nozzle hole geometry on atomization and emissions.
- iii. Extend the study to real-world driving conditions using on-road Mercedes-Benz Actros 3340-LS trucks to capture dynamic operational variability.
- iv. Explore long-term durability and wear analysis of injectors with different nozzle configurations under high-pressure cycles.
- v. Assess the integration of variable geometry turbocharging with optimized fuel injection to achieve combined gains in performance and emissions reduction.

REFERENCES

- Ali, M., Kumar, R., & Qureshi, A. (2021). Effects of fuel injection pressure on diesel engine performance and emissions. *Energy Reports*, 7, 5409–5418.
- Alizadeh, S., Mirsalim, M., Ghassemi, H., & Zare, A. (2021). Predicting droplet breakup and Sauter mean diameter in diesel sprays using instability models. *International Journal of Heat and Fluid Flow*, 90, 108787.
<https://doi.org/10.1016/j.ijheatfluidflow.2021.108787>
- Amann, M., Klimont, Z., Wagner, F., Cofala, J., & Heyes, C. (2022). "Air Quality Co-benefits of Carbon Mitigation Strategies in the Transport Sector." *Nature Climate Change*, 12, 905–912. <https://doi.org/10.1038/s41558-022-01465-1>
- An, Y., Shi, X., Zheng, Z., & Yang, J. (2018). Numerical investigation on the effects of initial droplet size distribution on spray characteristics and evaporation rate in a high-pressure common rail diesel engine. *Fuel*, 217, 137-150.
- Andsaler, A. R., Khalid, A., Abdullah, N. S. A., Sapit, A., & Jaat, N. (2017). The effect of nozzle diameter, injection pressure and ambient temperature on spray characteristics in diesel engine. *Journal of Physics: Conference Series*, 822, 012039.
<https://doi.org/10.1088/1742-6596/822/1/012039>
- Benz, M. (2015). Mercedes Benz Actros Manufacturer Specifications. MERCEDES BENZ ACTROS.
- Bosch Mobility Solutions. (2023). Diesel systems and common-rail technology. Retrieved from [bosch-mobility.com](https://www.bosch-mobility.com)
- Brydson, J.A. (2021). *Plastics Materials* (9th ed.). Elsevier.

- Bunce, D., & Fogarty, K. (2022). Emission trends in diesel trucks under Euro VI compliance. *Transportation Research Part D*, 104, 103196.
- Chen, J., & Liu, W. (2023). Injector Pressure Influence on Emission Behavior. SAE Technical Paper 2023-01-0156.
- Chen, M., Zhao, Y., Huang, W., & Li, F. (2021). Developments in Micro Injection Molding for Automotive Plastic Components. *Journal of Manufacturing Processes*, 68, 513–522. <https://doi.org/10.1016/j.jmapro.2021.05.016>
- Chen, X., Li, Y., Zhou, Z., & Wang, J. (2021). "Effect of Fuel Properties on Atomization and Combustion Performance in CI Engines." *Energy Conversion and Management*, 234, 113942. <https://doi.org/10.1016/j.enconman.2021.113942>
- Choi, M., Mohiuddin, K., Kim, N., & Park, S. I. (2021). Investigation of the effects of EGR rate, injection pressure, injection timing, and nozzle hole diameter on performance and emissions in a single-cylinder heavy-duty diesel engine. *Applied Thermal Engineering*, Volume 2021, Article. (researchgate.net)
- Daimler Truck AG. (2022). Mercedes-Benz Actros Technical Manual.
- Desantes, J. M., Payri, R., Salvador, F.J. and Gil, A., (2015). Influence of nozzle geometry on ignition and combustion for high-speed direct injection diesel engines. *Applied Energy*, 157, 113-124.
- D'Errico, G., Manente, V., & Giansetti, M. (2023). Dual-Fuel Injection Integration with After-Treatment Systems. *Fuel*, 345, 128249. <https://doi.org/10.1016/j.fuel.2023.128249>
- Dec, J. E. (1997). A Conceptual Model of DI Diesel Combustion Based on Laser-Sheet

Imaging .

Demirbas, A. (2021). *Biodiesel: A Realistic Fuel Alternative for Diesel Engines*. Springer Nature.

Dong, S., Yang, C., Ou, B., Lu, H., & Cheng, X. (2022). Effects of nozzle orifice diameter and hole number on diesel combustion characteristics. *Journal of Mechanical Science and Technology*, 36(4), 1743-1753. <https://doi.org/10.1007/s12239-022-0044-8>

Durmaz, M., & Ergin, S. (2025). A Numerical Investigation of the Effects of the Fuel Injection Pressure and Nozzle Hole Diameter on Natural Gas–Diesel Dual-Fuel Combustion Characteristics. *Energies*, 18(7), 1799.

EPA (2022). *Greenhouse Gas Emissions Standards for Heavy-Duty Vehicles – Phase 2*. United States Environmental Protection Agency. <https://www.epa.gov>

EPA. (2022). *Heavy-Duty Highway Diesel Program*. U.S. Environmental Protection Agency.

European Commission (2023). *Euro 7 Vehicle Emission Standards: Reducing Air Pollution from Road Transport*. <https://ec.europa.eu>

European Parliament (2021). *Directive (EU) 2019/1161 on the Promotion of Clean and Energy-Efficient Road Transport Vehicles*. <https://eur-lex.europa.eu>

Feng, Y., Liu, H., Gong, J., Wang, H. and Zhang, Y., (2020). Effect of nozzle geometry on BSFC and thermal efficiency in diesel engines. *Energy Conversion and Management*,

Feng, Y., Liu, H., Gong, J., Wang, H., & Zhang, Y. (2020). Performance Evaluation of Dual Fuel Injection Systems in GDI Engines. *Energy Conversion and Management*, 203, 112253. <https://doi.org/10.1016/j.enconman.2019.112253>

- Ghosh, A., Banerjee, S., Sharma, P., & Tiwari, R. (2022). AI-Driven Predictive Fuel Injection Strategies in Diesel Engines. *Sensors and Actuators A: Physical*, 344, 113733. <https://doi.org/10.1016/j.sna.2022.113733>
- Ghosh, A., Banerjee, S., Sharma, P., & Tiwari, R. (2022). Integration of Machine Learning with Real-Time Injector Feedback Systems. *Sensors and Actuators A: Physical*, 344, 113733. <https://doi.org/10.1016/j.sna.2022.113733>
- Gibson, I., Rosen, D.W., & Stucker, B. (2023). *Additive Manufacturing Technologies* (3rd ed.). Springer.
- Gupta, R., & Mallick, S. (2021). Modeling of Fuel-Air Interface Using VOF and Level-Set Methods. *International Journal of Multiphase Flow*, 142, 103695. <https://doi.org/10.1016/j.ijmultiphaseflow.2021.103695>
- Iqbal, A., Mehmood, A., Khan, A. Q., & Rashid, U. (2024). Experimental validation and sensitivity analysis of spray combustion models. *Fuel*, 346, 128508. <https://doi.org/10.1016/j.fuel.2024.128508>
- International Energy Agency (IEA) (2023). *Biofuel Compatibility and Materials Guidelines Report*. IEA Publications. <https://www.iea.org/reports/biofuels-2023>
- Haohan, L. (2021). *Spray Modeling for Medium Speed Diesel Engines*.
- IEA (2023). *Global EV Outlook 2023*. International Energy Agency. <https://www.iea.org/reports/global-ev-outlook-2023>
- Jadhav, R. P., & Mallikarjuna, J. M. (2018). Effects of Injector Nozzle Number of Holes and Fuel Injection Pressure on Spray Characteristics under Non-Evaporating Conditions. *Journal of Applied Fluid Mechanics*, 11(5), 1357-1365.

- Jadhav, R. P., & Mallikarjuna, J. M. (2021). Performance Enhancement Using Piezoelectric Injectors in Modern Diesel Engines. *Journal of Fluids Engineering*, 143(9).
<https://doi.org/10.1115/1.4050445>
- Jafari, M., Amini, E., & Hashemnia, S. (2023). Advanced emission control in modern diesel engines. *Applied Thermal Engineering*, 214, 119027
- Jain, R., & Kumar, P. (2023). Aftertreatment technologies in Euro VI diesel engines. *International Journal of Automotive Technology*, 24(1), 101–113.
- Kumbhar, V., Pandey, A. K., & Varghese, A. (2019). Effect of Fuel Injector Nozzle Hole Diameter on Emissions of CAT 3401 Diesel Engine Using CONVERGE™ CFD. *International Journal of Engineering and Advanced Technology (IJEAT)*, 8(6).
<https://doi.org/10.35940/ijeat.F8231.088619>
- Karimian, E., Moghaddam, M., Hashemi, S. H., & Tavakoli, M. (2022). Process Optimization in Selective Laser Melting for Fuel Injector Components. *Materials Today Communications*, 33, 104512. <https://doi.org/10.1016/j.mtcomm.2022.104512>
- Karimkashi, S., Yari, M., & Reitz, R. D. (2021). Effect of Injector Nozzle Geometry on Diesel Spray and Combustion Characteristics. *Journal of Energy Resources Technology*, 143(7), 072301. <https://doi.org/10.1115/1.4049740>
- Kim, H., & Lee, D. (2022). CFD-Based Assessment of Atomization Efficiency in High-Pressure Common-Rail Injectors. *Fuel*, 329, 125385.
<https://doi.org/10.1016/j.fuel.2022.125385>
- Kim, D., & Lee, Y. (2023). Spray Stability and Cavitation Analysis in Multi-Hole Injectors at Various Injection Pressures. *International Journal of Engine Research*, 25(1), 78–92.

<https://doi.org/10.1177/14680874231117154>

Kothiwale, G. R., Akkoli, K. M., Doddamani, B. M., Kattimani, S. S., Ağbulut, Ü., Afzal, A., Kaladgi, A. R., & Said, Z. (2022). Impact of injector nozzle diameter and hole number on performance and emission characteristics of CI engine powered by nanoparticles. *International Journal of Environmental Science and Technology*, 20(5), 5013–5034. <https://doi.org/10.1007/s13762-022-04397-0>

Kumar, N., & Thakur, D. (2022). Evolving trends in particulate emission control. *Clean Technologies*, 4(3), 345–359.

Kumbhar, V., Pandey, A. K., & Varghese, A. (2019). Effect of Fuel Injector Nozzle Hole Diameter on Emissions of CAT 3401 Diesel Engine Using CONVERGE™ CFD. *International Journal of Engineering and Advanced Technology*, 8(6), 927-931.

Lapuerta, M., Armas, O., & Herreros, J. M. (2021). Spray Characteristics of Biodiesel-Ethanol Blends in Common Rail Injectors. *Renewable Energy*, 179, 843–857. <https://doi.org/10.1016/j.renene.2021.07.004>

Lapuerta, M., Armas, O., & Herreros, J. M. (2021). Material Compatibility and Stability of Diesel-Biodiesel-Ethanol Blends. *Renewable Energy*, 179, 843–857. <https://doi.org/10.1016/j.renene.2021.07.004>

Li, X., Zhang, Y., & Sun, L. (2022). Advances in CNC Micro-Machining for Fuel Injector Orifices. *Precision Engineering*, 76, 509–520. <https://doi.org/10.1016/j.precisioneng.2022.03.014>

Li, Y., & Tan, Y. (2021). Ceramic Composites in Atomization Systems for Biofuel Compatibility. *Journal of Materials Science and Engineering*, 29(2), 77–88.

- Liu, Y., & Su, W. (2024). The influence of injector nozzle diameter on high-density and lean mixture combustion in heavy-duty diesel engines. *Energies*, 17(11), 2549. <https://doi.org/10.3390/en17112549>
- Markov, V. A., Sa, B., Kamaltdinov, V., Neverov, V., & Zherdev, A. (2022). Investigation on the effect of the flow passage geometry of diesel injector nozzle on injection process parameters and engine performances. *Energy Science & Engineering*, 10(2), 552–577. <https://doi.org/10.1002/ese3.1051>
- Manente, V., D'Errico, G., & Giansetti, M. (2023). Experimental and Simulation Study of E-Fuel Spray Characteristics in Diesel Injectors. *Fuel Processing Technology*, 243, 107615. <https://doi.org/10.1016/j.fuproc.2023.107615>
- Manin, J., Pickett, L. M., Malbec, L. M., & Venugopal, R. (2021). Influence of Spray Characteristics on Soot and Combustion Efficiency in Multi-hole Injectors. *International Journal of Engine Research*, 22(5), 1387–1401. <https://doi.org/10.1177/1468087420981461>
- Mercedes-Benz Trucks. (2023). Actros Series Overview and Performance Report. [mercedes-benz-trucks.com](https://www.mercedes-benz-trucks.com)
- Mishra, S. S., Mohapatra, T., Sahoo, S. S., & Mishra, P. (2022). Overall performance investigation and optimization of a multi-fuel operated compression ignition engine using coupled Taguchi and Grey relational analysis. *ACS Omega*, 7(37), 33,216–33,232. <https://doi.org/10.1021/acsomega.2c03566>
- Mohanraj, S., Karthikeyan, S., & Ravi, M. (2021). "Review of Atomization Techniques in Diesel Engines and their Impact on Combustion and Emission." *Fuel*, 305, 121614.

<https://doi.org/10.1016/j.fuel.2021.121614>

Most, J., & Duret, A. (2022). High-Fidelity CFD Analysis for Atomization Optimization in Diesel Injectors. *Applied Thermal Engineering*, 193, 117016.

<https://doi.org/10.1016/j.applthermaleng.2021.117016>

Mostafa, H., Zhang, Y., Chen, J., & Li, W. (2023). Digital Twin and CFD-Based Simulation of Spray and Combustion in Atomization Systems. *Computers & Fluids*, 258, 105873. <https://doi.org/10.1016/j.compfluid.2023.105873>

Musa, I., Bukenya, J., & Okello, C. (2023). Atomization Research in African Diesel Truck Applications. *East African Journal of Engineering*, 5(1), 78–85.

Nazemian, M., Nazemian, M., Hosseini Bohlooli, M., & Hosseinitazek, M. R. (2024). Role of Nozzle Hole Diameter in Modulating Spray Dynamics and Enhancing Combustion Performance in Reactivity-Controlled Compression Ignition Engines. *Automotive Science and Engineering (ASE)*.

NHTSA (2022). Corporate Average Fuel Economy (CAFE) Standards. U.S. Department of Transportation. <https://www.nhtsa.gov>

Park, S. J., Lee, Y. W., & Lee, H. (2021). CRDI Diesel Combustion Characterization. *Journal of Mechanical Science and Technology*, 35(4), 1123–1130.

Park, M., Lee, J., Kim, S., & Choi, H. (2023). Tribological Performance of DLC-Coated Fuel Injector Components Under Ultra-High Injection Pressure. *Tribology International*, 182, 108164. <https://doi.org/10.1016/j.triboint.2023.108164>

Payri, R., Marti-Aldaravi, P., & Bardi, M. (2020). Spray Analysis of Pilot and Main Injection Strategies in Diesel Engines. *Energy Conversion and Management*, 215,

112896. <https://doi.org/10.1016/j.enconman.2020.112896>

Payri, R., Salvador, F. J., Carreres, M., & Gimeno, J. (2020). Study of Visualization Experiment on the Influence of Injector Nozzle Diameter on Diesel Engine Spray Ignition and Combustion Characteristics. *Energies*, 13(9), 2345. <https://doi.org/10.3390/en13092345>

Payri, R., Salvador, F. J., & Martínez-López, J. (2021). Effect of Injector Geometry on Atomization and Emission Trends. *SAE Int. J. Engines*.

Prasad, B.K., Sridharan, S., & Kumar, R. (2022). "Fuel Spray and Atomization Characterization for Modern Diesel Engine Injectors." *Journal of Energy Resources Technology*, 144(3), 032302. <https://doi.org/10.1115/1.4053235>

RD Reitz, H Ogawa, R Payri, T Fansler, S Kokjohn, Y Moriyoshi, AK Agarwal, D Arcoumanis, D Assanis, C Bae, et al. *IJER editorial: The future of the internal combustion engine. International Journal of Engine Research*, 21(1):3–10, 2020.

Reitz, R.D., & Ogawa, H. (2022). "Advanced Compression-Ignition Combustion Strategies for High-Efficiency Engines." *Progress in Energy and Combustion Science*, 91, 100954. <https://doi.org/10.1016/j.pecs.2022.100954>

Rezaei, M., Naseri, M., Amini, E., & Ahmadi, G. (2023). Machine Learning-Based Injector Control for Real-Time Combustion Optimization. *Applied Energy*, 337, 120920. <https://doi.org/10.1016/j.apenergy.2023.120920>

Rezaei, M., Naseri, M., Amini, E., & Ahmadi, G. (2023). Transient spray simulation in direct injection engines with variable injection parameters. *Energy Conversion and Management*, 274, 116433. <https://doi.org/10.1016/j.enconman.2023.116433>

- Saleh, H.E., Youssef, T. A., & Elshaer, A. (2023). "Materials Compatibility of Biodiesel Blends with Aluminum Alloys in Diesel Engines." *Renewable Energy*, 202, 421–431. <https://doi.org/10.1016/j.renene.2023.02.023>
- Sharma, R., Patel, S., Verma, A., & Gupta, N. (2023). Real-Time Control of Diesel Engine Fuel Injection Based on Sensor Feedback for Improved Atomization. *Applied Thermal Engineering*, 217, 119243. <https://doi.org/10.1016/j.applthermaleng.2022.119243>
- Sharma, R., Patel, S., Verma, A., & Gupta, N. (2023). AI-based adaptive fuel injection control for combustion optimization. *Applied Thermal Engineering*, 217, 119243. <https://doi.org/10.1016/j.applthermaleng.2022.119243>
- Shehata, M. S. A., & Attia, A. M. A. (2018). Effect of nozzle hole and pump plunger diameters on the performance of a diesel engine fueled with *Jatropha* oil. *International Journal of Green Energy*, 15(2), 148-156.
- Shoaib, M., Ahmad, A., Khan, M. M., & Usman, M. (2022). Performance Degradation in Diesel Injectors Due to Biofuel Fouling and Deposits. *Energy Conversion and Management*, 269, 116073. <https://doi.org/10.1016/j.enconman.2022.116073>
- Singh, A., & Verma, M. (2022). Effect of atomization on particulate matter and combustion characteristics. *Fuel*, 310, 122421.
- Singh, R., & Verma, P. (2021). Heat Transfer Modeling in Multi-Component Fuel Spray Systems. *Thermal Science and Engineering Progress*, 24, 100927. <https://doi.org/10.1016/j.tsep.2021.100927>
- Singh, R., Kumar, A., & Mishra, S. (2022). Tool Steel Selection and Surface Treatments for Micro-Fuel Injection Components. *Manufacturing Review*, 9, 12.

<https://doi.org/10.1051/mfreview/2022009>

Singh, P., & Rao, V. (2022). Precision Finishing Technologies for High-Performance Injector Nozzles. *Journal of Manufacturing Processes*, 75, 788–796.

<https://doi.org/10.1016/j.jmapro.2022.01.011>

Singh, P., & Rao, V. (2022). Precision Grinding Technologies for Injector Components. *International Journal of Advanced Manufacturing Technology*, 119(9), 4551–4563.

<https://doi.org/10.1007/s00170-022-09592-z>

Singh, V., & Kumar, N. (2021). Numerical investigation of the effect of nozzle hole diameter on the combustion, emission, and spray characteristics in a diesel engine.

Energy Sources, Part A: Recovery, Utilization, and Environmental Effects, 47(1), 1–

18. <https://doi.org/10.1080/15567036.2021.1980155>

Song, H., Li, J., & Yang, Z. (2020). High-Temperature Fatigue Performance of Inconel 718 for Engine Applications. *Journal of Alloys and Compounds*, 819, 153034.

<https://doi.org/10.1016/j.jallcom.2020.153034>

Toledo, E., Guerrero, F., Amador, G., & Toledo, M. (2022). Experimental assessment of the performance and fine particulate matter emissions of a LPG-diesel dual-fuel

compression ignition engine. *Energies*, 15(23), 9035.

<https://doi.org/10.3390/en15239035>.

Tzanetakis, E., Bruneaux, G., & Pickett, L. M. (2022). Experimental diesel spray characterization of single- and multi-hole nozzle configurations: ECN and production

injectors. *Frontiers in Mechanical Engineering*, 8, 940891.

<https://doi.org/10.3389/fmech.2022.940891>

- UNECE (2023). World Forum for Harmonization of Vehicle Regulations (WP.29). United Nations Economic Commission for Europe. <https://unece.org>
- Wang, J., Zhang, T., & Guo, Q. (2018). Review on Plasma Sprayed Ceramic Coatings: Process, Materials, and Applications. *Materials*, 11(4), 651.
- Wang, J., Zhang, T., & Guo, Q. (2022). Review on Ceramic Coatings for High-Performance Engine Components. *Materials*, 15(2), 392.
<https://doi.org/10.3390/ma15020392>
- Wang, J., Zhang, T., & Guo, Q. (2022). Review of Advanced Coatings for Injector Wear Resistance. *Materials*, 15(2), 392. <https://doi.org/10.3390/ma15020392>
- Wang, J., Liu, T., Zhang, L., & Zhao, X. (2023). Role of Surface Treatments in Enhancing Injector Durability and Atomization Efficiency. *Surface and Coatings Technology*, 456, 129018. <https://doi.org/10.1016/j.surfcoat.2023.129018>
- Wang, J., Zhang, T., & Guo, Q. (2023). Injector Wear and Long-Term Durability in High-Pressure Diesel Systems. *Wear*, 518–519, 205613.
<https://doi.org/10.1016/j.wear.2023.205613>
- Wang, J., Liu, T., Zhao, X., & Feng, Y. (2023). Advances in coating technologies for fuel injector durability. *Surface and Coatings Technology*, 456, 129018.
<https://doi.org/10.1016/j.surfcoat.2023.129018>
- Wang, X., Chen, Y., & Huang, Z. (2021). Effects of nozzle geometry on soot formation in heavy-duty diesel engines. *Fuel*, 289, 119819.
<https://doi.org/10.1016/j.fuel.2020.119819>
- Wang, Y., Kumar, R., Li, S., & Huang, Z. (2023). Lagrangian–Eulerian spray simulation

for diesel and e-fuels. *Applied Thermal Engineering*, 219, 119558.

<https://doi.org/10.1016/j.applthermaleng.2023.119558>

Whyte, W., & Eaton, T. (2021). *Cleanroom Technology: Fundamentals of Design Design, Testing, and Operation*. (3rd ed.). Wiley.

Xu, H., Yang, J., Li, G., & Xu, M. (2020). A numerical study on the effects of nozzle hole diameter on multi-hole injector spray characteristics in a GDI engine. *Fuel*, 276, 118039

Yang, C., Liu, H., & Wang, B. (2023). Combustion and emissions optimization in heavy-duty diesel engines. *Fuel Processing Technology*, 240, 107513.

Yuan, Q., Lin, J., Xie, Z., & Gao, Y. (2023). 3D Metrology Techniques for Automotive Injector Inspection. *Measurement Science and Technology*, 34(7), 075009.

<https://doi.org/10.1088/1361-6501/acda2a>

Yuan, Q., Lin, J., Xie, Z., & Gao, Y. (2023). Hybrid Manufacturing of Fuel Injection Systems: Combining SLM and Machining. *Manufacturing Letters*, 35, 12–19.

<https://doi.org/10.1016/j.mfglet.2023.04.002>

Zhang, H., Li, M., & Zhang, Y. (2022). Optimization of Injector Configurations in Heavy-Duty Diesel Engines. *Energy Conversion and Management*, 267, 115854.

Zhang, H., Zhao, W., & Li, J. (2022). Fuel consumption benchmarks for commercial diesel engines. *Journal of Cleaner Production*, 371, 133622.

Zhang, L., Wang, J., Li, X., & Zhao, H. (2021). Corrosion and Fatigue Behavior of Stainless Steels in Fuel Injection Systems. *Surface and Coatings Technology*, 412,

127018. <https://doi.org/10.1016/j.surfcoat.2021.127018>

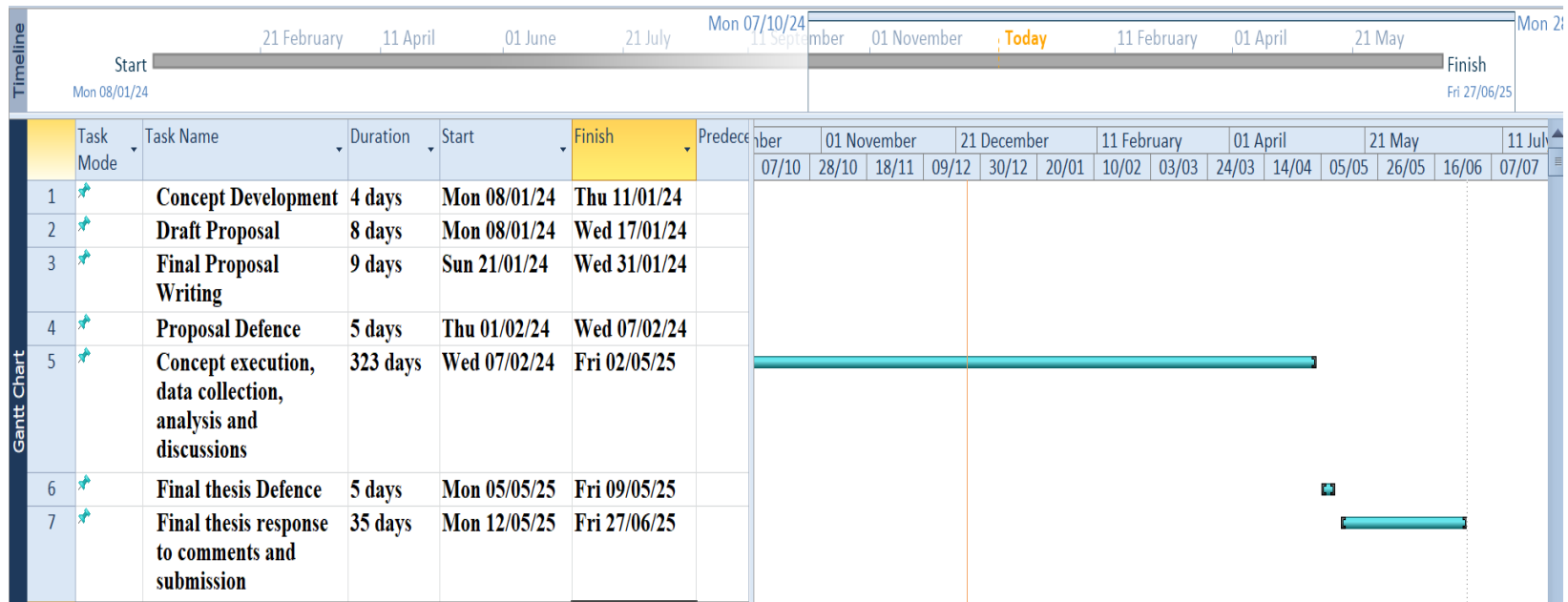
- Zhang, W., Liu, H., & Xu, T. (2023). Impact of injector nozzle hole diameter on combustion and emissions in heavy-duty diesel engines: A case study on Mercedes-Benz OM457. *Energy Conversion and Management*, 269, 116162. <https://doi.org/10.1016/j.enconman.2022.116162>
- Zhang, X., Chen, Y., Huang, Z., & Li, J. (2022). Integration of advanced combustion and injection systems for low emission engines. *Energy Conversion and Management*, 253, 115192. <https://doi.org/10.1016/j.enconman.2021.115192>
- Zhao, H., Liu, K., Wang, J., & Fang, R. (2023). "Challenges and Opportunities in Heavy-Duty Vehicle Electrification." *Applied Energy*, 344, 120265. <https://doi.org/10.1016/j.apenergy.2023.120265>
- Zhao, H., Liu, K., Fang, R., & Wang, T. (2022). Automation in Injector Assembly: A Review of Robotic Precision and Quality Control. *Procedia CIRP*, 112, 643–648. <https://doi.org/10.1016/j.procir.2022.09.104>
- Zhao, X., Li, B., Zhang, L., & Wang, H. (2022). Multiphase spray modeling in diesel combustion using hybrid Eulerian approaches. *Fuel Processing Technology*, 235, 107376. <https://doi.org/10.1016/j.fuproc.2022.107376>
- Zhang, X., Liu, Y., & Wu, H. (2022). Atomization and Spray Challenges in Advanced Emission-Compliant Diesel Engines. *Fuel*, 320, 123881. <https://doi.org/10.1016/j.fuel.2022.123881>
- Zheng, J., Zhang, G., & Liu, H. (2020). Effect of injector nozzle parameters on fuel consumption and soot emission of two-cylinder diesel engine for vehicle. *Energy Reports*, 6, 1-8. <https://doi.org/10.1016/j.egyr.2019.11.016>

Zhu, G., Chen, X., Zhang, Y., Wang, J., and Fang, L., (2016). Effects of droplet size on combustion and emissions in diesel engines. *International Journal of Engine Research*, 17(2), pp.123–132.

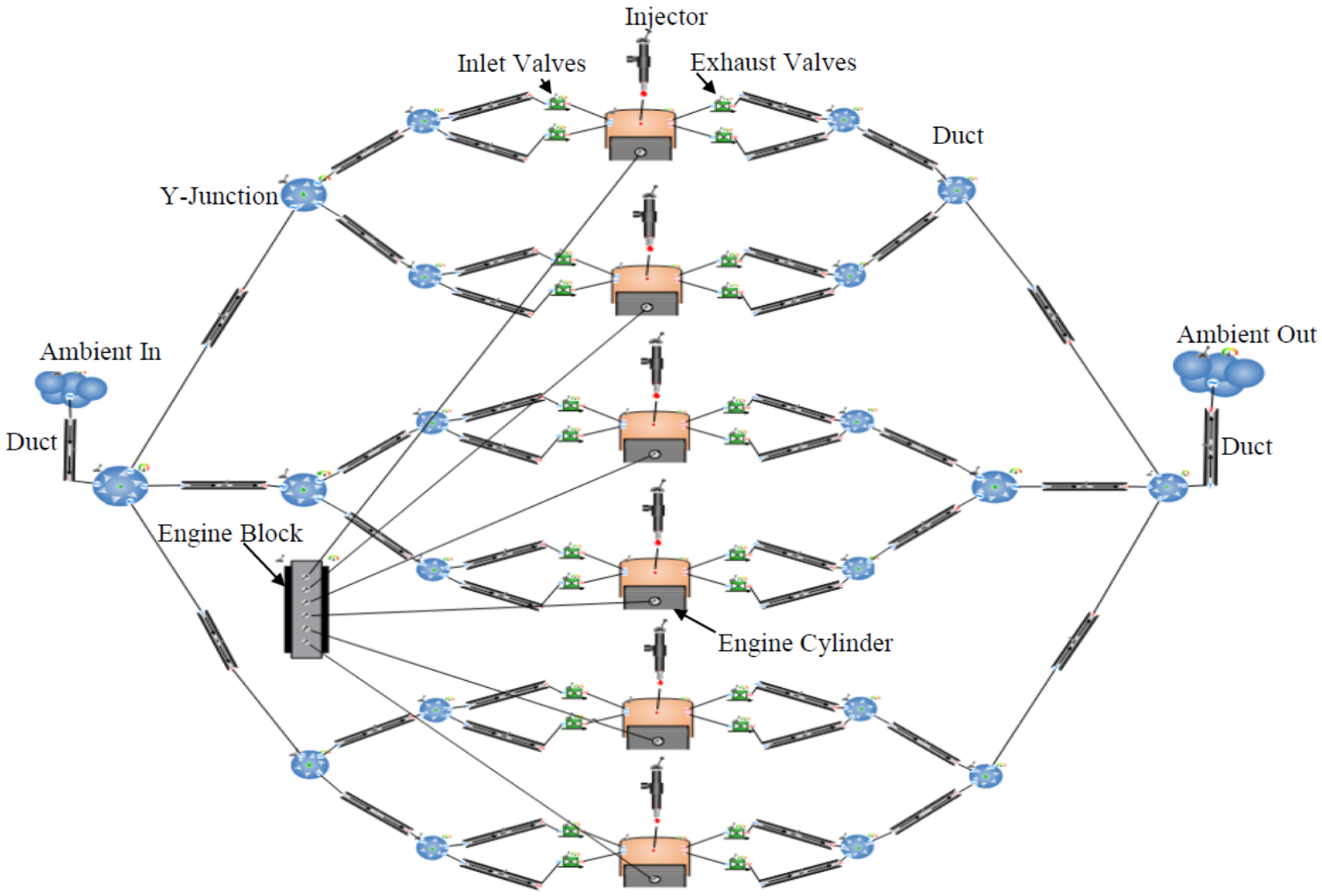
Zhu, G., Chen, X., Zhang, Y., Wang, J., and Fang, L., (2016). Effects of intake system design on volumetric efficiency and performance in internal combustion engines. *International Journal of Engine Research*,

APPENDICES

Appendix A1: Work Plan



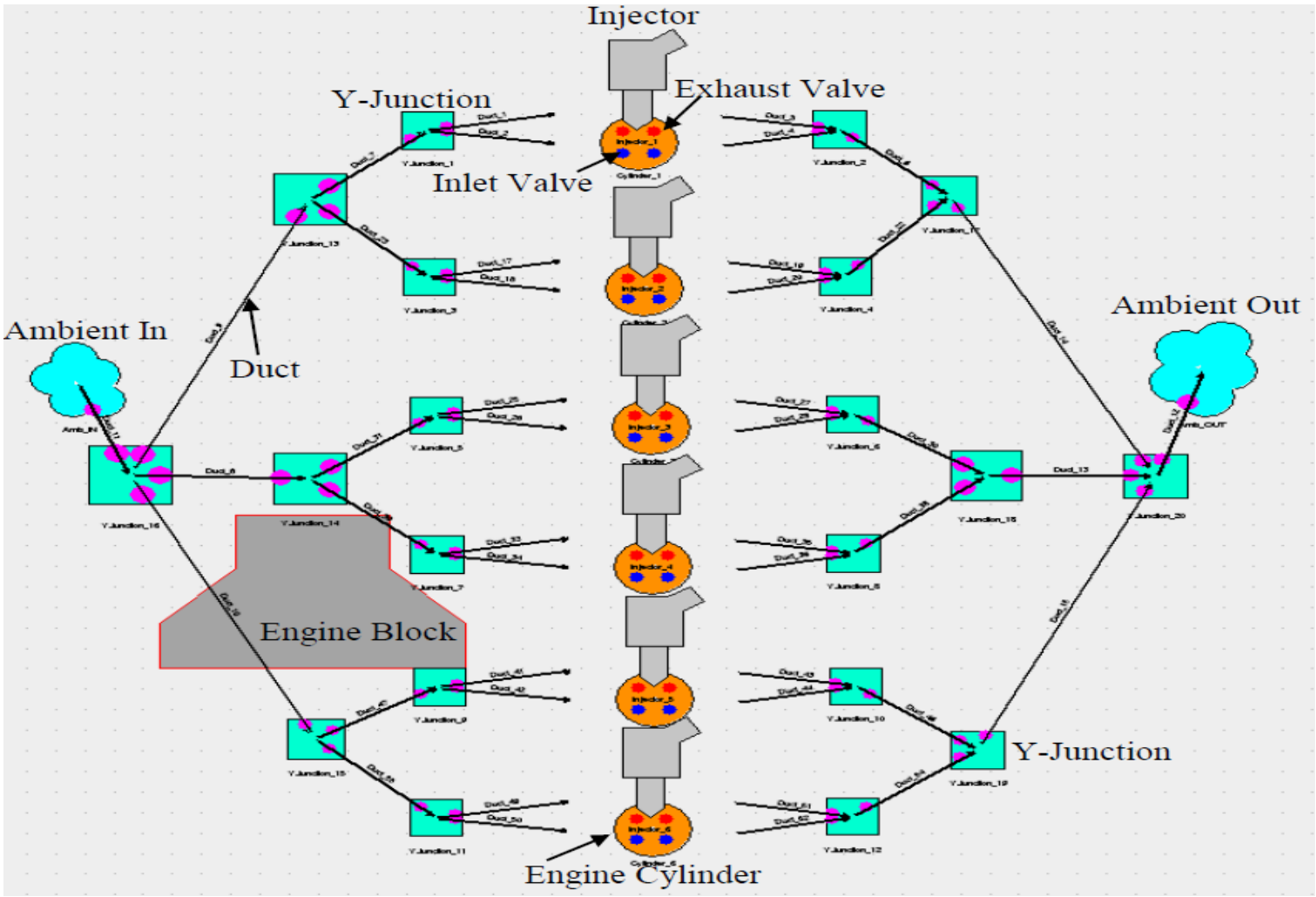
Appendix B1: Ricardo Wave Engine Model Developed



Appendix B2: Ricardo Wave Simulation Parametric Cases Definition

Show Editable ↓ ↓ ⊙ Sweep																
Search...																
	Name	Type	Units	Group	Comment	Case 1	Case 2	Case 3	Case 4	Case 5	Case 6	Case 7	Case 8	Case 9	Case 10	
Case Title						Case 1	Case 2	Case 3	Case 4	Case 5	Case 6	Case 7	Case 8	Case 9	Case 10	
Enabled						<input checked="" type="checkbox"/>	<input checked="" type="checkbox"/>	<input checked="" type="checkbox"/>	<input checked="" type="checkbox"/>	<input checked="" type="checkbox"/>	<input checked="" type="checkbox"/>	<input checked="" type="checkbox"/>	<input checked="" type="checkbox"/>	<input checked="" type="checkbox"/>	<input checked="" type="checkbox"/>	
Speed	Speed	Real	rpm		Engine Speed	700	900	1100	1300	1500	1700	1900	2100	2300	2500	
AFR	AFR	Real			Air Fuel Ratio	14.5	14.5	14.5	14.5	14.5	14.5	14.5	14.5	14.5	14.5	
Hole Diameter	Hole_Dia...	Real	mm		Nozzle Hole Dia...	0.194	0.203...	0.212...	0.222	0.231...	0.240...	0.25	0.259...	0.268...	0.278	
soinj	soinj	Real	deg		soinj	-11.5	-11.5	-11.5	-11.5	-11.5	-11.5	-11.5	-11.5	-11.5	-11.5	
NCYC	NCYC	Integer	cycle			20	20	20	20	20	20	20	20	20	20	
+																

Appendix B3: Ricardo Wave Post Model Image



Appendix C1: Budget

Particulars	Unit	Quantity	Rate (UGX)	Amount (UGX)
Transport	FUEL	N/A	1,500,000	1,500,000
Air Time	Freedom/Unlimited Bundles (5000 min of Airtel & Mtn)	2	75,000	150,000
Secretarial Work	N/A	1	700,000	700,000
Ricardo Wave Software	N/A	1	1,500,000	1,500,000
Internet	N/A	65GB	150,000	150,000
TOTAL				4,000,000

Appendix D1: Ricardo Wave Simulation Output File

```
Output
Executing Serial Solution
Translation finished successfully (0 errors, 0 warnings)
Executing Serial Solution
  WAVE Version 2019.1 Build 154161
  File: D:\JK Masters Thesis\RW MODEL\RW_MERCEDES_BENZ_3340_LS_ENGINE_MODEL_3_FINAL_THESIS_for_JK_WAVE
  Case 1 of 10

  BAS:OUTPUT_CONTROL
  BAS:CONSTANTS
  BAS:GENERAL
    I*** reading active.tags found in "C:\Program Files\Ricardo\2019.1\Products\WAVE\Config"
    I*** Loading property data: DIESEL: C:\Program Files\Ricardo\2019.1\Common\propty\data\fuels\d:
    Diesel
  BAS:PASSIVE_SCALAR_LIST
  BAS:OUTPUT
  BAS:COMPATIBILITY
  DUC:DUCT
  DUC:SHAPE
  DUC:REMS
```

```
Output
JUN:INITIAL
TAG:flowElements
  I*** 6 <cylinder> tags found
ENG:GEOMETRY

  FIRING SEQUENCE, FIRING TDC, AND FIRING INTERVALS
    1      5      3      6      2      4
    0.0 120.0 240.0 360.0 480.0 600.0
    120.0 120.0 120.0 120.0 120.0 120.0

  ENG:OPERATING
  VAL:VALVES
    I*** 433 POINTS READ FROM FILE: truck-in.val: C:\Program Files\Ricardo\2019.1\Products\WAVE\Exar
-in.val
    I*** 24 POINTS READ FROM FILE: CFTYP: C:\Program Files\Ricardo\2019.1\Products\WAVE\Tutorials\B
I*** VALVE #1: TVO = 336.2257, TVC = 537.7743 FLOW COEF BASED ON SEAT AREA
    I*** NV = 1 AEFMAX = 568.1 (mm2) DVALVE(NV) = 35.00 (mm) CDMAX = 0.42113
    I*** 485 POINTS READ FROM FILE: truck-ex.val: C:\Program Files\Ricardo\2019.1\Products\WAVE\Exar
-ex.val
    I*** 24 POINTS READ FROM FILE: CFTYP: C:\Program Files\Ricardo\2019.1\Products\WAVE\Tutorials\B
```

Appendix D2: Ricardo Wave Simulation Summary Data File

Default Summary Data - RW_MODEL_MERCEDES_BENZ_3340_LS_FINAL_THESIS_for_JK_WAVE_Solver_001.sum, Data for engine

Name Data for engine

Results Table

		699	900	1100	1299	1500	1700	1900	2100	2300	2500
1 Engine speed	rpm	699	900	1100	1299	1500	1700	1900	2100	2300	2500
2 Case	-	1	2	3	4	5	6	7	8	9	10
3 Subcase	-	0	0	0	0	0	0	0	0	0	0
4 Case title	-	Case 1	Case 2	Case 3	Case 4	Case 5	Case 6	Case 7	Case 8	Case 9	Case 10
5 Stoichiometric A/F	-	14.2205	14.2205	14.2205	14.2205	14.2205	14.2205	14.2205	14.2205	14.2205	14.2205
6 Trapped A/F	-	14.4985	14.498	14.4973	14.4964	14.4948	14.4929	14.4909	14.4862	14.4808	14.4734
7 Mass Airflow	kg/hr	204.922	237.834	256.386	262.731	260.562	251.389	237.675	220.628	201.637	180.539
8 Pseudo-volumetric efficiency	kg/hr/rpm	0.292746	0.26426	0.233078	0.202101	0.173708	0.147876	0.125092	0.105061	0.087668	0.0722156
9 Auxiliary Power	kW	0	0	0	0	0	0	0	0	0	0
10 BMEP	bar	7.34139	6.147	4.83684	3.55024	2.40156	1.3662	0.455832	-0.343324	-1.04088	-1.6586
11 Brake Power	kW	51.158	55.0736	52.9654	45.945	35.8611	23.1208	8.62176	-7.1773	-23.8322	-41.2781
12 Brake specific CO emissions	g/kW/hr	6.57553	12.9916	19.897	26.2404	34.5388	49.1707	108.79	-95.8085	-19.7648	-7.99316
13 BSFC	kg/kW/hr	0.276284	0.297874	0.333909	0.394489	0.501311	0.750294	1.90261	-2.12239	-0.584414	-0.302296
14 Brake specific unburned fuel emissions	g/kW/hr	0.271693	0.316048	0.390147	0.514819	0.735376	1.24076	3.53854	-4.41507	-1.35035	-0.769803
15 Brake specific NO2 emissions	g/kW/hr	21.6079	42.6917	65.3894	86.2288	113.498	161.58	357.497	-314.837	-64.9494	-26.2664
16 Charging efficiency	-	0.715007	0.635853	0.54294	0.452402	0.363912	0.279663	0.207027	0.144506	0.089755	0.174626
17 Delivered efficiency	-	0.714918	0.635741	0.542807	0.452249	0.363744	0.279487	0.206849	0.144332	0.0896056	0.174218
18 Total delivered efficiency	-	0.714918	0.635741	0.542807	0.452249	0.363744	0.279487	0.206849	0.144332	0.0896055	0.174219
19 Combined Displacement	m³	0.0119459	0.0119459	0.0119459	0.0119459	0.0119459	0.0119459	0.0119459	0.0119459	0.0119459	0.0119459
20 Brake thermal engine efficiency	%	30.444	28.2375	25.1901	21.3218	16.7784	11.2106	4.42087	-3.9631	-14.3926	-27.8244
21 EGR	-	-6.38246e-	-2.17917e-	-7.07805e-	-1.49868e-	-6.9184e-	-6.01485e-	2.35937e-	-6.96178e-	-1.70088e-	-4.02829e-0
22 FMEP	bar	1.26283	1.30757	1.35798	1.41279	1.47519	1.54466	1.62162	1.70214	1.7862	1.87143
23 Friction Energy Loss	%	5.23691	6.00662	7.07231	8.48483	10.3064	12.6749	15.7272	19.6483	24.6984	31.3948
24 Friction torque	Nm	120.048	124.302	129.099	134.303	140.236	146.839	154.156	161.91	169.801	177.904
25 Fuel mass flow	kg/hr	14.1342	16.405	17.6856	18.1248	17.9775	17.3474	16.4039	15.233	13.9279	12.4782
26 Fuel volume flow	L/hr	18.5354	21.5133	23.1927	23.7687	23.5756	22.7492	21.5119	19.9764	18.2649	16.3638
27 Engine out CO mass flow	g/s	0.0934421	0.198748	0.292762	0.334893	0.344055	0.315796	0.260546	0.191013	0.130845	0.0916506
28 GMEP	bar	9.34069	8.4912	7.45977	6.3898	5.42429	4.55134	3.79172	3.13248	2.56394	2.05922
29 GMEP from crossing point	bar	9.30678	8.41761	7.33594	6.20789	5.17678	4.24079	3.42932	2.73427	2.14227	1.63146
30 Engine out unburned fuel flow	g/s	0.00386092	0.00483498	0.00574008	0.00657037	0.00732530	0.0079687	0.0084745	0.0088023	0.00893943	0.00882666
31 Engine out NO2 mass flow	g/s	0.307061	0.653107	0.962048	1.10049	1.1306	1.03774	0.856182	0.627688	0.429969	0.301174
32 Heat Transfer Rate	W	43134.6	45906.1	48421.8	50350.1	52188.1	53741	55279	56915.3	58241.7	58716.6
33 Heat Transfer Loss	%	25.6693	23.5371	23.0292	23.3661	24.4174	26.0573	28.3447	31.427	35.1728	39.5792
34 Indicated Power	hp	80.4049	89.5651	90.9693	86.1317	77.6307	66.0609	52.6936	38.0936	22.8848	7.1032
35 IMEP	bar	8.60422	7.45457	6.19482	4.96303	3.87675	2.91086	2.07445	1.35881	0.745325	0.212834
36 ISAC	kg/kW/hr	3.41776	3.56099	3.7795	4.09058	4.50105	5.10315	6.0487	7.76682	11.8157	34.0842
37 ISFC	kg/kW/hr	0.235735	0.245625	0.260712	0.282193	0.310551	0.352149	0.41747	0.536251	0.816158	2.35578
38 Indicated Torque	N*m	817.941	708.653	598.897	471.799	368.535	276.715	197.408	128.173	70.8527	20.2326
39 Lambda	-	1.01955	1.01951	1.01946	1.0194	1.01928	1.01915	1.01901	1.01868	1.0183	1.01788

OK Apply Cancel Help

Default Summary Data - RW_MODEL_MERCEDES_BENZ_3340_LS_FINAL_THESIS_for_JK_WAVE_Solver_001.sum, Data for engine

Name Data for engine

Results Table

		699	900	1100	1299	1500	1700	1900	2100	2300	2500
40 Lower Heating Value	J/kg	4.28e+07	4.28e+07	4.28e+07	4.28e+07	4.28e+07	4.28e+07	4.28e+07	4.28e+07	4.28e+07	4.28e+07
41 Reference pressure	bar	1	1	1	1	1	1	1	1	1	1
42 Exhaust port pressure	bar	1.44222	1.56129	1.62972	1.65199	1.64286	1.60726	1.55784	1.50205	1.44515	1.38711
43 Trapped equivalence ratio	-	0.980828	0.980865	0.980908	0.980971	0.981081	0.981209	0.981343	0.981661	0.982025	0.98253
44 Intake port pressure	bar	0.960766	0.943416	0.929507	0.922136	0.920292	0.924219	0.929613	0.935368	0.94168	0.949579
45 PMEP	bar	-0.736476	-1.03663	-1.26495	-1.42677	-1.54753	-1.64048	-1.71427	-1.77367	-1.81862	-1.84638
46 PMEP from crossing point	bar	-0.702568	-0.963036	-1.14112	-1.24487	-1.30002	-1.32993	-1.35187	-1.37546	-1.39694	-1.41862
47 CO	ppm	1594.74	2922.57	3993.58	4457.95	4618.25	4393.35	3833.37	3028.08	2269.39	1774.72
48 HC	ppm	134.728	145.37	160.998	178.829	201.048	226.671	254.938	285.313	317.017	349.47
49 NOx	ppm	3189.40	5845.14	7987.17	8915.9	9236.49	8786.7	7666.75	6056.16	4538.77	3549.44
50 Pumping torque	N*m	-70.0115	-98.545	-120.25	-135.633	-147.113	-155.948	-162.963	-168.61	-172.883	-175.523
51 Plenum volumetric efficiency	-	0.72631	0.664685	0.594183	0.516557	0.442773	0.375346	0.315803	0.263865	0.219392	0.180181
52 Plenum volumetric efficiency (air-only)	-	0.726311	0.664686	0.594187	0.516557	0.442776	0.375346	0.315803	0.263865	0.219393	0.18018
53 Residual gas fraction	%	10.169	12.6407	15.2838	18.0914	20.9954	24.3223	28.159	32.7073	37.8809	43.8293
54 Scavenging efficiency	-	0.89831	0.873593	0.847162	0.819086	0.790046	0.756777	0.71841	0.672927	0.621191	0.561707
55 Scavenging ratio	-	0.898198	0.879438	0.846949	0.818809	0.789677	0.7563	0.717806	0.672116	0.620156	0.560394
56 Breakup length	m	0.0219299	0.0238639	0.0261644	0.0289084	0.0319211	0.0351711	0.0386377	0.0423352	0.0461423	0.0499828
57 Smoke emissions (Bosch smoke units)	-	4.6513	4.56304	5.12932	6.55575	7.67285	8.50256	8.85773	8.61763	7.71006	6.52568
58 Nozzle diameter	m	0.000194	0.00020333	0.00021266	0.000222	0.0002313	0.00024066	0.00025	0.00025933	0.00026866	0.000278
59 Mean droplet diameter	m	1.11696e-0	1.09115e-0	1.08441e-0	1.08573e-0	1.08991e-0	1.12295e-0	1.15482e-0	1.1317e-0	1.17403e-0	1.21825e-0
60 Injected fuel mass	kg	0.0001218	0.00010128	8.93389e-0	7.74769e-0	6.66098e-0	5.67185e-0	4.79952e-0	4.03371e-0	3.36859e-0	2.778e-0
61 Indicated specific mass flow of NO2	g/kW/hr	10.0733	7.19618	3.82274	1.36223	0.370998	0.029895	0.0363552	0.0054072	-0.0001256	-5.24088e-
62 Indicated power	hp	12.1	13.9697	14.2871	13.136	11.4142	9.45227	7.59123	5.8126	4.21735	2.84098
63 Indicated power	kW	9.02296	10.4172	10.6539	9.79549	8.51157	7.04856	5.66082	4.33446	3.14488	2.11852
64 Indicated mean effective pressure	psi	112.682	101.184	84.6281	65.87	49.6048	36.2457	26.0454	18.0435	11.9531	7.40793
65 Indicated mean effective pressure	bar	7.76918	6.97641	5.83766	4.54158	3.42013	2.49905	1.79577	1.24405	0.824138	0.510759
66 Indicated specific fuel consumption	lbm/hp/hr	0.429254	0.431554	0.454931	0.507118	0.578948	0.674672	0.794497	0.963848	1.21505	1.61681
67 Indicated specific fuel consumption	kg/kW/hr	0.261105	0.262550	0.276724	0.308468	0.352161	0.410388	0.483274	0.58287	0.739085	0.983471
68 Indicated thermal efficiency	%	29.9373	29.7777	28.2475	25.3406	22.1966	18.0473	16.1744	13.3327	10.5763	7.94815
69 Indicated thermal particulate emission	g/kW/hr	2.01318	2.13727	3.14681	6.3948	11.6557	22.527	66.4058	-79.0591	-17.1525	-6.8907
70 Emission NOx	ppm	1348.6	871.12	401.203	118.066	24.5602	3.9509	0.57945	0.0727889	0.00570239	0.00041704
71 Swirl ratio	-	1.96	1.96	1.96	1.96	1.96	1.96	1.96	1.96	1.96	1.96
72 Mean injection velocity	m/s	124.14	131.166	129.273	121.506	111.077	99.0409	86.805	74.9342	63.859	53.4633
73 Injection timing (ATDC)	deg	-11.5	-11.5	-11.5	-11.5	-11.5	-11.5	-11.5	-11.5	-11.5	-11.5
74 Ambient reference temperature	K	300	300	300	300	300	300	300	300	300	300
75 Exhaust gas temperature	K	1220.7	1287.8	1330.69	1362.49	1382.67	1388.77	1388.41	1385.47	1378.01	1365.79
76 Intake port gas temperature	K	291.772	282.236	269.189	256.604	239.805	217.219	191.154	159.796	119.69	65.965
77 Brake Torque	N*m	697.894	584.351	459.804	337.496	228.299	129.875	43.3327	-82.8378	-498.948	-157.671
78 Trapping ratio	-	1.00012	1.00017	1.00024	1.00034	1.00046	1.00063	1.00086	1.0012	1.00167	1.00235

OK Apply Cancel Help

Default Summary Data - RW_MODEL_MERCEDES_BENZ_3340_LS_FINAL_THESIS_for_JK_WAVE_Solver_001.sum, Data for engine

Name Data for engine

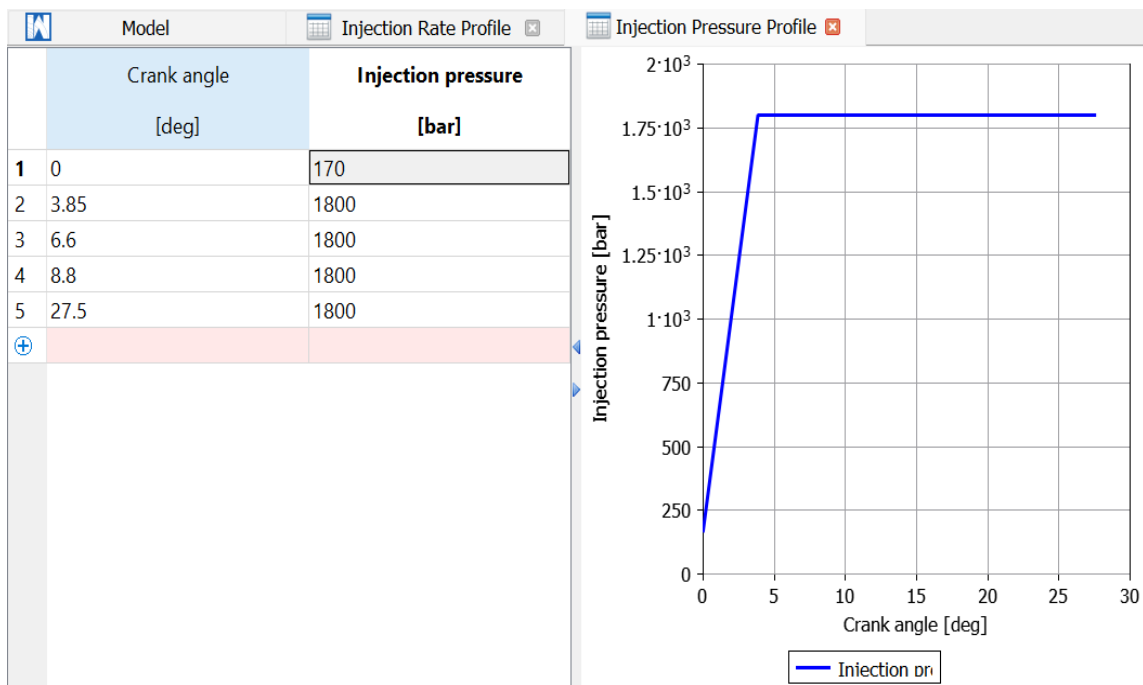
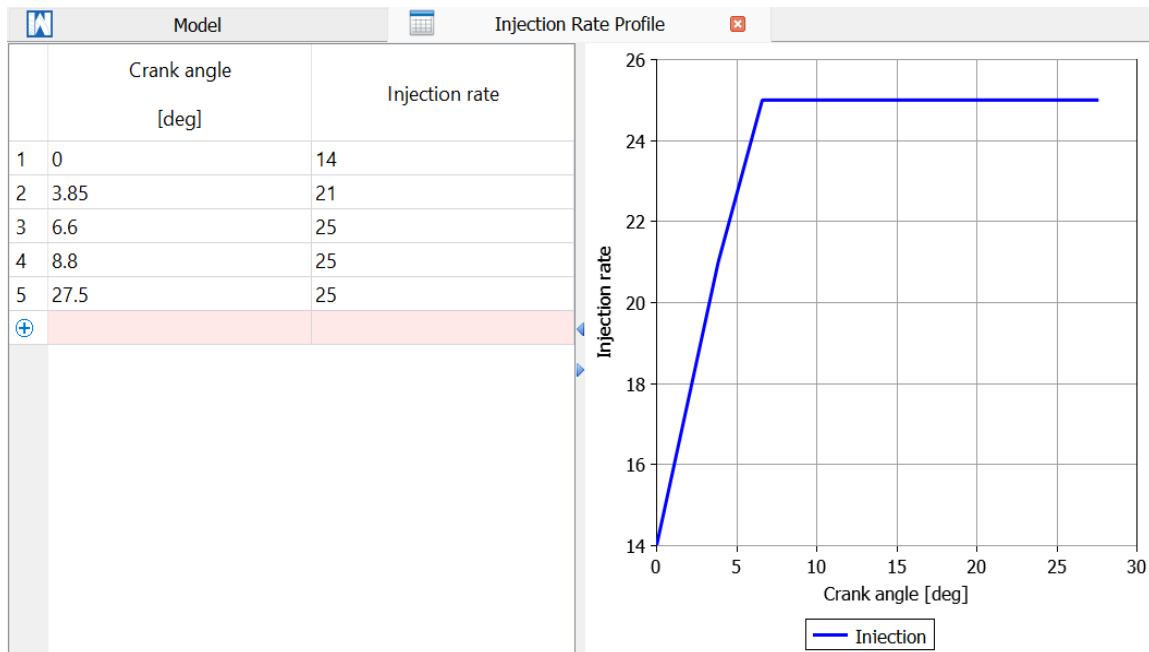
Results Table

43	Trapped equivalence ratio	-	0.980828	0.980865	0.980908	0.980971	0.981081	0.981209	0.981343	0.981661	0.982025	0.98253
44	Intake port pressure	bar	0.960766	0.943416	0.929507	0.922136	0.920922	0.924219	0.929613	0.935368	0.94168	0.949579
45	PMEP	bar	-0.736476	-1.03663	-1.26495	-1.42677	-1.54753	-1.64048	-1.71427	-1.77367	-1.81862	-1.84638
46	PMEP from crossing point	bar	-0.702568	-0.963036	-1.14112	-1.24487	-1.30002	-1.32993	-1.35187	-1.37546	-1.39694	-1.41862
47	CO	ppm	1594.74	2922.57	3993.58	4457.95	4618.25	4393.35	3833.37	3028.08	2269.39	1774.72
48	HC	ppm	134.728	145.37	160.098	178.829	201.048	226.671	254.938	285.313	317.017	349.47
49	NOx	ppm	3189.48	5845.14	7987.17	8915.9	9236.49	8786.7	7666.75	6056.16	4538.77	3549.44
50	Pumping torque	N*m	-70.0115	-98.545	-120.25	-135.633	-147.113	-155.948	-162.963	-168.61	-172.883	-175.523
51	Plenum volumetric efficiency	-	0.72631	0.664685	0.594183	0.516557	0.442773	0.375346	0.31582	0.263863	0.219392	0.180181
52	Plenum volumetric efficiency (air-only)	-	0.726311	0.664686	0.594187	0.516557	0.442776	0.375346	0.315813	0.263865	0.219393	0.18018
53	Residual gas fraction	%	10.169	12.6407	15.2838	18.0914	20.9954	24.3223	28.159	32.7073	37.8809	43.8293
54	Scavenging efficiency	-	0.89831	0.873593	0.847162	0.819086	0.790046	0.756777	0.71841	0.672927	0.621191	0.561707
55	Scavenging ratio	-	0.898198	0.873438	0.846949	0.818809	0.789677	0.7563	0.717806	0.672116	0.620156	0.560394
56	Breakup length	m	0.0219299	0.0238639	0.0261644	0.0289084	0.0319211	0.0351711	0.0386377	0.0423352	0.0461423	0.0499828
57	Smoke emissions (Bosch smoke units)	-	4.6513	4.56304	5.12932	6.55575	7.67285	8.50256	8.85773	8.61763	7.71006	6.52568
58	Nozzle diameter	m	0.000194	0.00020333	0.00021266	0.000222	0.0002313	0.00024066	0.00025	0.00025933	0.00026866	0.000278
59	Mean droplet diameter	m	1.11696e-0	1.09115e-0	1.08441e-0	1.08573e-0	1.09891e-0	1.12295e-0	1.15482e-0	1.3157e-05	1.67403e-0	2.17825e-0
60	Injected fuel mass	kg	0.00011218	0.00010128	8.93389e-0	7.74768e-0	6.66098e-0	5.67185e-0	4.79952e-0	4.03371e-0	3.36859e-0	2.778e-05
61	Indicated specific mass flow of NO2	g/kW/hr	10.0733	7.19618	3.82274	1.36223	0.370998	0.092995	0.0363552	-0.0054072	-0.0001256	-5.24088e-0
62	Indicated power	hp	12.1	13.9697	14.2871	13.136	11.4142	9.45227	7.59128	5.8126	4.21735	2.84098
63	Indicated power	kW	9.02296	10.4172	10.6539	9.79549	8.51157	7.04856	5.66082	4.33446	3.14488	2.11852
64	Indicated mean effective pressure	psi	112.682	101.184	84.6681	65.87	49.6048	36.2457	26.0454	18.0435	11.9531	7.40793
65	Indicated mean effective pressure	bar	7.76918	6.97641	5.83766	4.54158	3.42013	2.49905	1.79577	1.24405	0.824138	0.510759
66	Indicated specific fuel consumption	lbm/hp/h	0.429254	0.431554	0.454931	0.507118	0.578948	0.674672	0.794497	0.963848	1.21505	1.61681
67	Indicated specific fuel consumption	kg/kW/hr	0.261105	0.262505	0.276724	0.308468	0.352161	0.410388	0.483274	0.586287	0.739085	0.983471
68	Indicated thermal efficiency	%	29.9373	29.7777	28.2475	25.3406	22.1966	19.0473	16.1746	13.3327	10.5763	7.94815
69	Indicated specific particulate emission	g/kW/hr	2.01318	2.13727	3.14681	6.3948	11.6557	22.527	65.4058	-73.0591	-17.1525	-6.8907
70	Emission NOx	ppm	1348.6	871.12	401.203	118.066	24.5602	3.9509	0.57945	0.0727889	0.00570239	0.00041704
71	Swirl ratio	-	1.96	1.96	1.96	1.96	1.96	1.96	1.96	1.96	1.96	1.96
72	Mean injection velocity	m/s	124.14	131.166	129.273	121.586	111.077	99.0409	86.805	74.9342	63.859	53.4633
73	Injection timing (ATDC)	deg	-11.5	-11.5	-11.5	-11.5	-11.5	-11.5	-11.5	-11.5	-11.5	-11.5
74	Ambient reference temperature	K	300	300	300	300	300	300	300	300	300	300
75	Exhaust gas temperature	K	1220.7	1287.8	1330.69	1362.49	1382.67	1388.77	1388.41	1385.47	1387.01	1365.79
76	Intake port gas temperature	K	291.772	282.236	269.189	256.604	239.805	217.219	191.154	159.796	119.69	65.965
77	Brake Torque	N*m	697.894	584.351	459.804	337.496	228.299	129.875	43.3327	-32.6373	-98.9487	-157.671
78	Trapping ratio	-	1.00012	1.00017	1.00024	1.00034	1.00046	1.00063	1.00086	1.0012	1.00167	1.00235
79	Trapping ratio (air-only)	-	1.00012	1.00016	1.00023	1.00032	1.00043	1.00059	1.00082	1.00113	1.00158	1.00222
80	Trapped air volumetric efficiency	-	0.706322	0.637623	0.562423	0.487718	0.419248	0.356959	0.302027	0.253748	0.21183	0.174604
81	Total volumetric efficiency	-	0.70624	0.637518	0.562293	0.487562	0.419065	0.356746	0.301781	0.253456	0.211497	0.174218

Go to Settings to activate Windows.

OK Apply Cancel Help

Appendix E1: Injection Rate and Injection Pressure Profiles



Appendix E2: Characterized Design parameters for MB Actros Engine model 3340-LS.

Item	Specification
Engine Model Series	Mercedes Benz Actros 3340-LS, (2011-2024)
Engine Type	Four Stroke cycle - 6 cylinder In-line
Bore (mm)	130
Stroke (mm)	150
Connecting Rod Length (mm)	273
Engine Capacity (cc or cm ³)	11,950
Compression Ratio	17.75:1
Engine dry weight (kg)	940
Gross Vehicle Weight (tons) I.e. 7 t + 2x13 t	33
Maximum Power output (kW) @ 1800 rpm	294
Horse Power (hp)	394, Maximum is 400
Displacement (Ltr)	12.8
Maximum Torque (Nm) @ 1080 rpm	1900
Fuel Injection Type	Direct Injection via unit injectors
Injection Nozzle Type	6-hole injection nozzle, hole dia 0.194mm Simulations run between 0.194 mm – 0.278mm
Injection Pressure (Bar)	Up to 1800
Inlet and Exhaust lift	0.4 mm

Fuel Mixture Formation	Unit Pump System (UPS)
Cylinder arrangement	6-In-line
Ignition pressure	170 bars
Valve Technology	4-Valve Technology (2-Inlet & 2-Outlet)
Axil Configuration	6x4
Cooling	Water cooled with an electromagnetic fan
Exhaust	Stainless steel with SCR catalytic converter
Engine Brake	Brake flap & decomposition valve
Control (Engine Management)	Electronic Telligent engine management system
Emission Standard	Euro III Version
Fuel Type	Diesel of density 830 kg/m ³ , Cetane No. 48, Sulphur Content 0.05%
Combustion chamber diameter (mm)	98.8 Bowl type
Fuel Injection for low load	11.5 ⁰ C BTDC
Fuel Injection for high load	9.5 ⁰ C BTDC
Crank Radius (mm)	75
Firing order	1-5-3-6-2-4
AFR	14.5

Appendix F1: Plagiarism Report and Receipt



Digital Receipt

This receipt acknowledges that Turnitin received your paper. Below you will find the receipt information regarding your submission.

The first page of your submissions is displayed below.

Submission author: Josephat KALANZI
Assignment title: Thesis 2
Submission title: Examining The Effect Of Air-Fuel Atomization On Performance ...
File name: FINAL DISSERTATION_Report_for_JK-with_addressed_correctio...
File size: 4.5M
Page count: 134
Word count: 24,186
Character count: 139,598
Submission date: 08-Sep-2025 08:27PM (UTC+0100)
Submission ID: 2745435933

EXAMINING THE EFFECT OF AIR-FUEL ATOMIZATION ON THE
PERFORMANCE AND EMISSION OF HEAVY DUTY TRUCKS: A CASE STUDY
OF MERCEDES-BENZ ACTROS ENGINE MODEL 3004LS.

BY
KALANZI JOSEPHAT
(B.Eng. Mech & Materl. Eng. KYU)
22UGMEM400PE

A DISSERTATION SUBMITTED TO THE DIRECTORATE OF RESEARCH
AND GRADUATE TRAINING IN PARTIAL FULFILLMENT OF THE
REQUIREMENTS FOR THE AWARD OF THE DEGREE OF MASTER OF
SCIENCE IN ADVANCED MANUFACTURING SYSTEMS ENGINEERING
OF KYAMUGO UNIVERSITY

DECEMBER, 2024

KALANZI JESOUPHAT

ORIGINALITY REPORT

14%

SIMILARITY INDEX

11%

INTERNET SOURCES

9%

PUBLICATIONS

3%

STUDENT PAPERS

PRIMARY SOURCES

1

energy.sandia.gov

Internet Source

2%

2

www.researchgate.net

Internet Source

1%

3

www.mdpi.com

Internet Source

1%

4

www.westco.info

Internet Source

1%

5

biblio.ugent.be

Internet Source

<1%

6

worldwidescience.org

Internet Source

<1%

7

utpedia.utp.edu.my

Internet Source

<1%

8

www.grin.com

Internet Source

<1%

9

Submitted to 9659

Student Paper

<1%

10	erepository.uonbi.ac.ke Internet Source	<1%
11	Submitted to University of Wales, Lampeter Student Paper	<1%
12	www.nature.com Internet Source	<1%
13	propulsionejournal.com Internet Source	<1%
14	vdocuments.site Internet Source	<1%
15	makir.mak.ac.ug Internet Source	<1%
16	Balram Sahu, Dhananjay Kumar Srivastava. "A Numerical Investigation of Injector Hole Configuration and Injection Parameters in a Dimethyl Ether Fueled Engine ", Environmental Progress & Sustainable Energy, 2022 Publication	<1%
17	Arkadiusz Jamrozik. "Biodiesel/alcohol blends as fuel for compression ignition engines – a review", Journal of the Energy Institute, 2025 Publication	<1%
18	John E. Dec. "A Conceptual Model of DI Diesel Combustion Based on Laser-Sheet Imaging*",	<1%

SAE International, 1997

Publication

19	ir.jkuat.ac.ke Internet Source	<1%
20	Xandra Marcelle Margot, Raúl Payri Marín, José Ramón Serrano Cruz. "THIESEL 2022. Conference on Thermo-and Fluid Dynamics of Clean Propulsion Powerplants", Universitat Politecnica de Valencia, 2022 Publication	<1%
21	ir-library.ku.ac.ke Internet Source	<1%
22	kalaharijournals.com Internet Source	<1%
23	Ankit A Raut, J M Mallikarjuna. "Effects of direct water injection and injector configurations on performance and emission characteristics of a gasoline direct injection engine: A computational fluid dynamics analysis", International Journal of Engine Research, 2019 Publication	<1%
24	Rizal Mahmud, Toru Kurisu, Onur Akgol, Keiya Nishida, Yoichi Ogata. "Characteristics of Flat-Wall Impinging Spray Flame and Its Heat Transfer under Diesel Engine-Like Condition: Effects of Injection Pressure, Nozzle Hole	<1%

Diameter and Impingement Distance", SAE
International Journal of Advances and Current
Practices in Mobility, 2019

Publication

25	www.gallaherfleetsolutions.com Internet Source	<1 %
26	Sivakumar Ellappan, Silambarasan Rajendran, Ratchagaraja Dhariyasamy, Qasem M. Al-Mdallal et al. "Experimental investigation of ternary blends on performance, and emission behaviors of a modified low-heat rejection CI Engine", Case Studies in Thermal Engineering, 2024 Publication	<1 %
27	scholar.mzumbe.ac.tz Internet Source	<1 %
28	acikbilim.yok.gov.tr Internet Source	<1 %
29	wine.idaho.gov Internet Source	<1 %
30	www.ijeat.org Internet Source	<1 %
31	www.swamivivekanandauniversity.ac.in Internet Source	<1 %
32	Daisuke Tanaka, Koji Hiraya, Hirofumi Tsuchida, Hidetoshi Wakasa, Yutaka Murata,	<1 %

Jin Kusaka, Yasuhiro Daisho. "A Study of Gasoline Lift-off Combustion in a Spark Ignition Engine", SAE International Journal of Engines, 2008

Publication

33	Uwe Leuteritz, Amin Velji, Ernstwendelin Bach. "A Novel Injection System for Combustion Engines Based on Electrostatic Fuel Atomization", SAE International, 2000	<1 %
Publication		
34	dspace.nm-aist.ac.tz	<1 %
Internet Source		
35	Submitted to Addis Ababa University	<1 %
Student Paper		
36	Submitted to Middle East Technical University	<1 %
Student Paper		
37	afribary.com	<1 %
Internet Source		
38	liboasis.buse.ac.zw:8080	<1 %
Internet Source		
39	theses.hal.science	<1 %
Internet Source		
40	tind-customer-agecon.s3.amazonaws.com	<1 %
Internet Source		

41	Submitted to Kuwait Maastricht Business School Student Paper	<1%
42	Tan Chau Vo, Trung An Huynh. "Investigation of injection rate characteristics and applicability of palm-biodiesel blending ratios in various diesel injector nozzle geometries under simulated CI engine operating conditions", Transportation Engineering, 2025 Publication	<1%
43	Submitted to University of Sussex Student Paper	<1%
44	Hao Wu, Lingxia Zhu, Jianjun Cai, Huijuan Lv. "Effect of Sewage Sludge Addition on the Co-Combustion Characteristics of Municipal Solid Waste Incineration", Processes, 2024 Publication	<1%
45	Submitted to Louisiana Tech University Student Paper	<1%
46	Shanti Mehra, Avinash Kumar Agarwal. "Advanced NOx mitigation strategies in dimethyl ether-fuelled internal combustion engines", Fuel, 2025 Publication	<1%
47	Sulochana G, Venkata Prasad.CH, S.K. Bhatti, V.V. Venu.Madhav et al. "Impact of Multi-	<1%

Walled Carbon Nanotubes (MWCNTs) on Hybrid Biodiesel Blends for Cleaner Combustion in CI Engines", Energy, 2024

Publication

48	Wei Du, Juejue Lou, Fushui Liu. "Effects of Nozzle Hole Diameter on Diesel Sprays in Constant Injection Mass Condition", SAE International, 2017 Publication	<1%
49	epub.ub.uni-greifswald.de Internet Source	<1%
50	open.metu.edu.tr Internet Source	<1%
51	poltekkes-pontianak.ac.id Internet Source	<1%
52	tc.canada.ca Internet Source	<1%
53	www.ijat.net Internet Source	<1%
54	www.scribd.com Internet Source	<1%
55	"Renewable Fuels for Sustainable Mobility", Springer Science and Business Media LLC, 2023 Publication	<1%

56	Haohan Li, Tarek Beji, Sebastian Verhelst. "IMPROVING THE CALCULATION OF EVAPORATING SPRAYS FOR MEDIUM-SPEED MARINE-ENGINE-LIKE CONDITIONS", Atomization and Sprays, 2021 Publication	<1 %
57	Kundan Kumar, Barun Kumar Nandi, Vinod Kumar Saxena, Rakesh Kumar. "Experimental studies of thermal behavior, engine performance and emission characteristics of biodiesel / diesel / 1 pentanol blend in diesel engine", Alexandria Engineering Journal, 2024 Publication	<1 %
58	Y. Bai, L. Y. Fan, X. Z. Ma, H. L. Peng, E. Z. Song. "Effect of injector parameters on the injection quantity of common rail injection system for diesel engines", International Journal of Automotive Technology, 2016 Publication	<1 %
59	www.ecoeet.com Internet Source	<1 %
60	Submitted to Brunel University Student Paper	<1 %
61	Minhoo Choi, Khawar Mohiuddin, Namho Kim, Sungwook Park. "Investigation of the effects of EGR rate, injection strategy and nozzle specification on engine performances	<1 %

and emissions of a single cylinder heavy duty diesel engine using the two color method", *Applied Thermal Engineering*, 2021

Publication

62	Submitted to Queensland University of Technology Student Paper	<1 %
63	Submitted to Veermata Jijabai Technological Institute Student Paper	<1 %
64	Submitted to International Islamic University Malaysia Student Paper	<1 %
65	pdfcookie.com Internet Source	<1 %
66	www.nap.edu Internet Source	<1 %
67	www.total.co.ke Internet Source	<1 %
68	Murat Durmaz, Selma Ergin. "A Numerical Investigation of the Effects of the Fuel Injection Pressure and Nozzle Hole Diameter on Natural Gas–Diesel Dual-Fuel Combustion Characteristics", <i>Energies</i> , 2025 Publication	<1 %

69	N. Roeinfard, A. Moosavi. "Thermodynamic analysis and optimization of the organic Rankine and high-temperature Kalina cycles for recovering the waste heat of a bi-fuel engine", Fuel, 2022 Publication	<1 %
70	Submitted to Tikrit University Student Paper	<1 %
71	Submitted to University Tun Hussein Onn Malaysia Student Paper	<1 %
72	Submitted to University of Southampton Student Paper	<1 %
73	Varun, Paramvir Singh, Samaresh Kumar Tiwari, Rituparn Singh, Naresh Kumar. "Modification in combustion chamber geometry of CI engines for suitability of biodiesel: A review", Renewable and Sustainable Energy Reviews, 2017 Publication	<1 %
74	hdl.handle.net Internet Source	<1 %
75	libratez.cu.edu.tr Internet Source	<1 %
76	Papagiannakis, R.G.. "Emission characteristics of high speed, dual fuel, compression ignition	<1 %

engine operating in a wide range of natural gas/diesel fuel proportions", Fuel, 201007

Publication

77 Robert D. Chalgren, Gordon G. Parker, Oner Arici, John H. Johnson. "A Controlled EGR Cooling System for Heavy Duty Diesel Applications Using the Vehicle Engine Cooling System Simulation", SAE International, 2002 <1 %

Publication

78 Vaibhav Singh, Naveen Kumar. "Numerical investigation of the effect of nozzle hole diameter on the combustion, emission, and spray characteristics in a diesel engine", Energy Sources, Part A: Recovery, Utilization, and Environmental Effects, 2021 <1 %

Publication

79 ageconsearch.umn.edu <1 %

Internet Source

80 c.coek.info <1 %

Internet Source

81 www.ukessays.com <1 %

Internet Source

82 Qiang Cheng, Zeeshan Ahmad, Viljam Grahn, Jari Hyvönen, Larmi Martti, Ossi Kaario. "Multi-scale optical diagnostics for marine diesel spray", Energy, 2025 <1 %

Publication

83	catalysis.eprints.iitm.ac.in Internet Source	<1 %
84	eprints.utar.edu.my Internet Source	<1 %
85	open.library.ubc.ca Internet Source	<1 %
86	viralrang.com Internet Source	<1 %
87	www.globalgrowthinsights.com Internet Source	<1 %
88	Aditya Darbhamalla. "Analysis of the Internal Thermofluid-Dynamics in a Uniflow Scavenged Engine", Universitat Politecnica de Valencia, 2024 Publication	<1 %
89	Ayush Tripathi, Hardikk Valera, Avinash Kumar Agarwal. "Dimethyl ether fuelled genset engine development and optimisation of novel fuel injection equipment for improved performance and emissions", Fuel, 2024 Publication	<1 %
90	Chang Zhai, Junyu Zhang, Kuichun Li, Pengbo Dong, Yu Jin, Feixiang Chang, Hongliang Luo. "Comparative Analysis and Normalization of Single-Hole Vs. Multi-Hole Spray	<1 %

Characteristics: 1st Report on Spray
Characteristic Comparison", Green Energy
and Resources, 2025

Publication

- 91** Ioannis Nikiforakis, Gaurav Guleria, Mahmoud Koraiem, Dimitris Assanis, Curtis Collie, Tiago Costa, Piyush Kute, Alec Shkolnik. <1%
"Understanding Pre-Chamber Combustion Performance in a Closed-Cycle Model of a Novel Rotary Engine", SAE International, 2022
Publication
-

- 92** J. Christian Sacadura, Lionel Robin, Frederic Dionnet, David Gervais, Patrick Gastaldi, Afif Ahmed. <1%
"Experimental Investigation of an Optical Direct Injection S.I. Engine Using Fuel-Air Ratio Laser Induced Fluorescence", SAE International, 2000
Publication
-

- 93** Peiyong Ni, Haiyan Xu, Ziheng Zhang, Xuewen Zhang. <1%
"Effect of injector nozzle parameters on fuel consumption and soot emission of two-cylinder diesel engine for vehicle", Case Studies in Thermal Engineering, 2022
Publication
-

- 94** Swarup Kumar Nayak, Purna Chandra Mishra, Muhamad Mat Noor. <1%
"Simultaneous reduction of nitric oxide and smoke opacity in TDI dual fuel engine fuelled with calophyllum-

diesel blends and waste wood chip gas for modified inlet valve and injector nozzle geometry", Energy, 2019

Publication

95	Submitted to University of Kufa Student Paper	<1 %
96	Z Zhu, M Hao, G-X Gao, J Liu, S-H Liu, Y-J Wei. "Investigation of the injection process and combustion of a dimethyl ether engine with different nozzle flow areas", Proceedings of the Institution of Mechanical Engineers, Part D: Journal of Automobile Engineering, 2011 Publication	<1 %
97	academiascholaz.blogspot.com Internet Source	<1 %
98	bura.brunel.ac.uk Internet Source	<1 %
99	discovery.researcher.life Internet Source	<1 %
100	docplayer.net Internet Source	<1 %
101	eprints.utm.my Internet Source	<1 %
102	ndl.ethernet.edu.et Internet Source	<1 %

103	ouci.dntb.gov.ua Internet Source	<1 %
104	pleione.ehsst.org Internet Source	<1 %
105	psasir.upm.edu.my Internet Source	<1 %
106	research.nottingham.edu.cn Internet Source	<1 %
107	scholar.uoc.ac.in Internet Source	<1 %
108	vital.seals.ac.za Internet Source	<1 %
109	www.diplomarbeiten24.de Internet Source	<1 %
110	www.nhtsa.gov Internet Source	<1 %
111	"Design and Development of Heavy Duty Diesel Engines", Springer Science and Business Media LLC, 2020 Publication	<1 %
112	Ashkan Ghaedi, Rouzbeh Shafaghat, Omid Jahanian, Seyed Sadegh Motallebi Hasankola. "Comparing the performance of a CI engine after replacing the mechanical injector with a	<1 %

common rail solenoid injector", Journal of Thermal Analysis and Calorimetry, 2019

Publication

113

Nabi, Md.N.. "Experimental investigation of engine emissions with marine gas oil-oxygenate blends", Science of the Total Environment, 20100715

Publication

<1 %

114

R. Sakthivel, S. Sidharth, P. Ganesh Kumar, T. Mohanraj, A. Tamilvanan, B. Ashok. "Effect of engine design parameters in NOx reduction", Elsevier BV, 2022

Publication

<1 %

115

R.L. Evans. "Increasing the efficiency of lean-burn automotive engines", International Journal of Environmental Studies, 2006

Publication

<1 %

116

Raghu Palani, Venkatesan Subramanian. "Effect of nozzle hole number on performance and emissions of dual-fuel diesel engines with juliflora biodiesel blends and hydrogen additive", International Journal of Hydrogen Energy, 2025

Publication

<1 %

117

S.T.P. Purayil, SAB Al-Omari, E. Elnajjar. "Effect of hydrogen blending on the combustion performance, emission, and cycle-to-cycle

<1 %

variation characteristics of a single-cylinder
GDI spark ignition dual-fuel engine",
International Journal of Thermofluids, 2023
Publication

118 Selvakumar Periyasamy, Eduardo Alberto
López-Maldonado, R. Balachandran.
"Emerging Materials for Biofuel
Developments", CRC Press, 2025
Publication

119 Yang, W.M., H. An, S.K. Chou, K.J. Chua, B.
Mohan, V. Sivasankaralingam, V. Raman, A.
Maghbouli, and J. Li. "Impact of emulsion fuel
with nano-organic additives on the
performance of diesel engine", Applied
Energy, 2013.
Publication

120 agrifoodecon.springeropen.com
Internet Source

121 chiefengineerlog.com
Internet Source

122 coek.info
Internet Source

123 datahorizonresearch.com
Internet Source

124 dlib.hust.edu.vn:8080
Internet Source

125	drgan.org Internet Source	<1 %
126	dspace.sebhau.edu.ly Internet Source	<1 %
127	dspace.unza.zm Internet Source	<1 %
128	etd.aau.edu.et Internet Source	<1 %
129	link.springer.com Internet Source	<1 %
130	myscholar.umk.edu.my Internet Source	<1 %
131	oa.upm.es Internet Source	<1 %
132	research.library.mun.ca Internet Source	<1 %
133	www.akademiabaru.com Internet Source	<1 %
134	D.T. Hountalas. "Effect of injector flow rate on heavy-duty DI diesel engine performance and emissions for various injection pressures", International Journal of Vehicle Design, 2006 Publication	<1 %

135	H.H. Chiu, H.Y. Kim, E.J. Croke. "Internal group combustion of liquid droplets", Symposium (International) on Combustion, 1982	<1 %
Publication		
136	Sarbjot Singh Sandhu, Prem Kumar, Mandeep Singh. "Alcohol Fuels in Advanced Combustion Strategy Mode Diesel Engines", CRC Press, 2025	<1 %
Publication		
137	"Advances in IC Engines and Combustion Technology", Springer Science and Business Media LLC, 2021	<1 %
Publication		
138	"Hydrogen as Emerging Fuel for De-Fossilizing Transport Sector", Springer Science and Business Media LLC, 2025	<1 %
Publication		
139	Chang Zhai, Yu Jin, Keiya Nishida, Youichi Ogata. "Diesel spray and combustion of multi-hole injectors with micro-hole under ultra-high injection pressure – Non-evaporating spray characteristics", Fuel, 2021	<1 %
Publication		
140	Christopher Nkansah, Victor Oyebamiji Ojo, Maxwell Collins Bawuah, Abimbola Hannah Ojo, Odunola Latifah Odofin. "Assessment and performance of ferrocene nanoparticle-	<1 %

hibiscus cannabinus biodiesel admixed fuel blended with Hydrogen in direct injection (DI) engine", Springer Science and Business Media LLC, 2025

Publication

141

Paramvir Singh, Dhinesh Balasubramanian, Inbanaathan Papla Venugopal, Vineet Veer Tyagi et al. "A comprehensive review on the applicability of hydrogen and natural gas as gaseous fuel for dual fuel engine operation", Energy Sources, Part A: Recovery, Utilization, and Environmental Effects, 2024

Publication

<1 %

Exclude quotes Off

Exclude matches Off

Exclude bibliography On